IFM-GEOMAR
Leibniz-Institut für Meereswissenschaften
an der Universität Kiel

Adaptation Mechanisms of Antarctic Phytoplankton to Persistent Iron Limitation

Dissertation
zur Erlangung des Doktorgrades
der Mathematisch-Naturwissenschaftlichen Fakultät
der Christian-Albrechts-Universität zu Kiel

vorgelegt von

Linn Hoffmann

Kiel 2006

Hiermit erkläre ich, dass ich die vorliegende Arbeit selbständig und ohne unerlaubte Hilfe angefertigt habe. Es wurden keine anderen Hilfsmittel außer den angegebenen Quellen benutzt. Diese Arbeit wurde weder ganz noch zum Teil einer anderen Stelle im Rahmen eines Prüfungsverfahrens vorgelegt. Ferner habe ich noch keinen Promotionsversuch an dieser oder einer anderen Hochschule unternommen.

_____

Linn Hoffmann

Referentin: Prof. Dr. Karin Lochte

Koreferent: Prof. Dr. Franciscus Colijn

Tag der mündlichen Prüfung: 23. 01. 2007

Zum Druck genehmigt:

Der Dekan

LIST OF CHAPTERS

This doctoral thesis is based on the following publications and manuscripts:

I. Hoffmann, Linn J., Ilka Peeken, Karin Lochte, Philipp Assmy, Marcel Veldhuis. 2006.
Different reactions of Southern Ocean phytoplankton size classes to iron fertilization. Limnology and Oceanography 51(3): 1217–1229

II. Hoffmann, Linn J., Ilka Peeken, Karin Lochte.
Co-limitation by iron, silicate, and light of three Southern Ocean diatoms species. Submitted to Biogeosciences

III. Hoffmann, Linn J., Ilka Peeken, Karin Lochte.
Effects of iron on the elemental stoichiometry during EIFEX and in the diatoms *Fragilariopsis kerguelensis* and *Chaetoceros dichaeta*. Submitted to Biogeosciences

IV. Duggen, Svend, Peter Croot, Ulrike Schacht, and Linn Hoffmann. 2007.
Subduction zone volcanic ash can fertilize the surface ocean and stimulate phytoplankton growth: Evidence from biogeochemical experiments and satellite data. Geophysical Research Letters VOL. 34, L01612, doi:10.1029/2006GL027522, 2007

STATEMENT OF MY CONTRIBUTION

CHAPTER I:

This publication contains data that were collected by Ilka Peeken and me during the Southern Ocean iron fertilization experiment EIFEX and analyzed by me in the home laboratory. Philipp Assmy contributed cell counts. Samples for flow cytometric analysis were collected by me and analyzed by Marcel Veldhuis. The paper was written by me. Ilka Peeken, Karin Lochte, and Philipp Assmy contributed writing and provided scientific advice.

CHAPTER II:

Laboratory experiments were planned, performed and analyzed by me. Jesco Peschutter and Wiebke Schmidt assisted in laboratory work. The manuscript was written by me. Ilka Peeken and Karin Lochte contributed writing and provided scientific advice.

CHAPTER III:

Laboratory experiments were planned, performed and analyzed by me. Jesco Peschutter assisted in laboratory work. The manuscript was written by me. Ilka Peeken provided scientific advice.

CHAPTER IV:

The concept of this publication was derived by Svend Duggen and Peter Croot. I contributed the biological experiments which were planned, performed, and analyzed by me. The paper was written by Svend Duggen, I contributed writing the biological part.

Table of contents

1 SUMMARY

Antarctic phytoplankton is subjected to a variety of unfavorable environmental conditions that limit growth or require energy demanding adaptation mechanisms. Most severe are the low iron concentrations in the Southern Ocean (SO) that are known to limit phytoplankton growth throughout the year. Storm events frequently result in extremely deep mixing that exposes the primary producers to very low light intensities. Furthermore, the concentrations of silicate (Si), an essential nutrient for diatoms, are unequally distributed and can co-limit diatom growth in low Si areas north of the Polar Frontal Zone. The aim of this doctoral thesis is to investigate reactions and adaptation mechanisms of SO phytoplankton to these extreme abiotic factors, especially to iron limitation, during the European Iron Fertilization Experiment (EIFEX) and of SO diatom key species in laboratory experiments.

In agreement with other *in situ* iron fertilization experiments large, chain forming diatoms were the main beneficiaries of iron fertilization during EIFEX and showed the highest increase in carbon and chlorophyll concentrations. However, it was observed for the first time that small diatoms benefited as well from increased iron availability and were able to outgrow other small nanophytoplankton groups in the 2-8 μm size fraction (Chapter I). Changes in the species composition in all size classes are most likely the reason for the observed alterations in the elemental composition.

In laboratory experiments investigating the possible co-limitation of iron, light, and silicate in *Actinocyclus sp.*, *Chaetoceros dichaeta*, and *C. debilis* from the SO, growth was almost completely suppressed in the former two species at high light intensities similar to those found in about 1-28 m water depth during EIFEX (Chapter II). This indicates that light limitation of SO diatoms may be less common than hitherto suggested. Further, iron and silicate co-limitation in *C. dichaeta* resulted in distinct frustule malformation that would likely decrease grazing protection of this species in the field. The species specific differences in growth and grazing protection found in this study imply that the abiotic factors iron, light, and silicate have distinct implications for SO phytoplankton community structure. *C. debilis*, the smallest species tested, was less affected by high light

intensity and iron and silicate co-limitation. In the field this species would therefore possibly dominate over the other species tested in the absence of grazing.

Decreases in the elemental Si : C, Si : N, and Si : P ratios of diatoms under high iron concentrations were caused by different mechanisms instead of solely by the assumed decreased silicification (Chapter III). While cellular Si concentrations decreased in *Fragilariopsis kerguelensis*, cellular C, N, and P concentrations increased in *C. dichaeta*. The first will likely result in lower sinking rates, while vulnerability to grazing and remineralization are possibly enhanced and thus export might be reduced in consequence of iron fertilization in the field. In contrast, relative C, N, and P export of *C. dichaeta* might increase as this species would possible maintain equal sinking rates, grazing protection, and remineralization. Unlike other *in situ* iron fertilization experiments an increase in the Si : C, Si : N, and Si : P ratios was observed inside the iron fertilized patch during EIFEX (Chapter I and III). This is possibly caused by a shift in species composition due to a stronger response of heavily silicified diatoms compared to other phytoplankton groups and does not necessarily reflect the intensity of frustule silicification. Modeling biogenic export solely based on changes in the elemental composition will be susceptible to errors due to the different causes for similar changes in phytoplankton stoichiometry and their possible effect on export.

As iron limitation is a general pattern in the SO it is likely that diatoms are able to react rapidly to temporary iron inputs. Of various Fe inputs such as dust deposition and sea ice melting, volcanic ash provides an iron source whose importance for HNLC regions has been largely overlooked so far. In Chapter IV it is demonstrated for the first time that SO diatoms are able to use volcanic ash as an iron source and increase chlorophyll concentrations and photosynthetic efficiency significantly. In contact with seawater, the volcanic ash released high concentrations of iron and other trace metals and nutrients within minutes. This very fast mobilization shows that the majority of nutrients will be released while the ash passes the euphotic zone. These data suggest that major volcanic eruptions have the potential to affect marine biogeochemical cycles.

In conclusion, this thesis demonstrates the sensitivity of Antarctic phytoplankton to changes in abiotic factors, such as iron, silicate, and light availability. The species specific

reactions of SO diatoms in growth and grazing protection, as shown in Chapter II and III, are probably the reason for the observed changes in species composition after iron fertilization during EIFEX (Chapter I). Shifts in the phytoplankton community structure will likely affect the export of biogenic material. Since specific diatoms decrease cellular silicification or increase cellular C, N, and P (Chapter III) after an iron input, such as volcanic ash deposition (Chapter IV) or artificial fertilization, the contribution of these species to the community structure can decrease or increase the export of biogenic material.

2 ZUSAMMENFASSUNG

Das Phytoplankton des Südlichen Ozeans (SO) ist einer Reihe von unwirtlichen abiotischen Faktoren ausgesetzt, die das Wachstum limitieren oder energiereiche Anpassungsmechanismen erfordern. Besonders die niedrigen Eisenkonzentrationen in großen Teilen des SO limitieren die marine Primärproduktion. Regelmäßige Stürme führen zu einer sehr tiefen Durchmischung, wodurch das Phytoplankton zum Teil sehr niedrigen Lichtintensitäten ausgesetzt wird. Diatomeen können darüber hinaus in den Gebieten mit niedrigen Silikatkonzentrationen nördlich der Polarfront Eisen und Silikat co-limitiert sein. Ziel dieser Arbeit ist es, Reaktionen und Adaptionsmechanismen von antarktischem Phytoplankton während des European Iron Fertilization Experiment (EIFEX) und von antarktischen Diatomeen in Laborexperimenten zu untersuchen.

Wie bei anderen *in situ* Eisendüngungsexperimenten konnten große, kettenbildende Diatomeen am meisten von der Eisendüngung profitieren und zeigten die größten Zunahmen in der Kohlenstoff- und Chlorophyllkonzentration. Gleichzeitig wurde zum ersten Mal gezeigt, dass auch kleine Diatomeen positiv auf *in situ* Eisendüngung reagieren und stärker wachsen als andere Phytoplanktonarten in der Größenklasse von 2 bis 8 µm (Kapitel I). Der Grund für die Änderungen in den Elementverhältnissen sind vermutlich die Veränderungen in der Artzusammensetzung aller Größenklassen.

In Laborexperimenten wurde die mögliche Co-Limitation von Eisen, Licht und Silikat bei *Actinocyclus sp.*, *Chaetoceros dichaeta* und *C. debilis* untersucht (Kapitel II). Hohe Lichtintensitäten, die etwa denen in 1-28 m Tiefe während EIFEX entsprechen, unterdrückten das Wachstum bei den beiden erstgenannten Arten fast vollständig. Dieses Ergebnis lässt vermuten, dass Lichtlimitierung von antarktischen Diatomeen geringer sein könnte als bisher postuliert. Bei *C. dichaeta* führt Eisen und Silikat Co-Limitation zu einer deutlichen Missbildung der Silikatschalen. Unter den gleichen Bedingungen im Feld würde dies eine erhebliche Reduzierung des Fraßschutzes für diese Art bedeuten. Die artspezifischen Unterschiede im Wachstum und Fraßschutz implizieren, dass die abiotischen Faktoren Eisen, Licht und Silikat bedeutende Auswirkung auf die Zusammensetzung der Phytoplanktongemeinschaft haben. *C. debilis*, die kleinste der getesteten Arten, war am

wenigsten anfällig für hohe Lichtintensitäten und Eisen und Silikat Co-Limitation. Im Feld würde diese Art vermutlich über die anderen Arten dominieren, wenn es keinen Fraß gäbe.

Außerdem wurde gezeigt, dass sinkende Si : C, Si : N und Si : P Verhältnisse von Diatomeen durch Eisendüngung unterschiedliche Ursachen haben und nicht ausschließlich eine schwächere Verkieselung der Zellen bedeuten müssen (Kapitel III). Bei *Fragilariopsis kerguelensis* nahm der zelluläre Si Gehalt ab, während bei *C. dichaeta* der zelluläre C, N und P Gehalt zunahm. Ersteres könnte zur Folge haben, dass Eisendüngung im Feld zu geringeren Sinkgeschwindigkeiten führt, wobei vermutlich die Anfälligkeit für Fraß und Remineralisation erhöht und der Export verringert würde. Im Gegensatz dazu würde der relative C, N und P Export von *C. dichaeta* erhöht werden, da vermutlich Sinkgeschwindigkeit, Fraßschutz und Remineralisation gleich blieben. Anders als bei anderen *in situ* Eisendüngungsexperimenten stiegen die Si : C, Si : N und Si : P Verhältnisse während EIFEX im eisengedüngten Gebiet an (Kapitel I und III). Vermutlich resultiert dies aus einer Veränderung in der Artzusammensetzung durch ein stärkeres Wachstum der stark verkieselten Diatomeen im Verhältnis zu anderen Phytoplanktongruppen und lässt keine Rückschlüsse auf eine veränderte Verkieselung zu. Die unterschiedlichen Ursachen für gleiche Veränderungen in den Elementverhältnissen und deren mögliche Auswirkungen auf den biogenen Export zeigen, dass Exportmodelle, die nur auf diesen Verhältnissen basieren, anfällig für Fehler sind.

Diatomeen sind im SO einer permanenten Eisenlimitierung ausgesetzt und es ist daher wahrscheinlich, dass sie schnell und effektiv auf temporäre Eiseneinträge durch z.B. Eisschmelze, Staubeintrag oder aber auch Eintrag von Vulkanasche reagieren können. Die Bedeutung von Vulkanasche als Eisenquelle in HNLC Gebieten wurde bisher weitgehend vernachlässigt. Hier konnte zum ersten Mal gezeigt werden, dass antarktische Diatomeen Eisen aus Vulkanasche nutzen können und dadurch die Chlorophyllkonzentrationen und photosynthetische Effizienz deutlich erhöht werden (Kapitel IV). Bei Kontakt mit Seewasser wurden innerhalb von Minuten hohe Konzentrationen an Eisen, sowie anderen Spurenelementen und Nährstoffen freigesetzt. Diese sehr schnelle Mobilisierung zeigt, dass der Großteil der Nährstoffe freigesetzt wird, während die Asche die euphotische

Zone passiert. Diese Daten legen nahe, dass große Vulkaneruptionen das Potential haben marine biogeochemische Kreisläufe zu beeinflussen.

Zusammenfassend zeigt diese Arbeit, wie sensibel Antarktisches Phytoplankton auf Veränderungen der abiotischen Faktoren Eisen, Silikat und Licht reagiert. Artspezifische Reaktionen im Wachstum und Fraßschutz, wie in Kapitel II und III gezeigt, sind vermutlich der Grund für Veränderungen in der Artzusammensetzung als Folge der Eisendüngung während EIFEX (Kapitel I). Abhängig davon, ob nach einem Eiseneintrag, wie z. B. durch Vulkanasche (Kapitel IV) oder künstliche Düngung, Diatomeen das Phytoplankton dominieren, die ihre zelluläre Verkieselung verringern, oder den zellulärer C, N und P Gehalt erhöhen (Kapitel III) können diese Veränderungen in der Phytoplanktongemeinschaft den Export von biogenem Material erhöhen oder erniedrigen.

3 INTRODUCTION

Iron (Fe) is the fourth most abundant element in the Earth's crust and an essential trace nutrient for all living organisms. In heterotrophs Fe is an important component of several enzymes as well as of hemoglobin and myoglobin in higher animals and thus essential for oxygen transport. In autotrophs iron is an essential part of the photosystem (PS) I and II, cytochromes, and iron-sulfur redox proteins. These proteins are involved in key metabolic processes such as photosynthetic and respiratory electron transport, chlorophyll synthesis, nitrate and nitrite reduction, N_2 fixation, and detoxification of reactive oxygen species (Sunda, 2001).

The paradox of iron is that despite its high abundance in the Earth's crust and its major importance for living organisms, low iron availability limits primary production in major regions of the worlds' ocean. An explanation of this phenomenon can be found in the early evolution of live on our planet. In the primordial atmosphere no free O_2 was present and thus the ocean was suboxic. Under these conditions iron would have been soluble as Fe(II) and was presumably available in high concentrations (Turner et al., 2001). As iron availability was no limiting factor, the early stages of life were able to evolve high iron requirements. When O_2 concentrations increased in the atmosphere and in the ocean due to photosynthesis, the soluble Fe(II) was oxidized to Fe(III), which rapidly precipitates and thus the concentrations of bioavailable iron decreased by many orders of magnitude (Turner et al., 2001). This resulted in the paradox that the evolution of photosynthesis, the process iron is most important for, has reduced the availability of this important trace metal in the ocean. However, today 99 % of iron in seawater is bound to strong organic complexes, which increase its apparent solubility. Some phytoplankton groups have evolved uptake mechanisms to utilize parts of this ligand bound iron.

OCEANIC IRON INPUTS

There are three major pathways of iron input into the ocean. The majority of iron is transported to the sea by rivers. However, this source provides mainly particulate iron ($625 - 962 \times 10^{12}$ g year $^{-1}$), which is effectively trapped in estuaries and coastal areas

(Poulton and Raiswell, 2002). The dissolved iron input from rivers is estimated to be about 500 to 1000 times lower than the particulate and it remains unknown how much indeed reaches the open ocean (de Baar and de Jong, 2001). A second source of iron are hydrothermal and sediment inputs. Even if the global flux of dissolved iron from hydrothermal sources is very high (1 - 10 x 10^{12} g yr^{-1}) (Elderfield and Schultz, 1996), it is questionable if this source contributes significant amounts to the iron concentrations in the euphotic zone. As sediments in the surroundings of hydrothermal areas are highly enriched in iron it is assumed that the majority of the dissolved iron is rapidly precipitated at depth (Jickells et al., 2005; Ussher et al., 2004). Significant dissolved Fe(II) and Fe(III) inputs from sediments are only expected in anoxic areas, in areas with high turbidity, or if released as organically complexed Fe (Ussher et al., 2004). In polar regions, ice melting provides a regional iron source (Martin et al., 1990). Atmospheric dust particles accumulate in snow and ice, resulting in relatively high iron concentrations in sea ice. Many phytoplankton species are specialized in living directly underneath the ice cover and benefit from the high iron concentrations compared to the surrounding water. Especially in the Southern Ocean ice melting may be an important reason for regional phytoplankton blooms (Sedwick and DiTullio, 1997). However, globally, the dominant input of soluble and bioavailable iron to the euphotic zone of the open ocean is via atmospheric sources (Jickells and Spokes, 2001). Wind transported dust, mainly from the great deserts of the world, provides the major source of eolian iron input with about 14 - 35 x 10^{12} g $year^{-1}$ (Jickells and Spokes, 2001). About only 1 – 10 % of this Fe is estimated to be bioavailable (Johnson, 2001).

There are other possible contributors to atmospheric iron input, such as extraterrestrial dust, volcanic ash deposition, and anthropogenic sources (Jickells et al., 2005). The amount of soluble (presumably bioavailable) extraterrestrial iron input into the ocean is estimated to be 7 x 10^{9} g $year^{-1}$ (Johnson, 2001). Furthermore, large volcanic eruptions can contribute significantly to the eolian iron amounts. Dust and ash can be transported over month and years around the world before they are finally deposited. Significant amounts of volcanic ash are found in sediments all over the worlds' ocean including areas like the Southern Ocean, where only a relatively small number of active volcanoes exist (Kunz-Pirrung et al., 2002). There is evidence in the literature that the eruption of the

Pinatubo volcano on the Philippines in 1991 enhanced primary production in the Southern Ocean resulting in an observed atmospheric CO_2-drawdown and a parallel pulsed O_2 increase (Keeling et al., 1996; Sarmiento, 1993; Watson, 1997). However, the effect of volcanic eruptions as a source of iron containing aerosols on marine biogeochemistry is only poorly understood.

IRON LIMITATION IN THE OCEAN

Despite its ubiquity in the Earth's crust and the variety of oceanic iron inputs, iron is often only found at trace concentrations and can be limiting for phytoplankton growth in many regions of the world's ocean. In seawater there are various particulate and dissolved phases of iron (Fig. 1), whereas the concentration of each is dependent on the rates of the processes involved and on the composition of the seawater (Ussher et al., 2004). Iron mainly exists as Fe(III) in seawater which is poorly soluble. The majority of Fe(III) adsorbs to particles and is thus effectively exported to the deep sea by sedimentation (Fig. 2 A), resulting in low dissolved and biologically available Fe concentrations at the sea surface. However, organic ligands complex Fe and retain dissolved Fe species in the euphotic zone.

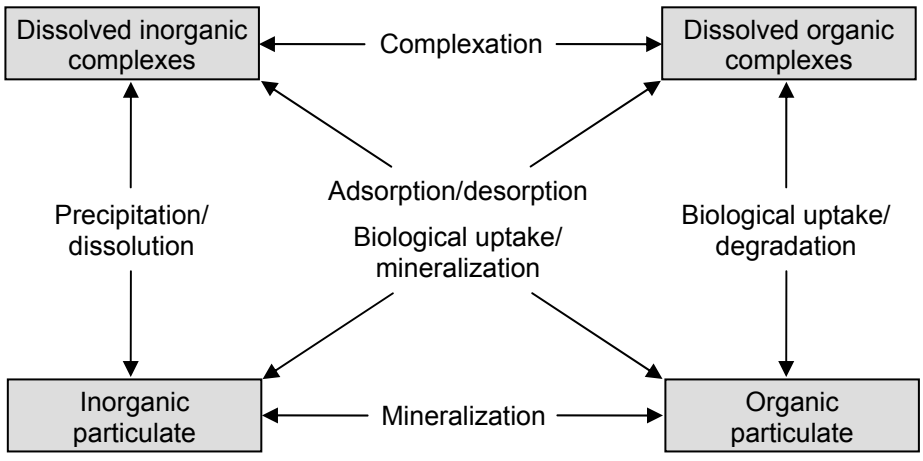

Figure 1: Phase transfer of iron and related processes in seawater. Modified after Ussher et al. (2004).

There are three major regions where iron limits phytoplankton growth, the subarctic Pacific, the equatorial Pacific, and the Southern Ocean. These High Nutrient Low Chlorophyll (HNLC) regions represent about 40 % of the worlds' ocean and are characterized by high concentrations of the macronutrients nitrate and phosphate throughout the year while chlorophyll concentrations remain generally low. Martin and Fitzwater (1988) were the first to show that this paradox is caused by low iron concentrations. Today, a variety of laboratory and ship incubation experiments as well as *in situ* iron fertilization experiments have supported these findings for all HNLC regions. It is surprising that, despite the extreme differences in light, temperature, and hydrography, the three HNLC regions show remarkable similarities in the ecosystem structure and its reaction to iron fertilization. Under iron limitation small phytoplankton species dominate the community in all HNLC regions. Because of their high surface to volume ratios these species are less affected by diffusion-limited iron uptake compared to larger species (see below) (Hudson and Morel, 1990; Morel et al., 1991). The iron requirements for nitrate uptake are relatively high and thus recycled nitrogen (ammonium and urea) are the preferred N sources under Fe limitation (Maldonado and Price, 1996; Wang and Dei, 2001). This and the observations that small phytoplankton communities generally have relative low sinking fluxes result in an ecosystem that is dominated by recycling production and thus has a low *f*-ratio (ratio of new production to total production) (Watson, 2001). The effects of iron fertilization on the ecosystem are again comparably in the HNLC regions. A collective result from all iron fertilization experiments is a strong response of the autotrophic community as shown in a significant increase in photosynthetic efficiency and chlorophyll concentrations (summarized in de Baar et al., 2005; Watson, 2001). Within the phytoplankton community, large diatoms responded most to increased iron availability, leading to a shift in community composition. The initial aim of *in situ* iron fertilization experiments was to prove the theory that iron limits phytoplankton growth in HNLC regions (Martin and Fitzwater, 1988). Martin and Fitzwater (1988) then postulated that lower atmospheric CO_2 concentrations during glacial periods, measured in ice cores, were caused by increased primary production due to higher oceanic Fe input by dust. This rapidly led to the idea to use oceanic iron fertilization as a potential climate regulating strategy by increasing the

efficiency of the biological pump and thus decreasing atmospheric CO_2 concentrations (Martin et al., 1990). Today, nine *in situ* iron fertilization experiments have been performed in the three HNLC regions. While the initiated phytoplankton blooms resulted in an increased CO_2 uptake from the atmosphere, actual carbon export to the deep sea is difficult to assess and could not be clearly demonstrated (de Baar et al., 2005). However, these experiments did improve our knowledge about these unique ecosystems and their complex response to changing nutritional conditions as for example during glacial/interglacial periods.

BIOLOGICAL UPTAKE MECHANISMS

It is not yet exactly known which form of iron is available for phytoplankton growth. It was primarily assumed that only the sum of all inorganic iron species (Fe') are bioavailable (Rich and Morel, 1990). However, as more than 99 % of iron in the surface ocean is organically complexed (Rue and Bruland, 1995), the remaining Fe' concentrations would be too low to sustain growth (Wells et al., 1995). Indeed some organic complexes were shown to be an important source of bioavailable iron for phytoplankton growth (Hutchins et al., 1999; Maldonado and Price, 1999).

In oceanic phytoplankton two major iron uptake systems exist: The siderophore system and ion membrane transporters. The siderophore system is commonly used by terrestrial bacteria, fungi, and also by some marine heterotrophic bacteria and cyanobacteria (Sunda, 2001). In these organisms low intracellular iron concentrations induce the production of iron chelators on the outer cell membrane (Fig. 2 C). These siderophores, having a very high iron affinity, are released into the seawater where they bind Fe that is chelated within existing complexes or adsorbed to particles. The Fe-siderophore complex is then transported back into the cell by specific transport proteins. In the cell iron is released and used for synthesis of iron proteins, while the siderophores are either discarded or recycled and transported back into the media. As not every species of marine bacteria is able to produce siderophores, many of them depend on siderophores produced by other microorganisms (Granger and Price, 1999). There is no proof that the siderophores are

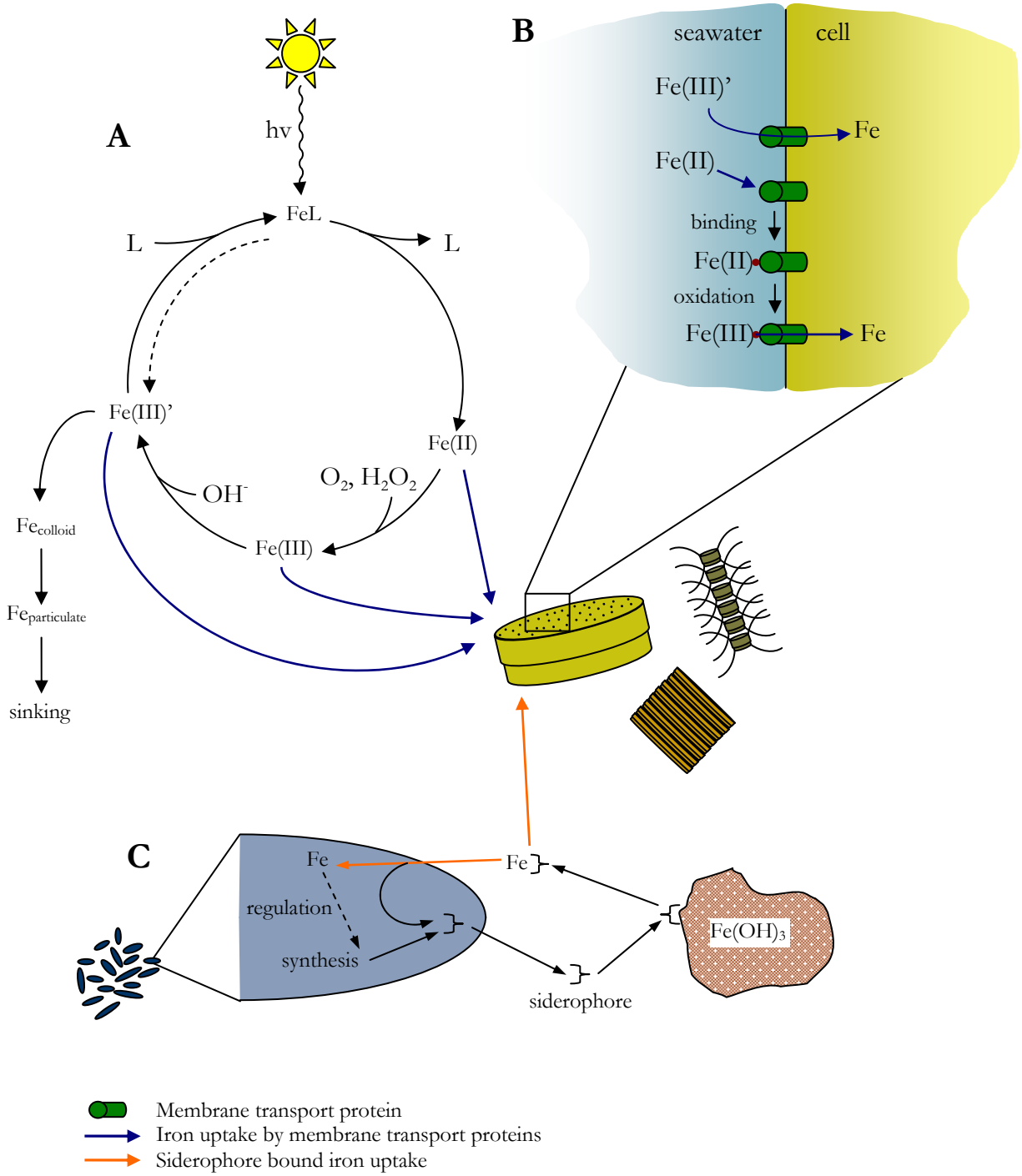

Figure 2: The redox cycling of iron in seawater (A). Iron uptake mechanisms of marine eukaryotes (B) and prokaryotes (C). Abbreviations are as follows: FeL = Ligand bound iron; L = ligand; Fe(III)' = sum of all inorganic Fe(III) species. Redrawn after (Sunda, 2001) and (Croot et al., 2005).

produced by eukaryotic marine phytoplankton, although they can utilize siderophore bound iron (Hutchins et al., 1999).

The main iron uptake mechanism for marine eukaryotic phytoplankton is by membrane transporters that directly access dissolved inorganic iron (Sunda, 2001) (Fig. 2 B). Here inorganic species of Fe(III) or Fe(II) react with a receptor on the outer cell membrane and then are transported inside the cell where they are released into the cell plasma. Fe(II) may be oxidized after it is bound to the transporter and finally shuttled into the cell as Fe(III) (Sunda, 2001). The limiting effect of this iron uptake mechanism is the concentration of bioavailable iron. However, this uptake mechanism is highly efficient as, normalized to cell surface area, iron uptake rates in eukaryotic phytoplankton are observed to be more than 30 times higher than those of bacteria (Maldonado and Price, 1999). Among eukaryotic phytoplankton however, iron uptake is highly dependent on the higher surface to volume ratio and thus small species are favored at low Fe concentrations.

Fe(III) is much less soluble compared to Fe(II) and forms much stronger complexes with organic ligands (Rue and Bruland, 1995). As aforementioned, most Fe(III)-ligand complexes are very stable and can not be taken up by phytoplankton and are thus not bioavailable. Sunlight can break down the strong Fe(III)-ligand complexes and reduce Fe(III) to Fe(II) (Barbeau et al., 2001). Fe(II) however, is rapidly re-oxidized to Fe(III) at seawater pH of about 8. The half life time ranges from a few minutes in warm waters to approximately half an hour in polar regions (Croot and Laan, 2002). This photochemical cycling though enhances the bioavailable Fe(II) and Fe(III) concentrations that can bind to the iron transport proteins on the cell surface (Fig. 2 A). Another mechanism of increasing the concentrations of bioavailable iron in seawater is described by Barbeau et al. (1996). They found that the presence of protozoan grazers increase the bioavailability of iron bound to strong complexes. They suggest that the large complexes are converted into smaller, more labile colloids and/or dissolved iron species due to the acidic conditions (pH 2-3) and the high enzymatic activity in the protozoan food vacuoles.

IMPORTANCE OF IRON FOR PHYTOPLANKTON CELLS

Photosynthesis and inorganic nitrogen assimilation are probably the two most important iron demanding processes for phytoplankton cells. Iron is an essential part of the iron-sulfur proteins and ferredoxin of the photosystems and the heme and iron-sulfur proteins of the cytchrom b_6f complex. Iron therefore plays an important role in the photosynthetic electron transfer and is essential for photosynthetic energy supply (Greene et al., 1991; Greene et al., 1992; Greene et al., 1994). Under iron limitation a visible decrease in chlorophyll concentration (chlorosis) as well as a decrease in the photosynthetic efficiency (Fv/Fm) is generally observed. Many marine and freshwater phytoplankton species as well as bacteria replace the iron-sulfur protein ferredoxin in the photosynthetic and/or respiratory electron transport chains by the non-iron-containing protein flavodoxin and thus reduce their cellular iron requirements efficiently when iron limits growth (Fillat et al., 1988; LaRoche et al., 1995; Vetter and Knappe, 1971; Zumpf and Spiller, 1971). The essential role of iron in photosynthesis is emphasized in combination with extremely low or high light intensities that require adaptation of the photosynthetic apparatus. Under low light intensities phytoplankton cells usually increase their cellular pigment content to enhance light harvesting efficiency. Such photoacclimation is hampered when pigment synthesis and energy supply are reduced due to iron limitation and thus a co-limitation of iron and light has been observed in laboratory experiments (Timmermans et al., 2001; van Leeuwe and Stefels, 1998). Additionally, iron is required to prevent the cell from photoinhibition under very high light intensities. Light energy supply that exceeds the light absorption capacity of the photosynthetic apparatus results in production of reactive superoxide radicals, which can cause severe damage to the photosynthetic apparatus. Xanthophylls and carotenoids are photoprotective pigments that can effectively prevent photoinhibition and photodamage under high light conditions. Geider et al. (1993) report that synthesis of these pigments is decreased under iron limitation.

The second important process iron is involved in is nitrate uptake. For the synthesis of amino acids nitrate has to be reduced to ammonium. This occurs in a two step reduction, where the energy is derived from Fe-dependent photosynthetic redox reactions. Both enzymes involved, nitrate and nitrite reductase, have a high iron content. Additionally

nitrite reductase uses reduced ferredoxin, an iron-sulfur redox protein, or the non-iron-containing flavodoxin to reduce nitrite to ammonium. Therefore, iron limitation leads to reduced nitrate uptake rates (Price et al., 1994) and lowers nitrate reductase activity (Timmermans et al., 1994). However, it is not known if the latter is due to a direct reduction in the enzyme activity or indirectly via a reduced supply of the reductant from photosynthesis. Besides nitrate, phytoplankton cells can directly take up ammonium and incorporate it into amino acids without the use of iron containing enzymes. Therefore the iron demand of phytoplankton cells is higher when growing on nitrate compared to ammonium as N source (Maldonado and Price, 1996; Raven, 1988). This implies that in low Fe waters like the SO ammonium uptake is preferred and new production is suppressed (Maldonado and Price, 1996) despite the surplus of nitrate. To fulfill the higher iron requirements for nitrate uptake, phytoplankton cells have higher iron uptake rates when growing on nitrate compared to ammonium (Wang and Dei, 2001). Additionally, the Fe assimilation efficiency in marine copepods is higher under nitrate replete conditions (Wang and Dei, 2001). The authors suggest that therefore in low iron, high nitrate regions the residence time of Fe in the surface water may increase.

Some phytoplankton species, the so-called diazotrophs, are able to utilize N_2 as a nitrogen source. Nitrogen fixation requires even higher cellular iron levels because additional Fe is needed for the Fe-Mo centers of the N_2 fixing enzyme nitrogenase. Initially the iron requirement of diazotrophs was calculated to be 100 times higher compared to phytoplankton species growing on nitrate (Raven, 1988). More recently, this was corrected to 3-5 times higher Fe requirements (Kustka et al., 2002; Sañudo-Wilhelmy et al., 2001). Therefore, diazotrophic growth is mainly restrained to oceanic regions with comparably high iron availability.

DIATOMS AND IRON LIMITATION

Diatoms are the phytoplankton group that contributes most to global carbon fixation and account for about 40 % of total marine primary production (Nelson et al., 1995; Tréguer et al., 1995). Additionally, in the Southern Ocean the siliceous frustules of diatoms account for almost all the silica sedimentation (Abelmann and Gersonde, 1991) and form

the circum-Antarctic silica belt. Nevertheless, diatoms are known to depend on high nutrient conditions (reviewed by Sarthou et al., 2005), which is likely caused by their relative large size resulting in a low surface to volume ratio. It is therefore not surprising that large diatom species benefit most from iron fertilization experiments in HNLC regions (de Baar et al., 2005). Because of their striking abundance in *in situ* iron fertilization experiments and their major contribution to carbon and chlorophyll concentrations, almost all research to date concentrated on large diatom species. However, there are also very small diatoms, belonging to the pico- and nanophytoplankton, whose reactions to enhanced iron availability and thus changing environmental conditions is far less understood.

As a response to low dissolved Fe concentrations, a variety of adaptation mechanisms of oceanic phytoplankton have evolved. In general small size can be considered as an adaptation to nutrient and thus also to iron limitation (Chisholm, 1992). As eukaryotic phytoplankton takes up iron by membrane transporters a larger surface to volume ratio can effectively increase relative iron uptake rates under limiting Fe conditions. Diatoms are known to reduce cell size under low iron conditions (reviewed by Sarthou et al., 2005). Further, in adaptation to low iron availability oceanic phytoplankton species have lower cellular iron requirements (Maldonado and Price, 1996; Muggli and Harrison, 1997; Muggli et al., 1996; Sunda and Huntsman, 1995; Sunda et al., 1991). The exact physiological mechanisms that enable the algae to reduce their cellular iron requirements are still unknown. However, possible adaptations include a more efficient exchange of iron within intracellular pools (Sunda and Huntsman, 1995), a minimization of iron rich metabolic pathways (Stefels and van Leeuwe, 1998), and/or a replacement of ferredoxin by the non-iron-containing protein flavodoxin (LaRoche et al., 1995). Another strategy to reduce cellular iron requirements has been recently described by Strzepek and Harrison (2004). They found that open ocean diatom species have developed a photosynthetic apparatus which contains less of the iron rich PS I and cytochrome b_6f components while being photosynthetically as effective as coastal species, possibly due to a higher effective absorption cross-section and turnover rate of PS I. Other planktonic species evolved exceptional ways to manage the low dissolved iron concentrations. The mixotrophic

flagellate *Ochromonas sp.*, for example, takes up iron in particulate form, by ingesting bacteria (Maranger et al., 1998).

Besides the general limiting effect of iron in the SO it is described that diatom growth is further affected by low silicate concentrations north of the Polar Frontal Zone (Brzezinski et al., 2005; Coale et al., 2004; Franck et al., 2000; Leblanc et al., 2005). Additionally, it has been generally accepted that light limitation due to extremely deep mixing limits primary production in the SO (Mitchell et al., 1991). In contrast to this assumption Takeda (1998) found higher growth rates of SO phytoplankton at 2,6 % of sea surface light intensity compared to 40 % using deck incubation experiments. However, laboratory experiments with SO diatom species under different light conditions are rare and often performed under light intensities that far exceed natural conditions. It thus remains questionable if SO phytoplankton suffers from regular light limitation or if they have evolved effective adaptation mechanisms resulting in an overestimation of this factor.

It is also described that the elemental composition of diatoms changes under different iron regimes (Price, 2005; Takeda, 1998; Timmermans et al., 2004). The C : N ratio is generally close to the Redfield ratio of 6.6 and shows only minor changes with iron availability (Arrigo et al., 1999; Coale et al., 2004; Price, 2005). However, large changes in the C : P and N : P ratios of diatoms are reported as an effect of changing iron concentrations. These changes are non-linear and differ remarkably between species. The mechanisms and reasons for this phenomenon are not well understood but lower nitrate uptake and the formation of internal P pools under iron limitation are thought to be the main reasons (Price, 2005). The Si : C, Si : N, and Si : P ratios of diatoms are known to be affected by a variety of factors such as temperature, light intensity, photoperiod, macronutrient, and iron limitation (reviewed by Ragueneau et al., 2000). It is generally assumed that higher silicification is caused by a reduction in growth rate and an increased duration of the cell in the G_2 + M phase of the cell cycle during which Si uptake occurs (Martin-Jézéquel et al., 2000). Nevertheless, it remains questionable if higher Si : C, Si : N, and Si : P ratios under iron limitation generally represent increased silicification in all diatom species. Changes in the C, N, and P composition could also affect the stoichiometry.

THIS THESIS

Aim of this thesis is to investigate reactions to changing iron availability and adaptation mechanisms to iron limitation of phytoplankton during the *in situ* iron fertilization experiment EIFEX and of Southern Ocean diatoms in laboratory experiments.

Chapter I deals with the question how different phytoplankton size classes react to iron fertilization in the field. Since former *in situ* iron fertilization experiments generally showed that large, chain forming diatoms are the main beneficiaries of iron fertilization, special attention was turned to diatom growth in the smaller size classes and to total phytoplankton community structure. Changes in species composition and implications for elemental ratios and carbon export modeling are discussed.

The impacts of iron, silicate, and light co-limitation of the two Antarctic diatom species *Actinocyclus sp.* and *Chaetoceros dichaeta* and the cosmopolitan species *C. debilis* are investigated in Chapter II. Key question of this study is if low light intensities limit growth of SO diatoms depending on iron and silicate availability and what the implications for diatom community structure are in the field. The results are discussed concerning their importance for growth and grazing protection of these species under similar light and nutrient regimes in the field.

The hypothesis that iron limitation increases cellular silicification and affects elemental stoichiometry of SO diatoms was investigated in Chapter III, using the important SO diatom species *Fragilariopsis kerguelensis* and *C. dichaeta* in laboratory experiments. The results are discussed in terms of the possible effects of iron fertilization on export of biogenic material in the field. Data of the size fractionated elemental Si : C, Si : N, and Si : P ratios during EIFEX are assessed and discussed concerning the changes in community structure observed in Chapter I and the laboratory results.

In Chapter IV it was examined if volcanic ash deposition into seawater has a potential fertilizing effect on phytoplankton growth, especially in HNLC regions. Geochemical data of the rapid trace metal and nutrient release from volcanic ash as well as the effect of ash on growth and photosynthetic efficiency of *C. dichaeta* in laboratory experiments are presented.

REFERENCES

Abelmann, A., and R. Gersonde, 1991. Biosiliceous particle flux in the Southern Ocean. Marine Chemistry, 35, 503-536.

Arrigo, K. R., D. H. Robinson, D. L. Worthen, et al., 1999. Phytoplankton community structure and the drawdown of nutrients and CO_2 in the Southern Ocean. Science, 283, 365-367.

Barbeau, K., J. W. Moffett, D. A. Caron, et al., 1996. Role of protozoan grazing in relieving iron limitation of phytoplankton. Nature, 380, 61-64.

Barbeau, K., E. L. Rue, K. W. Bruland, et al., 2001. Photochemical cycling of iron in the surface ocean mediated by microbial iron(III)-binding ligands. Nature, 413, 409-413.

Brzezinski, M. A., J. L. Jones, and M. S. Demarest, 2005. Control of silica production by iron and silicic acid during the Southern Ocean Iron Experiment (SOFeX). Limnology and Oceanography, 50(3), 810-824.

Chisholm, S. W., 1992, Phytoplankton size, in *Primary productivity and biogeochemical cycles in the sea*, edited by A.D. Woodhead, Plenum Press, New York.

Coale, K. H., K. S. Johnson, F. P. Chavez, et al., 2004. Southern Ocean iron enrichment experiment: carbon cycling in high- and low- Si waters. Science, 304, 408-414.

Croot, P. L., and P. Laan, 2002. Continuous shipboard determination of Fe(II) in polar waters using flow injection analysis with chemiluminescence detection. Analytica Chimica Acta, 466, 261-273.

Croot, P. L., P. Laan, J. Nishioka, et al., 2005. Spatial and temporal distribution of Fe(II) and H_2O_2 during EisenEx, an open ocean mesoscale iron enrichment. Marine Chemistry, 95, 65-88.

de Baar, H. J. W., P. W. Boyd, K. H. Coale, et al., 2005. Synthesis of iron fertilisation experiments: From the iron age in the age of enlightenment. Journal of Geophysical Research, 110, C09S16, doi:10.1029/2004JC002601.

de Baar, H. J. W., and J. T. M. de Jong, 2001, Distribution, sources and sinks of iron in seawater, in *The biogeochemistry of iron in seawater*, edited by K.A. Hunter, pp. 125-253, John Wiley and Sons, Chichester.

Elderfield, H., and A. Schultz, 1996. Mid-ocean ridge hydrothermal fluxes and the chemical composition of the ocean. Annual Review of Earth and Planetary Sciences, 24, 191-224.

Fillat, M. F., G. Sandmann, and C. Gomez-Moreno, 1988. Flavodoxin from the nitrogen-fixing cyanobacterium Anabaena PCC 7119. Archives of Microbiology, 150, 160-164.

Franck, V. M., M. A. Brzezinski, K. H. Coale, et al., 2000. Iron and silicic acid concentrations regulate Si uptake north and south of the Polar Frontal Zone in the Pacific Sector of the Southern Ocean. Deep-Sea Research II, 47, 3315-3338.

Geider, R. J., J. La Roche, R. M. Greene, et al., 1993. Response of the photosynthetic apparatus of *Phaeodactylum tricornutum* (Bacillariophyceae) to nitrate, phosphate, or iron starvation. Journal of Phycology, 29(6), 755-766.

Granger, J., and N. M. Price, 1999. The importance of siderophores in iron nutrition of heterotrophic marine bacteria. Limnology and Oceanography, 44(3), 541-555.

Greene, R. M., R. J. Geider, and P. G. Falkowski, 1991. Effect of iron limitation on photosynthesis in a marine diatom. Limnology and Oceanography, 36(8), 1772-1782.

Greene, R. M., R. J. Geider, Z. Kolber, et al., 1992. Iron-induced changes in light harvesting and photochemical energy-conversion processes in eukaryotic marine-algae. Plant Physiology, 100(2), 565-575.

Greene, R. M., Z. S. Kolber, D. G. Swift, et al., 1994. Physiological limitation of phytoplankton photosynthesis in the eastern equatorial Pacific determined from variability in the quantum yield of fluorescence. Limnology and Oceanography, 39(5), 1061-1074.

Hudson, R. J. M., and F. M. M. Morel, 1990. Iron transport in marine phytoplankton: Kinetics of cellular and medium coordination reactions. Limnology and Oceanography, 35(5), 1002-1020.

Hutchins, D. A., A. E. Witter, A. Butler, et al., 1999. Competition among marine phytoplankton for different chelated iron species. Nature, 400, 858-861.

Jickells, T. D., Z. S. An, K. K. Andersen, et al., 2005. Global iron connections between desert dust, ocean biogeochemistry, and climate. Science, 308(5718), 67-71.

Jickells, T. D., and L. J. Spokes, 2001, Atmospheric iron inputs to the oceans, in *The biogeochemistry of iron in seawater*, edited by K.A. Hunter, pp. 85-121, Whiley and Sons, Chichester.

Johnson, K., 2001. Iron supply and demand in the upper ocean: Is extraterrestial dust a significant source of bioavailable iron? Global Biogeochemical Cycles, 15(1), 61-63.

Keeling, R. F., S. C. Piper, and M. Heimann, 1996. Global and hemispheric CO2 sinks deduced from changes in atmospheric O2 concentration. Nature, 381, 218-221.

Kunz-Pirrung, M., R. Gersonde, and D. A. Hodell, 2002. Mid-Brunhes century diatom sea surface temperature and sea ice records from the Atlantic sector of the Southern Ocean (OCD Leg 177, sites 1093, 1094 and core PS2089-2). Palaeogeography Palaeoclimatology Palaeoecology, 182, 305-328.

Kustka, A., E. J. Carpenter, and S. A. Sanudo-Wilhelmy, 2002. Iron and marine nitrogen fixation: progress and future directions. Research in Microbiology, 153(5), 255-262.

LaRoche, J., H. Murray, M. Orellana, et al., 1995. Flavodoxin expression as an indicator of iron limitation in marine diatoms. Journal of Phycology, 31, 520-530.

Leblanc, K., C. E. Hare, P. W. Boyd, et al., 2005. Fe and Zn effects on the Si cycle and diatom community structure in two high and low-silicate HNLC areas. Deep-Sea Research I, 52, 1842-1864.

Maldonado, M., and N. M. Price, 1999. Utilization of iron bound to strong organic ligands by plankton communities in the subarctic Pacific Ocean. Deep-Sea Research II, 46, 2447-2473.

Maldonado, M. T., and N. M. Price, 1996. Influence of N substrate on Fe requirements of marine centric diatoms. Marine Ecology Progress Series, 141, 161-172.

Maranger, R., D. F. Bird, and N. M. Price, 1998. Iron acquisition by photosynthetic marine phytoplankton from ingested bacteria. Nature, 396(6708), 248-251.

Martin, J. H., and S. E. Fitzwater, 1988. Iron deficiency limits phytoplankton growth in the north-east Pacific subarctic. Nature, 331, 341-343.

Martin, J. H., R. M. Gordon, and S. E. Fitzwater, 1990. Iron in Antarctic waters. Nature, 345, 156-158.

Martin-Jézéquel, V., M. Hildebrand, and M. A. Brzezinski, 2000. Silicon metabolism in diatoms: implications for growth. Journal of Phycology, 36, 821-840.

Mitchell, B. G., E. A. Brody, O. Holmhansen, et al., 1991. Light limitation of phytoplankton biomass and macronutrient utilization in the Southern-Ocean. Limnology and Oceanography, 36(8), 1662-1677.

Morel, F. M. M., R. J. M. Hudson, and N. M. Price, 1991. Limitation of productivity by trace metals in the sea. Limnology and Oceanography, 36(8), 1742-1755.

Muggli, D. L., and P. J. Harrison, 1997. Effects of iron on two oceanic phytoplankters grown in natural NE subarctic seawater with no artificial chelators present. Journal of Experimental Marine Biology and Ecology, 212, 225-237.

Muggli, D. L., M. Lecourt, and P. J. Harrison, 1996. Effects of iron and nitrogen source on the sinking rate, physiology and metal composition of an oceanic diatom from the subarctic Pacific. Marine Ecology Progress Series, 132, 215-227.

Nelson, D. M., P. Tréguer, M. A. Brzezinski, et al., 1995. Production and dissolution of biogenic silica in the ocean: Revised global estimates, comparison with regional data and relationship to biogenic sedimentation. Global Biogeochemical Cycles, 9(3), 359-372.

Poulton, S. W., and R. Raiswell, 2002. The low-temperature geochemical cycle of iron: From continental fluxes to marine sediment deposition. American Journal of Science, 302, 774-805.

Price, N. M., 2005. The elemental stoichiometry and composition of an iron-limited diatom. Limnology and Oceanography, 50(4), 1159-1171.

Price, N. M., B. A. Ahner, and F. M. M. Morel, 1994. The equatorial Pacific Ocean: Grazer controlled phytoplankton populations in an iron-limited ecosystem. Limnology and Oceanography, 39(3), 520-534.

Ragueneau, O., P. Tréguer, A. Leynaert, et al., 2000. A review of the Si cycle in the modern ocean: recent progress and missing gaps in the application of biogenic opal as a paleoproductivity proxy. Global and Planetary Change, 26, 317-365.

Raven, J. A., 1988. The iron and molybdenum use efficiencies of plant growth with different energy, carbon and nitrogen sources. New Phytologist, 109, 279-287.

Rich, H. W., and F. M. M. Morel, 1990. Availability of well-defined iron colloids in the marine diatom *Thalassiosira weissflogii*. Limnology and Oceanography, 35(3), 652-662.

Rue, E. L., and K. W. Bruland, 1995. Complexation of iron(III) by natural organic ligands in the Central North Pacific as determined by a new competitive ligand equilibration/adsorptive cathodic stripping voltammetric method. Marine Chemistry, 50, 117-138.

Sañudo-Wilhelmy, S. A., A. B. Kustka, C. J. Gobler, et al., 2001. Phosphorus limitation of nitrogen fixation by *Trichodesmium* in the central Atlantic Ocean. Nature, 411(2001), 66-69.

Sarmiento, J. L., 1993. Atmospheric CO2 stalled. Nature, 365, 697-698.

Sarthou, G., K. R. Timmermans, S. Blain, et al., 2005. Growth physiology and fate of diatoms in the ocean: a review. Journal of Sea Research, 53(1-2), 25-42.

Sedwick, P. N., and G. R. DiTullio, 1997. Regulation of algal blooms in Antarctic shelf waters by the release of iron from melting sea ice. Geophysical Research Letters, 24(20), 2515-2518.

Stefels, J., and M. A. van Leeuwe, 1998. Effects of iron and light stress on the biochemical composition of Antarctic *Phaeocystis* sp. (Prymnesiophyceae). I. Intracellular DMP concentrations. Journal of Phycology, 34, 486-495.

Strzepek, R. F., and P. J. Harrison, 2004. Photosynthetic architecture differs in coastal and oceanic diatoms. Nature, 431, 689-692.

Sunda, W. G., 2001, Bioavailability and bioaccumulation of iron in the sea, in *The biogeochemistry of iron in seawater*, edited by K.A. Hunter, pp. 41-84, John Wiley and Sons, Chichester.

Sunda, W. G., and S. A. Huntsman, 1995. Iron uptake and growth limitation in oceanic and coastal phytoplankton. Marine Chemistry, 50, 189-206.

Sunda, W. G., D. G. Swift, and S. A. Huntsman, 1991. Low iron requirement for growth in oceanic phytoplankton. Nature, 351, 55-57.

Takeda, S., 1998. Influence of iron availability on nutrient consumption ratio of diatoms in oceanic waters. Nature, 393, 774-777.

Timmermans, K. R., M. S. Davey, B. van der Wagt, et al., 2001. Co-limitation by iron and light of *Chaetoceros brevis*, *C. dichaeta* and *C. calcitrans* (Bacillariophyceae). Marine Ecology Progress Series, 217, 287-297.

Timmermans, K. R., W. Stolte, and H. J. W. de Baar, 1994. Iron-mediated effects on nitrate reductase in marine phytoplankton. Marine Biology, 121, 389-396.

Timmermans, K. R., B. van der Wagt, and H. J. W. de Baar, 2004. Growth rates, half saturation constants, and silicate, nitrate, and phosphate depletion in relation to iron availability of four large open-ocean diatoms from the Southern Ocean. Limnology and Oceanography, 49(6), 2141-2151.

Tréguer, P., D. M. Nelson, A. J. Van Bennekom, et al., 1995. The silica balance in the World Ocean: A reestimate. Science, 268, 375-379.

Turner, D. R., K. A. Hunter, and H. J. W. de Baar, 2001, Introduction, in *The biogeochemistry of iron in seawater*, edited by K.A. Hunter, pp. 1-7, John Wiley and Sons, Chichester.

Ussher, S. J., E. P. Achterberg, and P. J. Worsfold, 2004. Marine biogeochemistry of iron. Environmental Chemistry, 1, 67-80.

van Leeuwe, M. A., and J. Stefels, 1998. Effects of iron and light stress on the biogeochemical composition of Antarctic *Phaeocystis sp.* (Prymnesiophyceae). II. Pigment composition. Journal of Phycology, 34, 496-503.

Vetter, H., and J. Knappe, 1971. Flavodoxin and ferredoxin of *Escherichia coli*. Zeitschrift für physiologische Chemie, 352, 433-446.

Wang, W.-X., and R. C. H. Dei, 2001. Biological uptake and assimilation of iron by marine plankton: influences of macronutrients. Marine Chemistry, 74, 213-226.

Watson, A. J., 1997. Volcanic Fe, CO_2, ocean productivity and climate. Nature, 385, 587-588.

Watson, A. J., 2001, Iron limitation in the oceans, in *The biogeochemistry of iron in seawater*, edited by K.A. Hunter, pp. 9-33, John Wiley & Sons Ltd., Chicester.

Wells, M. L., N. M. Price, and K. W. Bruland, 1995. Iron chemistry and its relationship to phytoplankton: a workshop report. Marine Chemistry, 48, 157-182.

Zumpf, W. G., and H. Spiller, 1971. Characterization of a flavodoxin from the green alga *Chlorella*. Biochemical and Biophysical Research Communications, 45(1), 112-118.

CHAPTER I

Different reactions of Southern Ocean phytoplankton size classes to iron fertilization

Linn Hoffmann, Ilka Peeken, Karin Lochte, Philipp Assmy, Marcel Veldhuis

Limnology and Oceanography 51(3) 1217-1229

LIMNOLOGY
AND
OCEANOGRAPHY

May 2006
Volume 51
Number 3

Limnol. Oceanogr., 51(3), 2006, 1217–1229

Different reactions of Southern Ocean phytoplankton size classes to iron fertilization

Linn J. Hoffmann,[1] *Ilka Peeken, and Karin Lochte*
Leibniz Institute of Marine Science at the University of Kiel, Duesternbrooker Weg 20, 24105 Kiel, Germany

Philipp Assmy
Alfred Wegener Institute for Polar and Marine Research, Am Handelshafen 12, 27570 Bremerhaven, Germany

Marcel Veldhuis
Royal Netherlands Institute for Sea Research, P.O. Box 59, 1790 AB Den Burg, Texel, The Netherlands

Abstract

During the European Iron Fertilisation Experiment (EIFEX), performed in the Southern Ocean, we investigated the reactions of different phytoplankton size classes to iron fertilization, applying measurements of size fractionated pigments, particulate organic matter, microscopy, and flow cytometry. Chlorophyll *a* (Chl *a*) concentrations at 20-m depth increased more than fivefold following fertilization through day 26, while concentrations of particulate organic carbon (POC), nitrogen (PON), and phosphorus (POP) roughly doubled through day 29. Concentrations of Chl *a* and particulate organic matter decreased toward the end of the experiment, indicating the demise of the iron-induced phytoplankton bloom. Despite a decrease in total diatom biomass at the end of the experiment, biogenic particulate silicate (bPSi) concentrations increased steadily due to a relative increase of heavily silicified diatoms. Although diatoms >20 μm were the main beneficiaries of iron fertilization, the growth of small diatoms (2–8 μm) was also enhanced, leading to a shift from a haptophyte- to a diatom-dominated community in this size fraction. The total biomass had lower than Redfield C : N, N : P, and C : P ratios but did not show significant trends after iron fertilization. This concealed various alterations in the elemental composition of the different size fractions. The microplankton (>20 μm) showed decreasing C : N and increasing N : P and C : P ratios, possibly caused by increased N uptake and the consumption of cellular P pools. The nanoplankton (2–20 μm) showed almost constant C : N and decreasing N : P and C : P ratios. Our results suggest that the latter is caused by a shift in composition of taxonomic groups.

The Southern Ocean is one of the three High Nutrient Low Chlorophyll (HNLC) regions of the world's oceans, where macronutrients abound but phytoplankton growth is limited by the availability of iron (Martin et al. 1990).

In situ iron fertilization experiments have been performed in all HNLC regions and all of them have in common that they induced strong phytoplankton blooms (*see* review in de Baar et al. 2005). The massive increase in chlorophyll *a* (Chl *a*) concentrations was mainly due to large or chain-forming diatoms, which benefit most from iron fertilization. Because iron uptake is dependent on cell surface area, smaller cells are favored under low iron concentrations due to their higher surface-to-volume ratios (Hudson and Morel 1990; Sunda and Huntsman 1997). The natural phytoplankton community of the iron-depleted Southern Ocean is therefore dominated by pico- and nanophytoplankton (Gervais et al. 2002). The small diatom *Chaetoceros brevis* did not change its growth rates under different iron concentrations in laboratory experiments, leading to the assumption that this species is not iron limited under natural conditions (Timmermans et al. 2001).

[1] Corresponding author (lhoffmann@ifm-geomar.de).

Acknowledgments

We thank Captain U. Pahl and the crew of RV *Polarstern* for their support. Without the help of V. Smetacek (chief scientist), H. Leach, V. Strass, H. Prandke, B. Cisewski (CTD sampling), and the other cruise participants, our work would have been impossible. Special thanks to K. Nachtigall, C. Krieger, S. Krug, and A. Kähler for their help with HPLC measurements. We also thank K. Nachtigall and P. Fritsche for POC/PON, POP, and bPSi measurements. The manuscript was greatly improved by the comments of two anonymous reviewers. This research was funded by the German Research Foundation (DFG) grant PE_565_5 awarded to Ilka Peeken.

Once iron becomes available, larger cells can increase their abundance due to increased growth rates (Timmermans et al. 2001, 2004) and better grazing protection. Mesozooplankton, which could feed effectively on these large diatoms, have relatively long generation times and therefore cannot control this fast-growing biomass. Microzooplankton, on the other hand, which have much shorter generation times, are too small to effectively consume large diatoms (Coale et al. 1996). There is evidence from the equatorial Pacific that growth rates of smaller phytoplankton groups were also stimulated, but could not build up high biomasses because of a concurrent increase in grazing pressure (Coale et al. 1996; Cavender-Bares et al. 1999). The overall effect of these changes leads to a shift in phytoplankton composition from an assemblage dominated by pico- and nanophytoplankton toward a nano- and microphytoplankton-dominated one (Gall et al. 2001*a*; Gervais et al. 2002).

Iron plays a major role in photosynthetic metabolism. Under low iron concentrations, the cellular chlorophyll concentrations and the efficiency of photosynthetic electron transfer (Fv/Fm) are known to be lower compared with high-iron conditions (Geider and LaRoche 1994). Besides enhanced growth rates, the natural phytoplankton community shows an increase in Fv/Fm (Boyd et al. 2000; Gervais et al. 2002; Coale et al. 2004) and higher cellular chlorophyll concentrations with iron fertilization in the Southern Ocean (Veldhuis and Timmermans unpubl. data). The increase in cellular chlorophyll concentrations is higher in larger cells, again indicating that these cells are more iron limited than smaller ones (Veldhuis and Timmermans unpubl. data).

Regions of the Southern Ocean where diatoms dominate the phytoplankton community have lower than Redfield C : P and N : P ratios, while those dominated by *Phaeocystis* exceed the Redfield ratio (Arrigo et al. 1999, 2002). Laboratory experiments have shown that the elemental composition of phytoplankton can differ significantly from the Redfield ratio and that diatoms in general have lower C : P and N : P ratios than other taxonomical phytoplankton groups (Ho et al. 2004; Klausmeier et al. 2004). The change in the elemental composition of the whole phytoplankton community may therefore be due to changing species composition. It is also known that the elemental composition of phytoplankton is variable, depending on the availability of macronutrients (Geider and La Roche 2002) and trace metals, such as iron (de Baar et al. 1997; Timmermans et al. 2004; Twining et al. 2004).

Changes in the elemental composition of phytoplankton during in situ iron fertilization experiments are of particular interest because the aim of these experiments is to increase biological production and carbon export. Carbon uptake and export is estimated by using the Redfield ratio so that even small deviations from this ratio will have significant effects on these calculations. Recent biogeochemical models differentiate between phytoplankton groups such as diatoms, pico/nanophytoplankton, and coccolithophores (Pasquer et al. 2005), and they require reliable information about possible changes in the group composition and associated variations in the elemental ratios due to iron fertilization.

It is still unknown whether the observed changes in community structure and elemental composition would be sustained during long-term fertilization and would have lasting effects on the ecosystem structure. Most field research is concentrated on the microphytoplankton because of its dominant increase in biomass after iron fertilization, while the response of smaller phytoplankton size classes is not well understood. The aim of this study was to identify the growth response of all phytoplankton size classes, as well as changes in the elemental ratios and species composition during the iron fertilization experiment EIFEX in the Southern Ocean.

Material and methods

The European Iron Fertilisation Experiment (EIFEX) was an in situ iron fertilization experiment carried out during the Southern Hemisphere autumn (21 Jan 04–25 Mar 04). To perform the experiment in a relatively stable water mass, an eddy, localized around 50°S and 2°E, was chosen. The eddy center was fertilized twice with an acidified iron sulfate solution. The first fertilization was carried out on day one after the initial sampling to determine the prefertilization conditions. All stations were located inside the eddy. Stations within the fertilized patch will be called in-stations, while the so-called out-stations were located inside the eddy but outside the iron-fertilized waters. Iron concentrations were approximately 0.08–0.2 nmol L^{-1} in the mixed layer before fertilization and reached about 2 nmol L^{-1} after the first fertilization. At day 15, the same water mass, as identified by high Fv/Fm, was fertilized again because iron concentrations had now decreased to only 2–3 times background. After the second infusion, iron concentrations remained significantly higher throughout the experimental patch compared with prefertilization conditions (Croot pers. comm.).

The indicator for photosynthetic efficiency Fv/Fm is known to increase with iron fertilization. To distinguish fertilized from unfertilized waters, the photosynthetic efficiency of phytoplankton was measured by Fast-Repetition-Rate-Fluororescence (FastTracka; Röttgers et al. 2005). Additionally, higher in vivo fluorescence of Chl *a* compared with the surrounding waters was measured by a fluorescence laser system (LIDAR) from a helicopter (Cembella et al. 2005).

Samples for size fractionated POC, PON, POP, bPSi, and measurements for algae pigment analysis by high-performance liquid chromatography (HPLC) were taken at in-stations and out-stations from 20-m depth using a CTD rosette sampler. All determinations are single measurements. Fractionated filtration was carried out to determine particulate organic matter (POM; which includes POC, PON, and POP) and pigment concentrations in different size classes. For POC and PON measurements, precombusted GF/F (Whatman) filters were used; bPSi determination was done on cellulose acetate (CA) filters (Millipore). For determination of the total amount, samples were directly filtered on the GF/F filters (25 mm in diameter) or

Table 1. Solvent gradient used for HPLC measurements. Solvent A: 30% 1 mol L^{-1} ammonium acetate, 70% methanol. Solvent B: 100% methanol.

Time (min)	Solvent A in %	Solvent B in %
0	65	35
1	50	50
12	15	85
15	0	100
20	0	100
25	65	35

CA filters of 0.8-μm pore size (25 mm in diameter) for bPSi, respectively. For size fractionation, samples were prefiltered through polycarbonate (PC) filters of the pore sizes 0.8 μm-, 2 μm-, 8 μm-, or a 20-μm gauze, each 47 mm in diameter. The larger surface area was chosen to avoid clogging of filters/gauze to prevent smaller cells from being retained. After filtration, the filters/gauze were rinsed and the filtrate was then filtered through GF/F or CA filters (each 25 mm in diameter) to collect the <0.8 μm, <2 μm, <8 μm, and <20 μm size fractions. The material on the 20-μm gauze was rinsed and collected on GF/F or CA filters for the >20-μm fraction. The fractions total, >20 μm, <20 μm, <8 μm, <2 μm, and <0.8 μm, were measured directly, the fractions 0.8–2 μm, 2–8 μm, 2–20 μm, and 8–20 μm were calculated by subtraction.

The volume of water filtered was between 1 and 6 L, depending on the amount of biomass in the water. POM filters were put in open Eppendorf tubes and immediately dried for at least 48 h in a drying oven. Afterward, the Eppendorf tubes were closed and stored with desiccant in closed plastic boxes. Immediately after filtration, the HPLC filters were stored in 1.5-mL cryo vials at -80°C until analysis.

POC/PON filters were exposed over night to 32% HCl to remove the inorganic carbon. The carbon and nitrogen content of the particulate, organic material was analyzed using a C/N Analyser (Euro EA Elemental Analyser) after Ehrhard and Koeve (1999). The POP content was determined colorimetrically using the method from Hansen and Koroleff (1999). BPSi was transformed to dissolved silicate by heating the filters in 0.1 mol L^{-1} NaOH solution to 85°C for 2 h. The dissolved silicate was then determined colorimetrically (Hansen and Koroleff 1999).

The HPLC samples were measured using a Waters 600 controller combined with a photodiode array detector (PDA; Waters 996) and an auto sampler (Waters 717plus). The method used was modified after Barlow et al. (1997) (Table 1). As an internal standard, 100 μL canthaxanthin were added to each sample. Identification and quantification of the different pigments were carried out using the program EMPOWER by Waters.

The whole phytoplankton community composition was classified into taxonomical groups applying the CHEMTAX program (Mackey et al. 1996). All Chl *a* concentrations of specific phytoplankton groups reported in this article are estimates based on the concentrations of their marker pigments according to this program. The input matrix was taken from Wright et al. (1996). This input matrix has been shown to provide reliable results, which correspond very well to cell counts in a former in situ iron fertilization experiment in the Southern Ocean (Peeken et al. unpubl. data). Nevertheless, we did not feel comfortable using these ratios for fractionated samples because it is likely that extremely different input ratios need to be considered for the various fractions. Therefore, fractionated samples are only presented as relative and absolute amounts of marker pigments.

At each station, 4-mL water samples for flow cytometric analysis of the phytoplankton composition were preserved with a drop of hexamine-buffered formaline solution on board and stored at -80°C until measurement. We tested this method in the past and found that the loss of cells for most groups was minor, ranging between 5% and 10%. This error is in the same range as for frozen samples reported by Vaulot et al. (1989). Flow cytometer samples were analyzed with a bench-top flow cytometer (Beckman Coulter XL-MCL) as described by Veldhuis and coworkers (Veldhuis and Kraay 2000). Samples were thawed immediately before analysis and up to 1.5-mL sample volume had to be analyzed because of the low phytoplankton density. Cell size, biovolume, and cell carbon were determined using size fractionated samples (Veldhuis and Timmermans unpubl. data). Chl *a* concentration per cell was determined from chlorophyll fluorescence derived by flow cytometry calibrated against direct chlorophyll measurements by HPLC. The carbon content of different groups was estimated using cell size. In order to avoid confusion of the carbon content of the autotrophic biomass with the directly measured carbon content of the entire plankton community, we will use a different notation. The carbon to Chl *a* ratio estimated by flow cytometry will be called C : Chl, while POC : Chl will be used for the ratio of directly measured particulate organic carbon to Chl *a* concentrations determined by HPLC.

For quantitative assessment of the phytoplankton assemblage, 200-mL water samples were preserved with hexamine-buffered formaline solution at a final concentration of 2% and stored at 4°C in the dark for microscopic analysis in the home laboratory. Due to the use of buffered formaline solution, the pH of the preserved samples was kept at in situ levels (pH 8). Cell counts were performed using inverted light and epifluorescence microscopy (Axiovert 25, Axiovert 135, and IM 35; Zeiss) according to the method of Utermöhl (1958). For phytoplankton cells >10 μm, water samples were settled in 50-mL sedimentation chambers (Hydrobios) for 48 h. For specifically counting diatoms <10 μm, solitary *Phaeocystis antarctica*, and *Emiliania huxleyi*, phytoplankton samples were settled in 10-mL sedimentation chambers for 72 h to assure that all cells had settled. Organisms were counted at magnifications of $\times$200–640 according to the size of the organisms examined. Each sample was examined until at least 500 cells had been counted. In order to acquire information on species-specific mortality, recognizable empty and broken diatom frustules were counted. Broken and empty diatom frustules were identified to species or genus level and

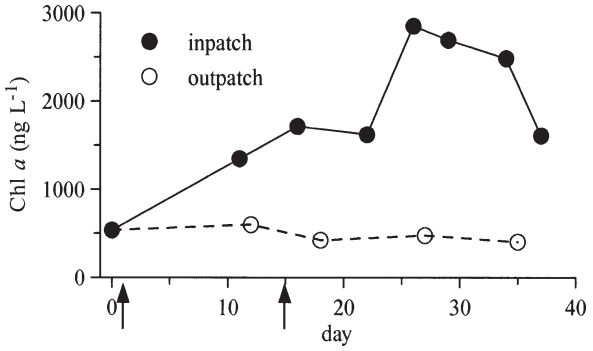

Fig. 1. Total Chl *a* concentration inside and outside the fertilized patch at 20-m depth. Arrows indicate days of iron fertilization.

otherwise grouped into size classes. Only broken diatom frustules of which >50% of the frustule was intact were counted. We cannot totally exclude dissolution of intact, empty, and broken frustules prior to examination of the samples by the storage, but the presence of empty and broken frustules of very delicate species, such as *Cylindrotheca closterium*, *Leptocylindrus mediteraneus*, and small *Chaetoceros* species, indicated that dissolution was of minor importance. Furthermore, some samples were counted again 9 months later and showed no significant differences in full, empty, as well as broken diatom cells between the two counts.

To investigate changes in the diatom community composition and its impact on bPSi accumulation, we compared heavily silicified species to the total diatom assemblage. The diatom species *Thalassiothrix antarctica, Fragilariopsis kerguelensis, F. obliquecostatalritscheri, Thalassiosira lentiginosa, Thalassionema nitzschioides*, and *Thalassiosira gracilis* are known to occur in Antarctic sediments (Zielinski and Gersonde 1997). The accumulation of frustules of these species in the sediment is taken as an indication of their strong silification, as compared with the majority of species that dissolve before reaching the sea floor. In the following, these species will be grouped as heavily silicified diatoms.

Results

Total plankton community response to iron fertilization—The total Chl *a* and POM concentrations showed a strong increase inside the fertilized patch, indicating a general biomass increase. The values were constantly higher than at the out-stations (Figs. 1 and 2). Chl *a* concentration increased more than fivefold through day 26, from 536 to 2853 ng L^{-1}, inside the patch and decreased thereafter. POC, PON, and POP concentrations roughly doubled during the first 30 days at the in-stations, while the concentrations at the out-stations did not increase and were constantly lower. Noticeable is a distinct dip at day 22 and a decline after day 30 inside the iron-fertilized patch; only bPSi showed a steady increase throughout the sampling period, reaching more than three times the initial concentrations (Fig. 2). At the out-stations, the bPSi concentrations were constantly lower but more variable compared with the POC, PON, and POP values. The POC : Chl *a* ratio of the total biomass decreased strongly inside the patch, from 180.8 to 55.5, at day 26 and increased thereafter to 86.9 (Fig 3).

While the Chl *a* concentrations at the out-stations gave the impression of a homogenous water mass surrounding the fertilized patch with approximately prefertilization conditions (Fig. 1), other data, like the bPSi concentrations (Fig. 2), the POC : Chl *a* ratio (Fig. 3), and pigments (Fig. 4B), showed larger variability. This might be partly explained by the occurrence of slightly different water masses, which lead to changes in temperature and salinity (Walter et al. 2005). Compared with the large changes following fertilization, the variability at the out-stations is relatively small. However, especially for the calculation of

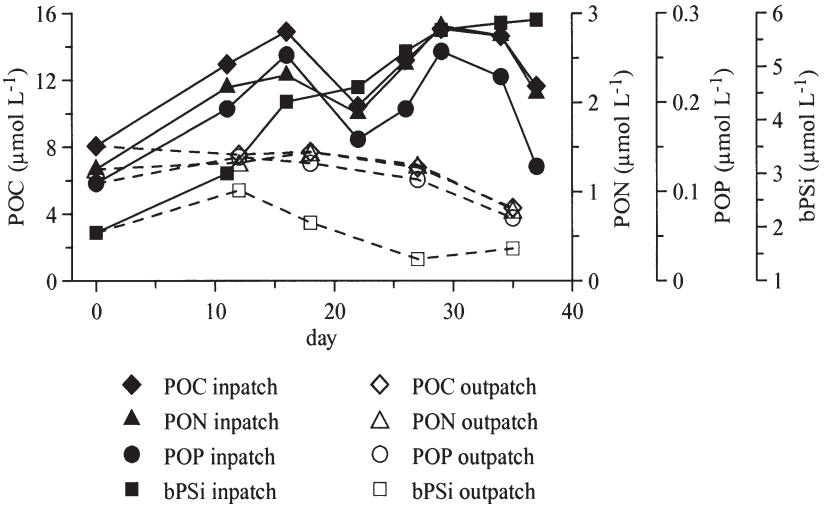

Fig. 2. Particulate organic carbon (POC), nitrogen (PON), phosphorus (POP), and biogenic silicate (bPSi) inside and outside the fertilized patch at 20-m depth.

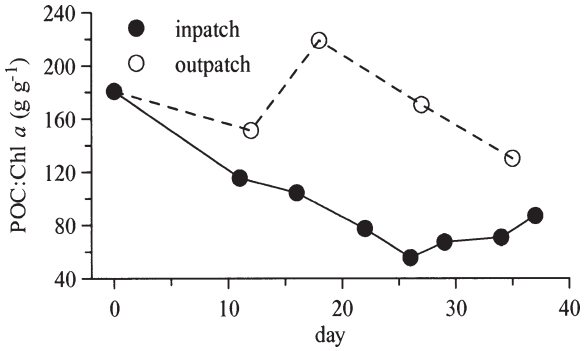

Fig. 3. Ratio of particulate organic carbon to Chl *a* inside and outside the fertilized patch at 20-m depth.

relative values and ratios, such as the percentage of total carbon and the elemental ratios, these minor deviations resulted in huge differences. We therefore omitted two stations that were clearly outliers and present the elemental ratios of three remaining out-stations as means and standard deviation in Fig. 6.

The CHEMTAX program (Mackey et al. 1996) provides estimates of the contribution of taxonomic phytoplankton groups to the total Chl *a* concentration based on their specific pigment composition. Using this method, we were able to distinguish between the seven phytoplankton groups chlorophytes, cyanobacteria, diatoms, dinoflagellates, pelagophytes, and two haptophyte types (*Phaeocystis* and *Emiliania huxleyi* type). According to these estimates, diatoms tended to dominate the phytoplankton community before and during the experiment and showed the greatest response to iron fertilization (Fig. 4A). They doubled their contribution to total Chl *a* from day 1 to day 26 (data not shown). The absolute diatom Chl *a* concentration increased five times in that time, while total diatom cell numbers increased almost three times (Fig. 4A). Based on the CHEMTAX results, the haptophyte type *Phaeocystis* was the second most abundant alga and increased its absolute Chl *a* concentration more than three times until day 29. Its relative abundance was about 20% of total Chl *a* and increased only marginally. Chlorophytes, cyanobacteria, dinoflagellates, and pelagophytes decreased in relative abundance because of the massive increase of diatom Chl *a* but did not change much in absolute Chl *a* concentrations and remained lower than 130 ng Chl *a* L^{-1} during the experiment (Fig. 4A). The haptophyte type *Emiliania huxleyi* was the only group that decreased almost four times in absolute Chl *a* concentration during this experiment. Outside the fertilized patch, the phytoplankton community was also dominated by diatoms and absolute Chl *a* values of all phytoplankton groups remained more or less at the prefertilization level (Fig. 4B).

The number of full, broken, and empty total diatom cells increased up to days 29 and 32, respectively, and decreased thereafter (Table 2). Heavily silicified diatoms increased more than other diatoms during the experiment. This leads to an increase in the ratio of full heavily silicified diatoms to full total diatoms from 0.13 to 0.25 during the experiment. Empty and broken diatom frustules were counted as well

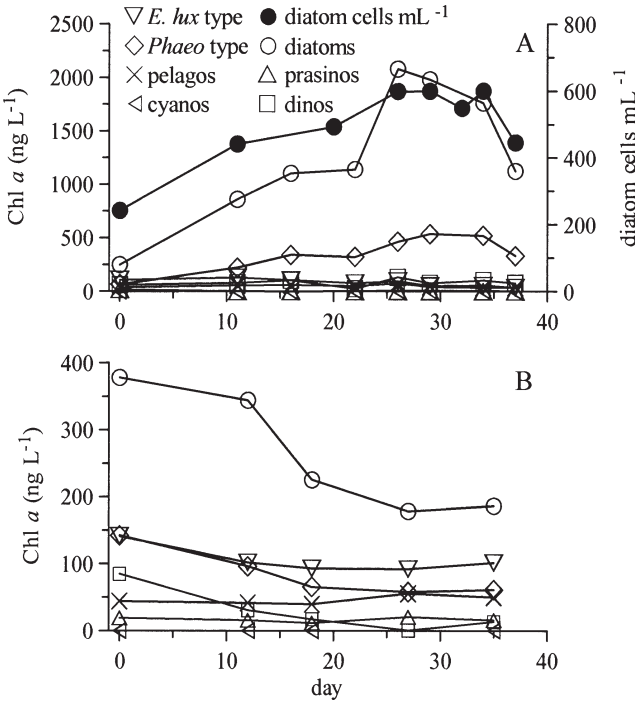

Fig. 4. Estimated Chl *a* concentration of the different phytoplankton groups based on the CHEMTAX program and total diatom cell numbers at 20-m depth (A) inside the fertilized patch and (B) outside the fertilized patch. Abbreviations are as follows: *E. hux* type for haptophyte type *Emiliania huxleyi, Phaeo* type for haptophyte type *Phaeocystis antarctica*, pelagos for pelagophytes, cyanos for cyanobacteria, prasinos for prasinophytes, and dinos for dinophytes.

because they contribute to bPSi concentrations. The sum of full, empty, and broken heavily silicified diatoms to the sum of full, empty, and broken total diatoms increased from 0.24 to 0.46 in the fertilized patch.

The biomass distribution of the total diatom community showed a relative decrease in large *Chaetoceros* species, while *Thalassiothrix antarctica*, *Corethron inerme*, and *Rhizosolenoids* (including *Guinardia*, *Proboscia*, and *Rhizosolenia* species) increased their relative contribution. Other species, like *Fragilariopsis kerguelensis*, *Pseudo-nitzschia* spp., and *Dactyliosolen antarcticus*, were important in terms of biomass throughout the whole experiment, with only minor changes in their relative contribution to the total diatom biomass (Assmy et al. unpublished).

Analysis by flow cytometry—In general, four populations of phytoplankton differing in size and chlorophyll fluorescence were distinguished. The smallest cells had an equivalent spherical diameter (esd) of ca. 0.6 μm; furthermore, three groups of picophytoplankton with an esd of ca. 1.1 μm (pico-Euk), 1.2 μm (Euk I), and 1.8 μm (Euk II) and one group of the nanophytoplankton with an esd of 3.9 μm (Euk III) were present. No significant numbers of phycoerythrin-containing cyanobacteria were detected. Because of their extremely low numerical abundance, the smallest phytoplankton group detected (esd 0.6 μm and

Table 2. The ratio of bPSi : POC of the total community, full, empty, and broken total diatom cells mL^{-1}, and the ratio of heavily silicified diatoms to total diatoms from 20-m depth inside the fertilized patch.

		Total diatom cells (mL^{-1})			Heavily silicified cells : total cells			
Day	bPSi : POC	Full	Empty	Broken	Full	Empty	Broken	Sum of full, empty, and broken
0	0.24	242	61	13	0.13	0.22	0.28	0.24
11/16*	0.23/0.29*	441	49	13	0.11	0.26	0.42	0.28
20/22*	0.44*	492	86	29	0.17	0.28	0.28	0.30
26	0.40	598	87	31	0.19	0.31	0.36	0.33
29	0.38	599	95	34	0.16	0.23	0.33	0.26
32	-	548	123	28	0.22	0.33	0.30	0.40
34	0.40	599	90	26	0.16	0.41	0.45	0.39
37	0.50	445	60	27	0.25	0.45	0.34	0.46

* At days 16 and 22, only data for bPSi and POC are available.

contribution to total biomass of <1%) was not included in the data analysis. With respect to the chlorophyll content of the different phytoplankton groups, temporary higher cellular chlorophyll values (up to day 24) were observed in pico-Euk, Euk I, and in the largest group detected by flow cytometry (Euk III; Fig. 5). As a result of the minor changes in the cellular Chl *a* content, changes in the C : Chl ratio in these groups also can be observed. Whereas the C : Chl ratio of the picoeukaryotes (pico-Euk) remained virtually constant, Euk I showed higher C : Chl ratios in the second half of the experiment. Euk II responded with an increase in the ratio of C : Chl after day 26. Finally, the largest group (Euk III) showed a temporary decline in the C : Chl ratio during the first 24 days, rising to the initial ratio thereafter. Noticeable is an abrupt change in cellular Chl *a* concentrations and the C : Chl ratio between days 24 and 26 especially in Euk I–III. At that time, distinct changes in many variables can be observed and may be explained by the beginning decay of the iron-induced bloom (Figs. 1, 3, 7, 8).

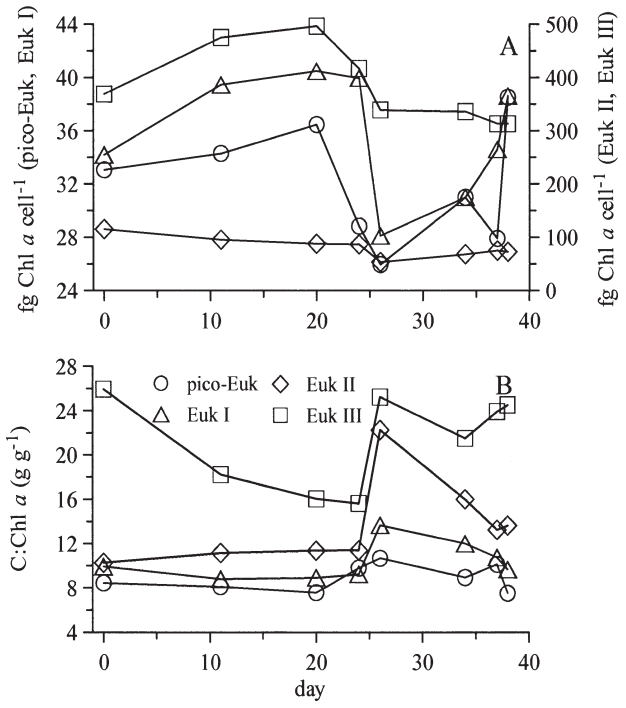

Fig. 5. (A) Estimated cellular Chl *a* concentration and (B) the ratio of C : Chl *a* of the four phytoplankton groups identified by flow cytometry inside the fertilized patch at 20-m depth.

Changes in the elemental composition—As described above, the elemental ratios at the out-stations differed extremely. They are here presented as mean and standard deviations (Fig. 6). In response to iron fertilization, the elemental composition of the pico-, nano-, and microplankton, estimated from size-fractionated POC, PON, and POP measurements, followed different trends (Fig. 6). The C : N ratio of the total community as well as of the pico- and nanoplankton (<2 and 2–20 μm) showed only minor changes during the experiment. The values did not differ much from those of the out-stations, which were slightly lower than the Redfield C : N ratio (5.9 and 5.7). In contrast, the >20 μm size fraction had higher than Redfield values prior to fertilization (11.2), which decreased rapidly during the first 22 days and were constant thereafter at about 5.2.

The N : P ratio of the picoplankton increased during the experiment from close to Redfield ratios (16.1) to higher values (24.9) at the end. The N : P ratio of the nanoplankton was lower at the out-stations (about 6) than at the in-stations. It decreased from close to Redfield start values (17.1) at the in-stations to 7.7 on day 34 and was higher again at the last station (14.7). Microplankton N : P ratios showed a different trend. They increased from well below Redfield (4.9) to close to Redfield ratios after iron fertilization (14.6). At the out-stations, the ratios were constantly low at about 5. The N : P ratio of the total community in- and outside the fertilized patch was slightly lower than the Redfield ratio and did not reflect the changes in the different size classes.

The C : P ratio of the picoplankton did not show any trend and was constantly below the Redfield ratio, except for one outlier at the last station. The out-stations had a mean C : P ratio of 83, which is far below the Redfield ratio of 106. The C : P ratios of the nano- and microplankton and of the total community showed in general the

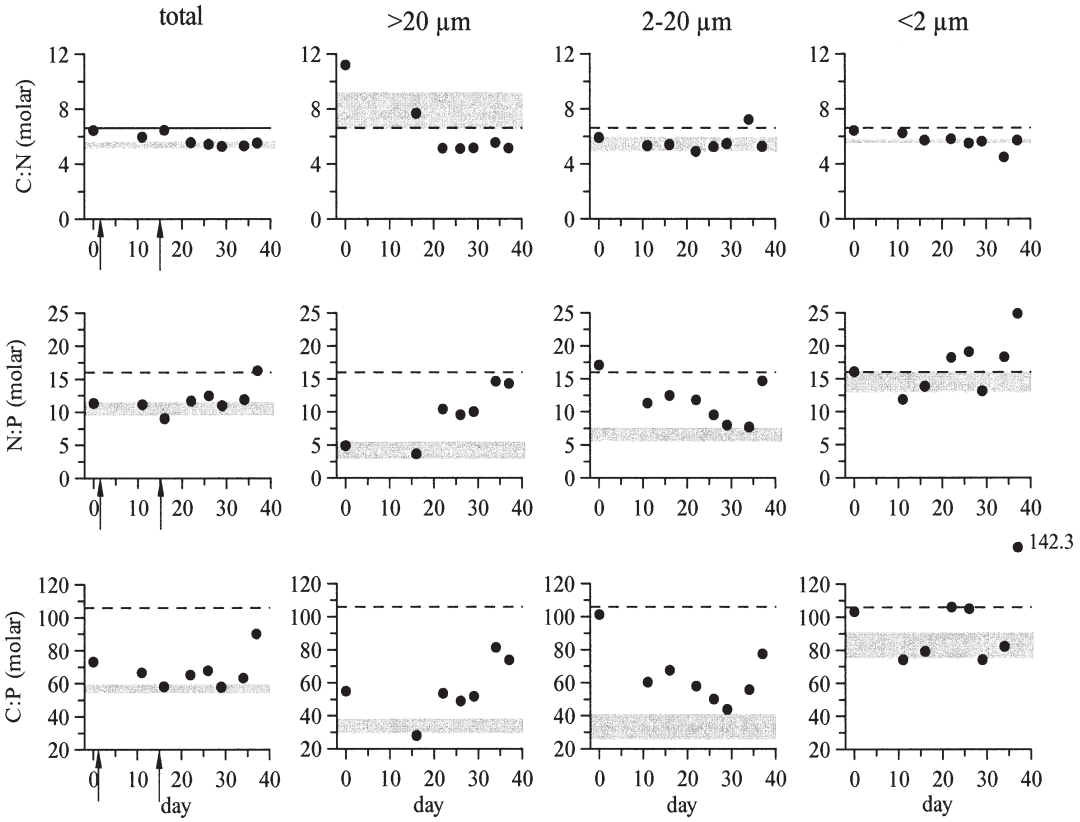

Fig. 6. Elemental composition of the total community and of the micro- (>20 μm), nano- (2–20 μm), and picoplankton (<2 μm) at 20-m depth. The grey area represents the mean and standard deviation of three out-stations. The dashed line represents the Redfield ratio, and arrows indicate days of iron fertilization.

same trend as the N : P ratios, which indicates that the changes are mainly driven by variations in POP concentrations. The C : P ratio of the nanoplankton decreased from 101.3 to 43.9 at day 29 and increased again at the last station to 77.5 inside the fertilized patch. Outside the patch, the ratio was about 33. The microplankton C : P ratio was 54.9 at the initial station, decreased to 27.9 at day 16, and increased to 81.3 at day 34, while they were about 34 at the out-stations. Generally, the N : P and C : P ratios were extremely low in the >20 μm size fraction in unfertilized waters, rising after iron fertilization.

However, the elemental composition of the total community conceals these diverse responses of the individual size classes. Especially the two dominant size fractions, >20 μm and 2–20 μm, show an opposite trend for the N : P and C : P ratios, which almost cancelled each other out.

Shifts in composition of taxonomic groups—To distinguish between pico- (<2 μm), nano- (2–20 μm), and microphytoplankton (>20 μm) reactions to iron fertilization, we analyzed changes in pigment composition of size-fractionated samples. The percentage of total Chl *a* within the different size classes (Fig. 7A,B) clearly shows different developments in smaller and larger organisms. Picophytoplankton contributed less than 20% of total Chl *a* before fertilization and did not change much during the experiment (Fig. 7A). The dominant size class during the course of the experiment was nanophytoplankton, which accounted for 44% to 71% of total Chl *a*. Microphytoplankton showed the strongest biomass increase as seen in percent of total Chl *a* and carbon biomass (data not shown). It increased its relative amount from 12% to 46% of total Chl *a* between days 11 and 26 and decreased again thereafter.

The additional size fractionation performed for the HLPC pigment samples split the 2–20-μm fraction into 2–8 and 8–20 μm (Fig. 7B). Here, the 8–20 μm was clearly the dominant fraction within the nanophytoplankton group, while the 2–8-μm fraction only accounted for less than 20% of total Chl *a* in the beginning and decreased to less than 10% during the experiment. The additional fragmentation of the <2-μm fraction into <0.8 μm and 0.8–2 μm did not show any changes. This relative contribution of Chl *a* by different size classes was also confirmed by the flow cytometer-derived chlorophyll measurements (for the fractions <20 μm, data not shown).

HPLC pigment measurements showed that fucoxanthin and chlorophyll *c* 1.2 (Chl *c* 1.2) were the most abundant pigments after Chl *a* in the microphytoplankton (Fig. 8A). The absolute concentration of both increased more than 13 times through day 26 from 65.5 to 886.6 ng L^{-1} for

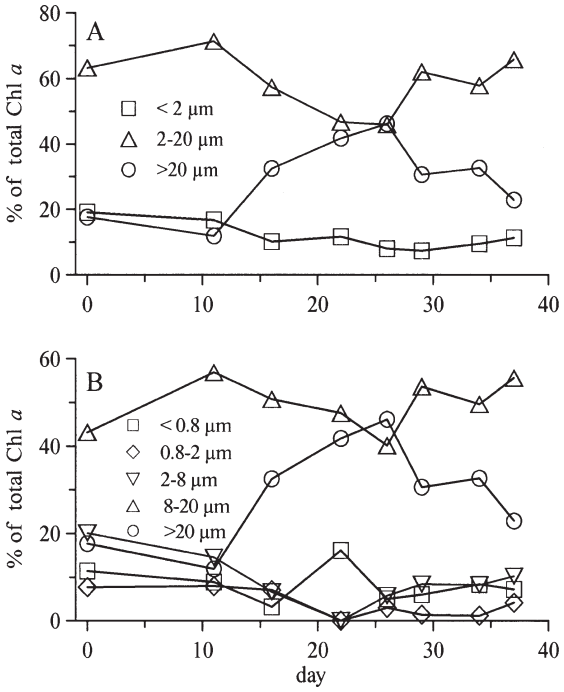

Fig. 7. Percentage of total Chl *a* at 20-m depth (A) inside the fertilized patch of the pico- (<2 μm), nano- (2–20 μm), and microphytoplankton (>20 μm), and (B) inside the fertilized patch of two groups of the picophytoplankton (<0.8 μm and 0.8–2 μm), two groups of the nanophytoplankton (2–8 μm and 8–20 μm), and the microphytoplankton (>20 μm).

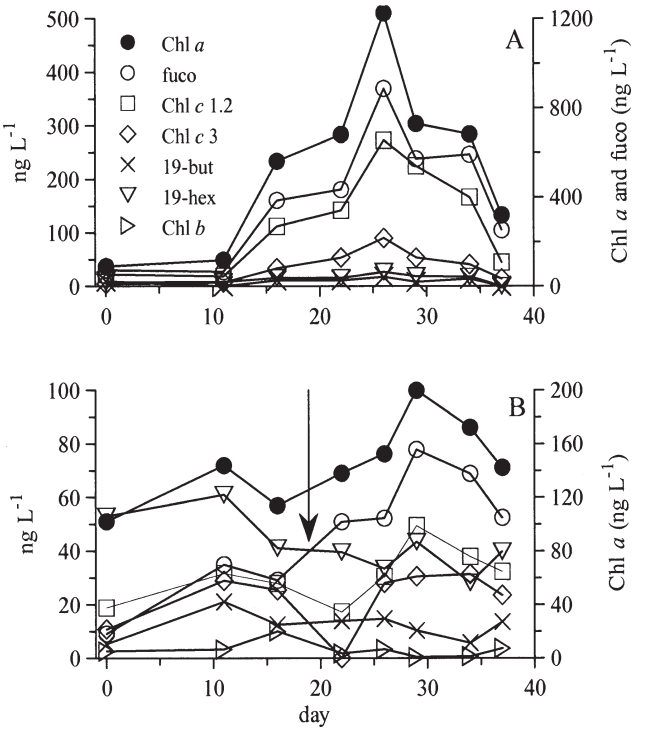

Fig. 8. Pigment composition at 20-m depth of (A) the >20 μm size fraction and (B) the 2–8-μm size fraction. The arrow indicates the shift from high 19-hex to high fucoxanthin concentrations between days 16 and 22.

fucoxanthin and from 18.6 to 272.7 ng L^{-1} for Chl *c* 1.2. Chl *c* 1.2 is the marker pigment of the group of chromophytes consisting of dinoflagellates, pelagophytes, cryptophytes, and diatoms. Fucoxanthin is a marker pigment, which mainly occurs in diatoms. The ratio of fucoxanthin to Chl *a* was very high throughout the experiment, ranging between 0.56 and 0.87, which indicates that the microphytoplankton size fraction consisted primarily of diatoms. Chlorophyll *c* 3 (Chl *c* 3) and 19-hexanoyloxyfucoxanthin (19-hex) increased in concentration from 4.8 to 90.2 ng L^{-1} for Chl *c* 3 and from 7.6 to 26.9 ng L^{-1} for 19-hex. Both pigments are markers for haptophytes. Haptophytes are small cells, belonging to the pico- or nanophytoplankton. Therefore, they must have been present in the colonial form of the haptophyte type *Phaeocystis* to be found in the >20 μm size class at the beginning of the experiment.

The 2–8-μm size fraction was only a minor part of the total Chl *a* (5.7–20.1%; Fig. 7B), and absolute Chl *a* concentrations only doubled. But unlike all other size fractions, it is striking that the other pigments did not follow the same trend as Chl *a* (Fig. 8B). Fucoxanthin increased almost 8.7 times, while 19-hex, the most abundant pigment after Chl *a* in the beginning, almost halved. This resulted in fucoxanthin being the most abundant pigment next to Chl *a* after day 22 (see arrow in Fig. 8B). The marker pigment of pelagophytes 19-butanoyloxyfucoxanthin (19-but), decreased 1.8 times, while all other pigments showed almost no changes.

Relative changes in the proportion of five marker pigments are summarized in Fig. 9. They clearly show the massive fucoxanthin increase in the 8–20-μm and >20-μm fractions. However, in both size fractions, fucoxanthin was the dominant pigment from the beginning, while in the 2–8-μm fraction, there was a shift from high 19-hex to high fucoxanthin concentrations. This relative increase of the marker pigment of diatoms was mainly caused by the overwhelming increase in the absolute fucoxanthin concentrations in every size fraction larger than 2 μm.

Microscopic cell counts of the small diatom species *Fragilariopsis cylindrus*, *Cylindrotheca closterium, Chaetoceros* sp. (solitary cells), and an unidentified small pennate diatom as well as the two haptophytes, *Phaeocystis antarctica* (solitary cells) and *Emiliania huxleyi*, which all fit into the 2–8-μm size fraction, also showed a higher increase of the diatoms than the haptophytes after day 22 (Fig. 10).

Discussion

Biomass response to iron fertilization—During EIFEX, the fifth in situ iron fertilization experiment in the Southern Ocean, we induced a massive phytoplankton bloom in austral fall. The 5.3-fold increase in Chl *a* concentration (Fig. 1) was of the same magnitude as in the two Southern Ocean in situ iron-fertilization experiments SOIREE (6-fold) and EisenEx (about 4.6-fold) (Boyd et al. 2000; Gervais et al. 2002). The SOFEX North and South

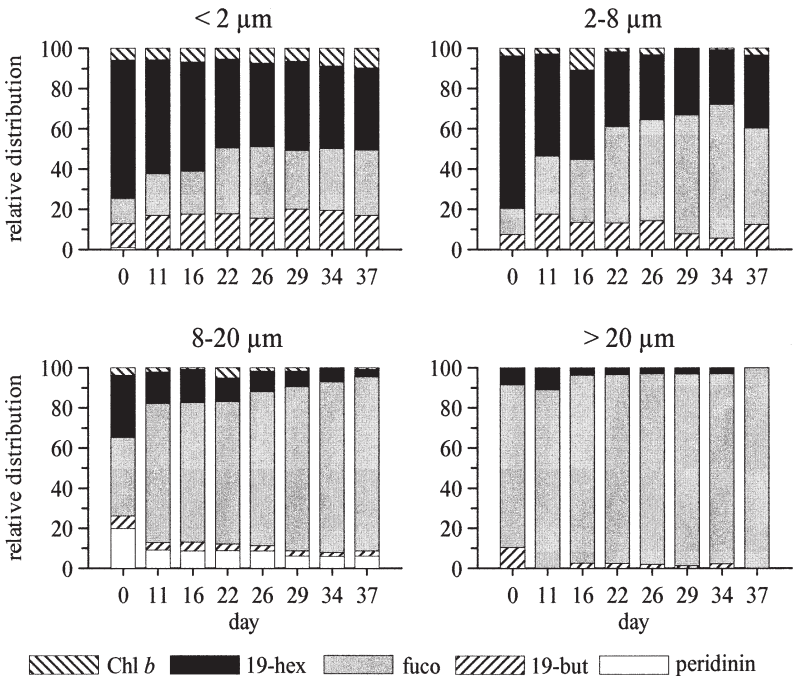

Fig. 9. Relative distributions of the marker pigments chlorophyll *b* (Chl *b*, chlorophytes), 19-hexanoyloxyfucoxanthin (19-hex, haptophytes), fucoxanthin (diatoms), 19-butanoyloxyfucoxanthin (19-but, pelagophytes), and peridinin (dinoflagellates) in the four size classes: <2 μm, 2–8 μm, 8–20 μm, and >20 μm at 20-m depth.

experiments showed higher Chl *a* increases (10- and 20-fold), which were mostly due to the lower prefertilization concentrations (Coale et al. 2004). The maximum Chl *a* concentration in 20-m depth of more than 2,800 ng L^{-1} reached during EIFEX were higher than those measured during SOIREE (about 1,800 ng L^{-1}), EisenEx (2,310 ng L^{-1}), and SOFEX North (about 2,600 ng L^{-1}), but lower than those found at SOFEX South (about 3,800 ng L^{-1}; Boyd et al. 2000; Gervais et al. 2002; Coale et al. 2004). The decline in the Chl *a*, POC, PON, and POP concentrations toward the end of the experiment suggests the demise of the iron-induced bloom (Figs. 1 and 2). This is in contrast with previous shorter experiments, where the phytoplankton biomass remained high until the end of the observations.

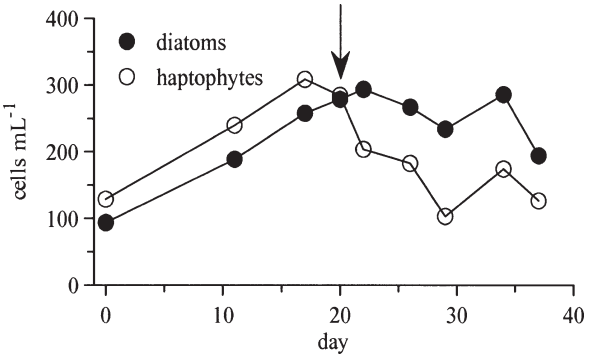

Fig. 10. Cell numbers of the diatom species *Fragilariopsis cylindrus*, *Cylindrotheca closterium, Chaetoceros* sp. (solitary cells), one unidentified small pennate diatom, and the two haptophytes species *Phaeocystis antarctica* (solitary cells) and *Emiliania huxleyi* in the 2–8-μm size fraction at 20-m depth. The arrow indicates the shift from higher haptophyte cell numbers to higher diatom cell numbers at day 20.

The POC, PON, and POP data result from measurements of the total particulate material and include autotrophic as well as heterotrophic biomass. An interpretation of changes in the autotrophic community from these parameters alone is therefore not unequivocal. However, all particulate organic matter components showed similar temporal patterns as Chl *a*, indicating that these changes are dominated by phytoplankton development. A similar trend was found during EisenEx, where Chl *a*, POC, and PON concentrations at 20-m depth inside the fertilized patch increased constantly until day 21 (Riebesell pers. comm.).

The strong decline in the POC : Chl *a* ratio of the whole plankton community inside the iron-enriched patch indicated a proportional increase in autotrophic biomass relative to the heterotrophic plankton component (Fig. 3). A similar trend was observed during SOIREE and EisenEx, where the POC : Chl *a* ratio was reduced by a factor of two in a time span of 13 days (Boyd et al. 2000) and by a factor of 4.4 within 21 days (Riebesell pers. comm.). To some extent, this could have been due to enhanced chlorophyll synthesis upon iron repletion (chlorosis; Geider and LaRoche 1994). In cultures of the diatom *Phaeodactylum tricornutum*, cellular Chl *a* concentrations increased by

Table 3. Changes in the absolute (ng L^{-1}) and relative (% of total) amounts of Chl *a* of the pico- (<2 μm), nano- (2–20 μm), and microphytoplankton (>20 μm) during the first 26 (*29) days of EIFEX and 21 days of EisenEx (Gervais et al. 2002). EIFEX samples were taken from 20-m depth and EisenEx data are mean values of all measurements between 0 m and 80 m.

Size fraction	EIFEX (ng L^{-1})	EisenEx (ng L^{-1})	EIFEX (% of total)	EisenEx (% of total)
>20 μm	89.7 → 1,225	50 → 1,100	12 → 46	10 → 43
2–20 μm	321.5 → 1,477*	250 → 1,100	63.2 → 45.9	50 → 44
<2 μm	97.2 → 212.7	200 → 300	±15	42 → 13

a factor of 4.4 and the ratio POC : Chl *a* decreased by a factor of 3.2 upon iron addition (Greene et al. 1991). Also during the present survey, the cellular Chl *a* content determined by flow cytometry increased slightly in the picophytoplankton group pico-Euk and Euk I and the nanophytoplankton group Euk III through day 20 (Fig. 5). Using the same method during EisenEx, cellular Chl *a* values were found to increase by a factor of two for the picophytoplankton community and up to a factor of four for the nanophytoplankton (Veldhuis and Timmermans unpubl. data). The small increase in cellular Chl *a* content observed during EIFEX cannot explain the strong decrease in POC : Chl *a*. Therefore, the observed decline in the total plankton carbon to phytoplankton chlorophyll ratio was predominantly due to preferential increase of mainly larger phytoplankton relative to the heterotrophic community.

BPSi can be used as an indicator for diatom biomass, as cell numbers of other organisms bearing silicious skeletons, like radiolarians, were insignificant compared with diatoms during EIFEX (Henjes pers. comm.). Surprisingly, the bPSi concentration did not decline toward the end of our observation (Fig. 2), while the diatom abundance, as determined by pigment measurements and cell counts, decreased after day 26 (Fig. 4A). A relative increase in the abundance of full cells and broken and empty frustules of heavily silicified diatoms compared with total diatom cell numbers was observed toward the end of the experiment (Table 2). This may be the cause for the slight increase in total bPSi concentration while total diatom cell numbers decreased. This assumption is also supported by the bPSi : POC ratio of the total community that increased from 0.24 to 0.5 during the experiment (Table 2).

Iron-induced growth in different size classes—A shift in the phytoplankton size distribution toward larger cells as a result of iron fertilization has been described for different HNLC regions (Cavender-Bares et al. 1999; Gervais et al. 2002; Eldridge et al. 2004). Cavender-Bares et al. (1999) found a dramatic change from a picoplankton-dominated community to one dominated by diatoms larger than 10 μm within 1 week in the equatorial Pacific. These findings are comparable with those of in situ iron-fertilization experiments in the Southern Ocean, despite the large physicochemical and biological differences of the two areas. During SOIREE, the first iron-fertilization experiment performed in the Southern Ocean in austral fall, the phytoplankton community was dominated by picoplankton (40% of total Chl *a* integrated over 65-m depth) before iron fertilization, while micro- and nanoplankton both contributed 30% (Gall et al. 2001*a*). During the 13 days of the experiment, microphytoplankton Chl *a* concentrations increased by one order of magnitude, nanoplankton sixfold, and picoplankton threefold. Gall et al. (2001*b*) showed that nano- and microphytoplankton increased their primary production strongly while picophytoplankton primary production did not change much.

The absolute and relative changes in the nano- and microphytoplankton during EIFEX, conducted during austral fall, and a previous iron fertilization experiment in the Southern Ocean (EisenEx), conducted during austral spring, show generally similar developments (Table 3). There are some differences in the changes of picoplankton, which had twice as high Chl *a* concentration at the start of EisenEx compared with EIFEX. The initial Chl *a* concentrations of the nano- and microphytoplankton were both higher during EIFEX. Another difference is that, while the Chl *a* increase of the nanophytoplankton was similar in both experiments (factor of 4.6 during EIFEX and 4.4 during EisenEx), the microphytoplankton increased its biomass much more during EisenEx (22 times) compared with EIFEX (13.7 times). The difference in the rate of microphytoplankton biomass increase between the two experiments was mainly due to a stronger response of the fast-growing diatom species *Pseudo-nitzschia lineola* during EisenEx than EIFEX, based on microscopic cell counts (Assmy unpubl. data). Irrespective of the absolute and relative initial composition of the phytoplankton community, iron fertilization induced a massive increase of microphytoplankton biomass independent of the season. The amount of pico- and nanophytoplankton growth seems to be less stimulated by iron addition and may also be strongly dependent on grazing pressure. The latter may exert a strong influence but cannot be evaluated from our data.

Stimulation of diatoms by iron fertilization—The pigment fucoxanthin is mainly found in diatoms and therefore is used as a marker pigment for diatom biomass. However, fucoxanthin can be found in other phytoplankton groups as well, such as haptophytes (van Leeuwe and Stefels 1998). They describe that the fucoxanthin content of *Phaeocystis* increases due to iron fertilization. Part of the increasing fucoxanthin concentration found in the 2–8-μm fraction (size of solitary *Phaeocystis* cells) and in the >20-μm fraction (size of *Phaeocystis* colonies) may therefore result from *Phaeocystis* instead of diatom growth. As microscopic cell counts showed that diatoms clearly dominated the microphytoplankton during EIFEX (Assmy et al. 2005), we

assume that this is of minor importance for the >20-μm size fraction. In the 2–8-μm size fraction, the Chl *c* 1.2 concentration increased as well as the fucoxanthin concentration (Fig. 8B). Chl *c* 1.2 is only found in the group of chromophytes (diatoms, dinoflagellates, pelagophytes, and cryptophytes), but not in haptophytes. We conclude that the increase in fucoxanthin was therefore primarily caused by rising diatom concentrations. The fucoxanthin concentration overtook the 19-hex concentration (indicator for haptophytes) after day 22. This suggests that, before iron fertilization, mainly haptophytes were present, which were exceeded by diatoms from day 22 on. Apart from pigment analysis, cell counts support these findings and show that diatoms between 2-μm and 8-μm size increased their abundance stronger than haptophytes of the same size (Fig. 10). Gall et al. (2001*a*) describe similar and more pronounced changes in the composition of the whole phytoplankton community during SOIREE. Initially, the haptophyte type *Phaeocystis*, as determined by HPLC pigment measurements, dominated the total phytoplankton community. After an initial increase of these algae, diatoms became the dominant group about 1 week after iron fertilization.

Size-fractionated pigment analysis and microscopic cell counts (Assmy et al. 2005) indicated that diatoms >20 μm were the main beneficiaries of iron addition during EIFEX, leading to a massive growth of long, chain-forming diatoms. This corresponds very well with other field data and incubation experiments after iron enrichment (Hutchins and Bruland 1998; Boyd et al. 2000; Gervais et al. 2002). The reason for this is thought to be the higher iron requirement of large cells due to the lower surface-to-volume ratio compared with smaller ones (Sunda and Huntsman 1995; Timmermans et al. 2001, 2004). Nevertheless, our pigment data suggest that iron fertilization stimulates diatom growth not only in the >20-μm size class, but in every size fraction larger than 2 μm (Fig. 9). The ratio of fucoxanthin to Chl *a* increased 4.4 times in the 2–8-μm size fraction, while the increase was smaller in the 8–20-μm size fraction (1.6). This implies that even the very small diatoms enhance their growth rates due to iron fertilization. In the microphytoplankton, a massive growth of long, chain-forming diatoms occurred, but it did not change the relative group composition because diatoms were already dominant at the start of the experiment.

During EIFEX, diatoms dominated the phytoplankton community already prior to the fertilization experiment under iron-limiting conditions, and they were able to increase their biomass to a greater extent than other phytoplankton groups when iron became available (Fig. 4). The reason why diatoms in general tend to have an advantage over other phytoplankton groups under high nutrient conditions is thought to be their relatively high half-saturation constants (Sarthou et al. 2005). This is often explained by a low surface-to-volume ratio, which is only true for large cells but not for diatoms in general. Laboratory experiments with a large (*Chaetoceros dichaeta*) and a small (*C. brevis*) Southern Ocean diatom species showed that *C. brevis* could not increase its growth rate with increasing iron availability (Timmermans et al. 2001), which is in contrast with our findings. Hence, the success of diatoms under iron-rich conditions may not only be because of high half-saturation constants but may be caused by several adaptive strategies. First, diatoms have a generally better ability to take up and store iron compared with other taxonomical groups. Sunda and Huntsman (1995) describe that diatoms were able to accumulate iron and reach Fe : C values that were 20–30 times higher than those needed for maximal growth, while coccolithophores and dinoflagellates had only two to three times higher Fe : C values than required for optimal growth. Such luxury uptake of iron can be a major advantage in regions where iron is only temporarily available. This could allow diatoms to keep higher growth rates while total iron concentrations in the surrounding water are depleted. Second, diatoms are better protected against grazing pressure by their silica frustules compared with other, naked phytoplankton groups.

Changes in the elemental composition—The increasing N : P and C : P ratios of the microphytoplankton as a result of increased iron availability is a phenomenon that has been previously described in the literature (de Baar et al. 1997). The opposite trend within the nanophytoplankton through day 29 and the increase thereafter has, to our knowledge, not been described yet and is likely due to a shift in the group composition in this size class. This is indicated by strong changes in the marker pigment distribution of the whole nanophytoplankton and especially the 2–8-μm size fraction as well as by cell counts of the latter size fraction as described above.

Klausmeier et al. (2004) show that the N : P ratios of different freshwater and marine species range between 7.1 and 43.3, although the median of 17.7 was close to Redfield. The elemental composition of phytoplankton can vary over a wide range between species or functional groups, and diatoms in general have lower than Redfield N : P and C : P ratios, ranging between 9.3–14.1 and 62–100, respectively (Arrigo et al. 1999; Quigg et al. 2003; Ho et al. 2004). Arrigo et al. (1999, 2002) describe that waters of the Southern Ocean that are dominated by diatoms have lower than Redfield N : P and C : P ratios of the above-said range, while those dominated by the haptophyte *Phaeocystis antarctica* exceed the Redfield ratio and range between 17.2 and 19.5 for N : P and 120 and 154 for C : P. This is assumed to be caused by luxury P uptake and the formation of internal P pools in diatoms as a response to iron stress (Tremblay and Price unpubl.). The observed decrease in the N : P and C : P ratios of the nanoplankton may therefore be primarily due to a species shift from haptophytes to diatoms. Furthermore, it could explain why the N : P and C : P ratios of the microphytoplankton, which mainly consisted of diatoms, were already far below those of the nano- and picoplankton at the start of the experiment.

The increasing N : P and C : P ratios of the microphytoplankton cannot be explained by a shift in assemblage composition, as pigment data and cell counts indicate that this size fraction was dominated by diatoms from the beginning. However, species-specific shifts within the

diatom assemblage, as observed during EIFEX, might impact these ratios. It is likely that there are different adaptation strategies of smaller and larger phytoplankton species to iron limitation that result in different elemental compositions. Additionally, nitrate uptake is inhibited under iron limitation (Franck et al. 2003) because the enzymes essential for nitrate uptake, nitrate and nitrite reductase, are iron rich (Timmermans et al. 1994). Low nitrate uptake and the possible formation of internal P pools (Tremblay and Price unpubl.) result in a low N : P ratio under low iron concentrations. With iron fertilization, the growth rates of large diatoms increase in culture experiments (Timmermans et al. 2004) and in situ fertilization experiments. Increase in N uptake with iron fertilization (de Baar et al. 1997; Franck et al. 2003; Timmermans et al. 2004) and consumption of internal P reserves at enhanced growth rates may be the reason for the strong increase in N : P and C : P ratios in the microphytoplankton (Fig. 6).

Biogeochemical models assessing the carbon export from the upper ocean generally assume fixed elemental Redfield ratios in the exported organic material. Our investigations showed that the mean C : N and C : P ratios of the total community inside the fertilized patch were 13% and 36% lower than the Redfield ratio. This would result in a significant overestimation of the carbon export based on N or P uptake. Our data indicate that iron fertilization causes more changes, especially in the species composition of the small phytoplankton community, than hitherto assumed. Part of this change is likely to be caused by grazing. As the microphytoplankton is generally too large to be consumed by most microzooplankton grazers and too fast growing for mesozooplankton grazers when iron becomes available (Coale et al. 1996), mainly smaller phytoplankton groups are exposed to grazing pressure. Changes in the pico- and nanophytoplankton community structure and elemental ratios and, thus, changes in the main food source of microzooplankton grazers will have impacts on the composition of fecal pellets. Besides cell aggregates, fecal pellets are an important transport mechanism of carbon to the deep ocean after a phytoplankton bloom. Recent biogeochemical models consider different phytoplankton groups and size classes (Pasquer et al. 2005) and, hence, a detailed understanding of mechanisms influencing the elemental composition of all phytoplankton size classes is important.

The question remains whether the short-term changes observed by these investigations also apply for long-term iron fertilization. If continuous iron input would generally alter the composition of the phytoplankton community and size classes, the export of nutrients from the upper water column would be different from the present iron-limited situation. The observed slight increase in N : P and C : P ratios would indicate a lesser export of P and perhaps a higher export of N. However, these assumptions do not take into account potential changes in grazing pressure from micro- to mesozooplankton that may result from prolonged iron fertilization, and therefore the combined effects on the nutrient export are difficult to predict.

References

Arrigo, K. R., R. B. Dunbar, M. P. Lizotte, and D. H. Robinson. 2002. Taxon-specific differences in C/P and N/P drawdown for phytoplankton in the Ross Sea, Antarctica. Geophy. Res. Lett. **29** [doi:10.1029/2002GL015277].

———, D. H. Robinson, D. L. Worthen, R. B. Dunbar, G. R. DiTullio, M. VanWort, and M. P. Lizotte. 1999. Phytoplankton community structure and the drawdown of nutrients and CO_2 in the Southern Ocean. Science **283:** 365–367.

Assmy, P., J. Henjes, K. Schmidt, V. Smetacek, and M. Montresor. 2005. The wax and wane of an iron-induced diatom bloom in the Southern Ocean. Berichte zur Polar und Meeresforschung **500:** 89–100.

Barlow, R. G., D. G. Cummings, and S. W. Gibb. 1997. Improved resolution of mono- and divinyl chlorophylls *a* and *b* and zeaxanthin and lutein in phytoplankton extracts using phase C-8 HPLC. Mar. Ecol. Prog. Ser. **161:** 303–307.

Boyd, P. W., and others. 2000. A mesoscale phytoplankton bloom in the polar Southern Ocean stimulated by iron fertilization. Nature **407:** 695–702.

Cavender-Bares, K. K., E. L. Mann, S. W. Chisholm, M. E. Ondrusek, and R. R. Bidigare. 1999. Differential response of equatorial Pacific phytoplankton to iron fertilisation. Limnol. Oceanogr. **44:** 237–246.

Cembella, C., H. Rohr, K. Loquay, and V. Strass. 2005. Mapping horizontal spreading of a developing phytoplankton bloom using an airborne chlorophyll *a* fluorescence LIDAR. Berichte zur Polar und Meeresforschung **500:** 38–43.

Coale, K. H., and others. 1996. A massive phytoplankton bloom induced by an ecosystem-scale iron fertilization experiment in the equatorial Pacific Ocean. Nature **383:** 495–501.

———, and others. 2004. Southern Ocean iron enrichment experiment: Carbon cycling in high- and low-Si waters. Science **304:** 408–414.

de Baar, H. J. W., M. A. van Leeuwe, R. Scharek, L. Goeyens, K. M. J. Bakker, and P. Fritsche. 1997. Nutrient anomalies in *Fragilariopsis kerguelensis* blooms, iron deficiency and the nitrate/phosphate ratio (A. C. Redfield) of the Antarctic Ocean. Deep-Sea Res. II **44:** 229–260.

———, and others. 2005. Synthesis of iron fertilisation experiments: From the Iron Age in the age of enlightenment. J. Geophys. Res. **110.** C09S16, [doi:10.1029/2004JC002601].

Ehrhard, M., and W. Koeve. 1999. Determination of particulate organic carbon and nitrogen, p. 437–444. *In* K. Grasshoff, K. Kremling and M. Ehrhard [eds.], Methods of seawater analysis. Wiley-VCH.

Eldridge, M. L., and others. 2004. Phytoplankton community response to a manipulation of bioavailable iron in HNLC waters of the subtropical Pacific Ocean. Aquat. Microb. Ecol. **35:** 79–91.

Franck, V. M., K. W. Bruland, D. A. Hutchins, and M. A. Brzezinski. 2003. Iron and zinc effects on silicic acid and nitrate uptake kinetics in three high-nutrient, low-chlorophyll (HNLC) regions. Mar. Ecol. Prog. Ser. **252:** 15–33.

Gall, M. P., P. W. Boyd, J. Hall, K. A. Safi, and H. Chang. 2001*a*. Phytoplankton processes. Part 1: Community structure during the Southern Ocean Iron RElease Experiment (SOIREE). Deep-Sea Res. Part II **48:** 2551–2570.

———, R. Strzepek, M. Maldonado, and P. W. Boyd. 2001*b*. Phytoplankton processes. Part 2. Rates of primary production and factors controlling algal growth during the Southern Ocean Iron RElease Experiment (SOIREE). Deep-Sea Res. Part II **48:** 2571–2590.

GEIDER, R. J., AND J. LAROCHE. 1994. The role of iron in phytoplankton photosynthesis, and the potential for iron-limitation of primary productivity in the sea. Photosynthesis Res. **39:** 275–301.

———, AND ———. 2002. Redfield revisited: Variability of C : N : P in marine microalgae and its biogeochemical basis. Eur. J. Phycol. **37:** 1–17.

GERVAIS, F., U. RIEBESELL, AND M. Y. GORBUNOV. 2002. Changes in primary productivity and chlorophyll *a* in response to iron fertilization in the Southern Polar Frontal Zone. Limnol. Oceanogr. **47:** 1324–1335.

GREENE, R. M., R. J. GEIDER, AND P. G. FALKOWSKI. 1991. Effect of iron on photosynthesis in a marine diatom. Limnol. Oceanogr. **36:** 1772–1782.

HANSEN, H. P., AND F. KOROLEFF. 1999. Determination of nutrients, p. 159–228. *In* K. Grasshoff, K. Kremling and M. Ehrhard [eds.], Methods of seawater analysis. Wiley-VCH.

HO, T. Y., A. QUIGG, Z. V. FINKEL, A. J. MILLIGAN, K. WYMAN, P. G. FALKOWSKI, AND F. M. M. MOREL. 2004. The elemental composition of some marine phytoplankton. J. Phycol. **39:** 1145–1159.

HUDSON, R. J. M., AND F. M. M. MOREL. 1990. Iron transport in marine phytoplankton: Kinetics of cellular and medium coordination reactions. Limnol. Oceanogr. **35:** 1002–1020.

HUTCHINS, D. A., AND K. W. BRULAND. 1998. Iron-limited diatom growth and Si : N uptake ratios in a coastal upwelling regime. Nature **393:** 561–564.

KLAUSMEIER, C. A., E. LITCHMAN, T. DAUFRESNE, AND S. A. LEVIN. 2004. Optimal nitrogen-to-phosphorus stoichiometry of phytoplankton. Nature **429:** 171–174.

MACKEY, M. D., D. J. MACKEY, H. W. HIGGINS, AND S. W. WRIGHT. 1996. CHEMTAX—a program for estimating class abundances from chemical markers: Application to HPLC measurements of phytoplankton. Mar. Ecol. Prog. Ser. **14:** 265–283.

MARTIN, J. H., S. E. FITZWATER, AND R. M. GORDON. 1990. Iron deficiency limits phytoplankton growth in Antarctic waters. Global Biogeochem. Cycles **4:** 5–12.

PASQUER, B., G. LARUELLE, S. BECQUEVORT, W. SCHOEMANN, H. GOOSSE, AND C. LANCELOT. 2005. Linking ocean biogeochemical cycles and ecosystem structure and function: Results of the complex SWAMCO-4 model. J. Sea Res. **53:** 93–108.

QUIGG, A., AND OTHERS. 2003. The evolutionary inheritance of elemental stoichiometry in marine phytoplankton. Nature **425:** 291–294.

RÖTTGERS, R., F. COLIJN, AND M. DIBBERN. 2005. Algal physiology and biooptics. Berichte zur Polar und Meeresforschung **500:** 82–88.

SARTHOU, G., K. R. TIMMERMANS, S. BLAIN, AND P. TREGUER. 2005. Growth physiology and fate of diatoms in the ocean: A review. J. Sea Res. **53:** 25–42.

SUNDA, W. G., AND S. A. HUNTSMAN. 1995. Iron uptake and growth limitation in oceanic and coastal phytoplankton. Mar. Chem. **50:** 189–206.

———, AND ———. 1997. Interrelated influence of iron, light and cell size on marine phytoplankton growth. Nature **390:** 389–392.

TIMMERMANS, K. R., W. STOLTE, AND H. J. W. DE BAAR. 1994. Iron-mediated effects on nitrate reductase in marine phytoplankton. Mar. Biol. **121:** 389–396.

———, B. VAN DER WAGT, AND H. J. W. DE BAAR. 2004. Growth rates, half saturation constants, and silicate, nitrate, and phosphate depletion in relation to iron availability of four large open-ocean diatoms from the Southern Ocean. Limnol. Oceanogr. **49:** 2141–2151.

———, AND OTHERS. 2001. Growth rates of large and small Southern Ocean diatoms in relation to availability of iron in natural seawater. Limnol. Oceanogr. **46:** 260–266.

TWINING, B. S., S. B. BAINES, AND N. S. FISHER. 2004. Element stoichiometries of individual plankton cells collected during the Southern Ocean Iron Experiment (SOFeX). Limnol. Oceanogr. **49:** 2115–2128.

UTERMÖHL, H. 1958. Zur Vervollkommnung der quantitativen Phytoplankton-Methodik. Mitt. int. Verein. theor. angew. Limnol. **9:** 1–38.

VAN LEEUWE, M. A., AND J. STEFELS. 1998. Effects of iron and light stress on the biogeochemical composition of Antarctic *Phaeocystis* sp. (Prymnesiophyceae). II. Pigment composition. J. Phycol.y **34:** 496–503.

VAULOT, D., C. COURTIES, AND F. PARTENSKY. 1989. A simple method to preserve oceanic phytoplankton for flow cytometric analyses. Cytometry **10:** 629–635.

VELDHUIS, M. J. W., AND G. W. KRAAY. 2000. Application of flow cytometry in marine phytoplankton research: Current applications and future perspectives. Sci. Mar. **64:** 121–134.

WALTER, S., I. PEEKEN, K. LOCHTE, A. WEBB, AND H. W. BANGE. 2005. Nitrous oxide measurements during EIFEX, the European Iron Fertilization Experiment in the subpolar South Atlantic Ocean. Geophys. Res. Lett. **32** [doi:10.1029/2005GL024619].

WRIGHT, S. W., D. P. THOMAS, H. J. MARCHANT, H. W. HIGGINS, M. D. MACKEY, AND D. J. MACKEY. 1996. Analysis of phytoplankton of the Australian sector of the Southern Ocean: Comparisons of microscopy and size frequency data with interpretations of pigment HPLC data using the 'CHEMTAX' matrix factorisation program. Mar. Ecol. Prog. Ser. **144:** 285–298.

ZIELINSKI, U., AND R. GERSONDE. 1997. Diatom distribution in Southern Ocean surface sediments (Atlantic sector): Implications for paleoenvironmental reconstructions. Palaeogeogr. Palaeoclimatol. Palaeoecol. **129:** 213–250.

Received: 12 July 2005
Amended: 19 December 2005
Accepted: 30 December 2005

CHAPTER II

Co-limitation by iron, silicate, and light of three Southern Ocean diatom species

Linn Hoffmann, Ilka Peeken, Karin Lochte

Accepted in Biogeosciences Discussions

Abstract:

The effect of combined iron, silicate, and light co-limitation was investigated in two Southern Ocean diatom species, *Chaetoceros dichaeta* and *Actinocyclus sp.*, and one cosmopolitan species, *Chaetoceros debilis*, all isolated in the Southern Ocean (SO). We found species specific differences in the level of nutrient limitation and its effect on physiological and morphological parameters.

Growth of all species tested was clearly co-limited by iron and silicate, reflected in a 4 to 40 times higher increase in cell numbers in the high iron, high silicate treatments compared with the controls. However, the effect of iron and silicate availability on chain length and frustules structures was species specific. Most drastic frustule malformation was found under iron and silicate co-limitation in *C. dichaeta* while Si limitation caused a strong cell elongation in both *Chaetoceros* species. Additional a significant increase in chain length was observed in these species under high iron conditions. Therefore, species composition in the SO is likely also indirectly affected by these nutrients via different effects on diatom grazing protection. These morphological changes may offer a potential as biological markers in sediments for the growth history of chain forming species.

High light conditions, comparable with light intensities found in the upper 28 m of the SO, showed a negative impact on growth of the endemic species *C. dichaeta* and *Actinocyclus sp.* This is in contrast to the assumed light limitation of SO diatoms and indicates an adaptation strategy to the deep mixing and resulting low light conditions in the SO. In contrast to that, the cosmopolitan species *C. debilis* was not negatively affected by increased light intensity, indicating adaptation to a broader light environment. These results suggest that light limitation of SO phytoplankton due to deep wind mixed layers may play a minor role than hitherto assumed.

Introduction:

Diatoms are an extraordinary phytoplankton class, which play a major role in global carbon fixation in all regions of the world's ocean (Sarthou et al., 2005). Especially in the SO, diatoms tend to dominate the phytoplankton community and account for as much as ~75% of the annual primary production (Nelson et al., 1995; Tréguer et al., 1995). Diatoms can build up enormous blooms and, since there is only little frustule dissolution during the transport to the deep sea (Tréguer et al., 1989), they are responsible for almost all of the silica sedimentation in the SO (Abelmann and Gersonde, 1991). Besides the macro nutrients nitrate and phosphate that are essential for the growth of all algae, diatoms also depend on the availability of silicic acid ($Si(OH)_4$) to produce their frustules.

While nitrate concentrations are high everywhere in the SO (about 25 μM Dafner and Mordasova, 1994; Tréguer and Jacques, 1992) dissolved Si concentrations vary from 1 to 15 μM north of the Polar Frontal Zone (PFZ) to about 40 to 60 μM on the south side (Coale et al., 2004; Franck et al., 2000; Tréguer and Jacques, 1992). The high Si concentrations south of the PFZ create a favorable environment for diatoms while the low Si concentrations can limit diatom growth (Brzezinski et al., 2005; Coale et al., 2004; Franck et al., 2000; Leblanc et al., 2005).

Besides Si the trace metal iron is known to limit phytoplankton growth in general in the SO. Several *in situ* iron fertilization experiments in the SO proved that especially the growth of large, chain-forming diatoms was enhanced due to iron addition (see review in de Baar et al., 2005). Nevertheless recent studies showed that diatoms in all size classes were able to benefit from iron fertilization (Hoffmann et al., 2006). Besides the effect on cell growth, iron fertilization increases the maximum specific uptake rates of silicic acid in SO diatoms and enables them to fulfill their silica needs even in water with very low Si concentrations (Brzezinski et al., 2005; De La Rocha et al., 2000; Franck et al., 2003; Franck et al., 2000). It is suggested that this is caused by an increase in the number of active Si transporters in the cell membrane (De La Rocha et al., 2000). Therefore iron is often described as the proximate limiting factor for community production (Blain et al., 2002; Hutchins et al., 2001; Sedwick et al., 2002) but a co-limitation of iron and silicate is suggested for SO diatoms (Leblanc et al., 2005). It is further suggested that besides

growth parameters phytoplankton composition is also affected by iron and silicate and the sensitive interaction of both in the SO (Banse, 1991; Hutchins et al., 2001; Leblanc et al., 2005). Iron requirements of different diatom species seem to be variable and dependent on their photosynthetic architecture as published by Strzepek and Harrison (2004). They describe that open ocean diatoms have developed low iron requirements in general, while coastal species have the ability to adapt to low Fe. This would suggest that diatoms of low Fe regions, such as the SO, can maintain high growth rates under low Fe because they have developed a photosynthetic apparatus that is as effective as others under high Fe.

The extremely deep mixing and the resulting low light intensities are discussed as a third main factor influencing algal growth in the SO (Mitchell et al., 1991; Timmermans et al., 2001; van Oijen et al., 2004). A significant negative correlation of the wind mixed layer (WML) depth and maximum chlorophyll a concentrations (mg m^{-3}) were found in almost all *in situ* iron fertilization experiments (de Baar et al., 2005). Since light serves as the source of energy for photosynthesis, light intensity and duration determines the degree of photosynthetic activity. The majority of intracellular iron is required in the photosynthetic apparatus and iron limitation lowers the photosynthetic efficiency of phytoplankton (Greene et al., 1994). This suggests that phytoplankton species growing in iron limited regions are suffering more from low light conditions. In other words the cellular iron demand is enhanced under low irradiation (Raven, 1990; Strzepek and Price, 2000). Light limited cells of the diatom *Thalassiosira weissflogii* contained four times more Fe per C compared to controls (Strzepek and Price, 2000). Based on these findings they suggest that photoacclimation of phytoplankton could be affected by the availability of Fe and that Fe limitation could be modulated by light. Since the SO is characterized by low iron and low light conditions most of the year, phytoplankton growth is thought to be co-limited by both factors in this High Nutrient Low Chlorophyll (HNLC) region (Timmermans et al., 2001). However, laboratory experiments suggest species specific differences in the exact impact of iron and light co-limitation (Sunda and Huntsman, 1997; Timmermans et al., 2001).

Here we present the first study examining the effect of iron, light, and silicate co-limitation on two Antarctic diatom species *Actinocyclus sp.* and *Chaetoceros dichaeta* and one

cosmopolitan species *Chaetoceros debilis*, all isolated in the SO, in laboratory experiments. The species are important contributors to the phytoplankton community in the SO and were chosen because of their different size in order to investigate possible size dependent reactions. Further, both *Chaetoceros* species are chain forming and we intended to compare those to a solitary species. We especially turned our attention to the interaction of these three abiotic factors on diatom growth, as well as on physiological conditions and morphologies, and the implications for the SO phytoplankton community structure and paleooceanographic record.

Material and methods:

The three diatom species *Actinocyclus sp.*, *Chaetoceros dichaeta*, and *Chaetoceros debilis* were isolated on board RV "Polarstern" during the SO iron fertilization experiments EisenEx (*Actinocyclus sp.*) and EIFEX (*Chaetoceros dichaeta*, and *Chaetoceros debilis*). Single cells were isolated under a light microscope using small glass pipettes and rinsed at least three times in sterile filtered Antarctic seawater.

The species were grown under iron limitation in the IfM-GEOMAR culture collection at 3 °C. Special care was taken to prevent contamination with iron. Every procedure was done under trace metal clean conditions in a laminar flow bench. All materials coming into contact with the cultures and/or the medium were HCl rinsed before use. Sterile filtered Antarctic seawater enriched with macronutrients, vitamins, and EDTA buffered trace metals (except for iron), all in f/2 concentrations, was used as culture medium. The light climate was 30 µmol photons m^{-2} s^{-1} provided by cool fluorescence tubes (OSRAM FLUORA L18 W/77 and BIOLUX 18 W /965) at a 16 h : 8 h light : dark cycle.

Sub samples of the same start cultures were transferred to the eight different treatments with three replicates each for every species and treatment (table 1). The culture media for all experimental treatments was prepared as described above except for iron and silicate concentrations. Handling during the experiment was again done under trace metal clean conditions as described above. In the four low iron treatments no iron was added to the culture media and the picomolar iron concentrations in the Antarctic seawater are buffered by the EDTA addition. In the four high iron treatments 100 nM Fe were added.

In these treatments free iron concentration were 1.55 nM Fe' (all inorganic Fe species) estimated after Timmermans et al. (2001).

The iron, silicate, and light conditions of the different treatments are shown in table 1. The high silicate treatments were grown in 200 μM Si, which is the concentration commonly recommended in f/2 media for diatoms. The 10 times lower Si concentrations in the low Si treatments (20 μM Si) resulted in a NO_3^- : $Si(OH)_4$ ratio of 44, which is close to the ratio that can be found in low Si regions of the Southern Ocean, where Si concentrations are depleted to < 1 μM (Brzezinski et al., 2005; Coale et al., 2004; Franck et al., 2000; Sigmon et al., 2002). The light : dark cycle was kept at 16 : 8 hours for all treatments. All cultures were grown in 250 ml polycarbonate bottles. Before use the bottles were HCl cleaned three times for at least 48 hours followed by triple rinsing with Milli-Q water.

Table 1: Iron and silicate concentrations and light intensities of the eight treatments A-H.

Treatment	Iron	Light μmol photons m^{-2} s^{-1}	Silicate μM
A	No addition	30	200
B	No addition	30	20
C	No addition	90	200
D	No addition	90	20
E	1.55 nM Fe'	30	200
F	1.55 nM Fe'	30	20
G	1.55 nM Fe'	90	200
H	1.55 nM Fe'	90	20

Because of the extremely different growth behavior, sampling times and experiment periods were different between the species and partly between the treatments as well. Sampling times for cell counts, Fv/Fm, and Chl measurements are listed in table 2.

Table 2: Sampling times of cell counts, Fv/Fm, and Chl measurements in the three experiments.

Day	Cell counts	Fv/Fm	Chl
Actinocyclus sp.			
0	All treatments	All treatments	All treatments
3	All treatments	All treatments	
7	All treatments	All treatments	
11	All treatments	All treatments	
21	All treatments	All treatments	
28	All treatments	All treatments	
36	E, F, G, H	All treatments	
42	All treatments	All treatments	
46	All treatments	All treatments	All treatments
57	A, B, E, F	All treatments	
77		All treatments	A, B, E, F
Chaetoceros dichaeta			
0	All treatments	All treatments	All treatments
3		All treatments	
7		All treatments	
10		All treatments	
13		All treatments	
16		All treatments	
18		All treatments	
21	All treatments	All treatments	All treatments
23	A, C, E	All treatments	
28	B, C, D, F, G,	All treatments	
31		All treatments	
35		All treatments	
Chaetoceros debilis			
0	All treatments	All treatments	All treatments
6		All treatments	
9	A, B, D, E, F,	All treatments	All treatments
12	A, B, C, D, E,	All treatments	
15	C, D, F, G	All treatments	All treatments
21		All treatments	All treatments
27	All treatments	All treatments	All treatments
30			All treatments
47	A, E	All treatments	All treatments

In all high light treatments (C, D, G, and H see table 1) of *Actinocyclus sp.* no growth was detectable based on cell counts and Fv/Fm until day 46 so the experiment was stopped thereafter. In the low light treatments (A, B, E, and F) we followed the experiment until day 77, but only treatment E showed a significant increase in cell numbers and Chl concentrations after day 46. Therefore Fv/Fm and cell counts of the treatments A, B, and F are also only shown until day 46 (Fig. 1 and 2). Chl per cell was determined at day 46 for *Actinocyclus sp.*, day 21 for *Chaetoceros dichaeta*, and day 27 for *C. debilis* except for treatment F and H. Here Chl per cell was estimated at day 9 as Chl concentrations decreased thereafter.

Samples for chlorophyll measurements were filtered on GF/F filters (Whatman) and immediately stored at -20 °C until analysis. The frozen filters were put in polypropylene vials and 11 ml 90 % acetone and glass beads (2 mm and 4 mm) were added. Thereafter the closed vials were put in a cell mill for at least 5 minutes until the filters were completely homogenized. The vials were then centrifuged at -5 °C (10 min at 5000 rpm). The extract was carefully taken by a pipette and filled in 5 cm glass cuvettes. Extinction was measured photometrically based on Jeffrey and Humphrey (1975).

The photosynthetic efficiency (Fv/Fm) was measured using a PhytoPAM (Walz, Germany) based on Kolbowski and Schreiber (1995). Samples were dark adapted for 10 minutes and kept on ice directly before measurement.

For determination of cell numbers 2 ml samples were fixed with 40 µl Lugol's Solution (iodine – potassium iodide solution 1 %, MERCK) and stored at 3 °C in the dark until analysis. Cells counts were performed using light microscopy (Utermöhl and Axiovert 100) at different magnifications according to the size of the organisms. In each sample at least 500 cells were counted. In the *Actinocyclus* cultures, the whole sample volume was counted because of the very low cell numbers.

Fixation with Lugol's Solution broke cell chains after some months of storage, which was not expected by the authors. We therefore decided only to use data of chain length of samples counted within one week after fixation. Unfortunately this led to an incomplete dataset. In *C. debilis* cultures data of chain length had to be taken from different days for the same reason. Chain length was taken from day 9 (treatments A, B), day 12 (treatments

F, H and E) and day 15 (treatments C, D, G). Chain length of *C. dichaeta* was determined at day 21 of the experiment for all treatments.

Length and width of the cells were measured under the light microscope during counting. Assuming a cylindrical shape of the cells, cell volume was calculated using the formula volume = $\pi \cdot (0.5 \text{ width})^2 \cdot \text{length}$.

For statistical analysis Students t-test was used. Differences found are reported as significant in the text if $p < 0.05$.

Results:

Morphological changes

Iron and silicate both had an effect on cell morphology in both *Chaetoceros* species. While cells grown under iron replete conditions had a healthier appearance, iron limitation led to a visible loss in cellular chlorophyll concentrations in *C. dichaeta* and *C. debilis* (Fig. 1 and 2). Under silicate limitation a distinct elongation of the cells was observed (Fig. 1 and 2, treatment B, D, F, H). Iron and silicate co-limitation resulted in frustule malformation in *C. dichaeta* (Fig. 2, treatment B and D). No visible effect of light intensity on cell morphology could be established for both *Chaetoceros* species. *Actinocyclus* showed no clear differences in cell morphology in the different treatments. The variance in cell size and pigmentation shown in Fig. 3 was found in all treatments. However, in treatment F the cells had a higher cellular chlorophyll content. All morphological changes described here were found in at least 60 % of all cells; in most cases all cells were affected.

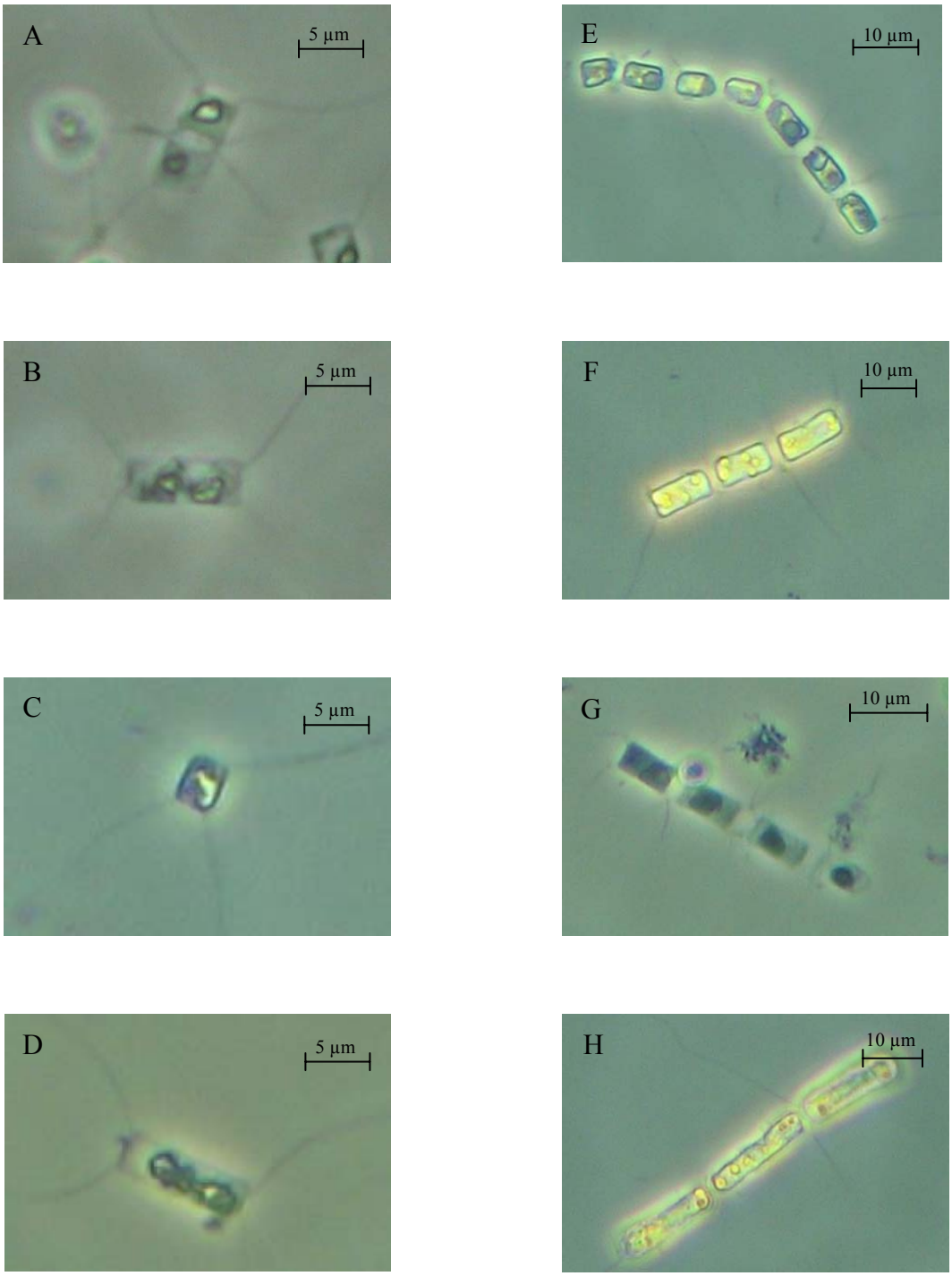

Figure 1: Light microscopy pictures of *C. debilis* in the treatments A-H.

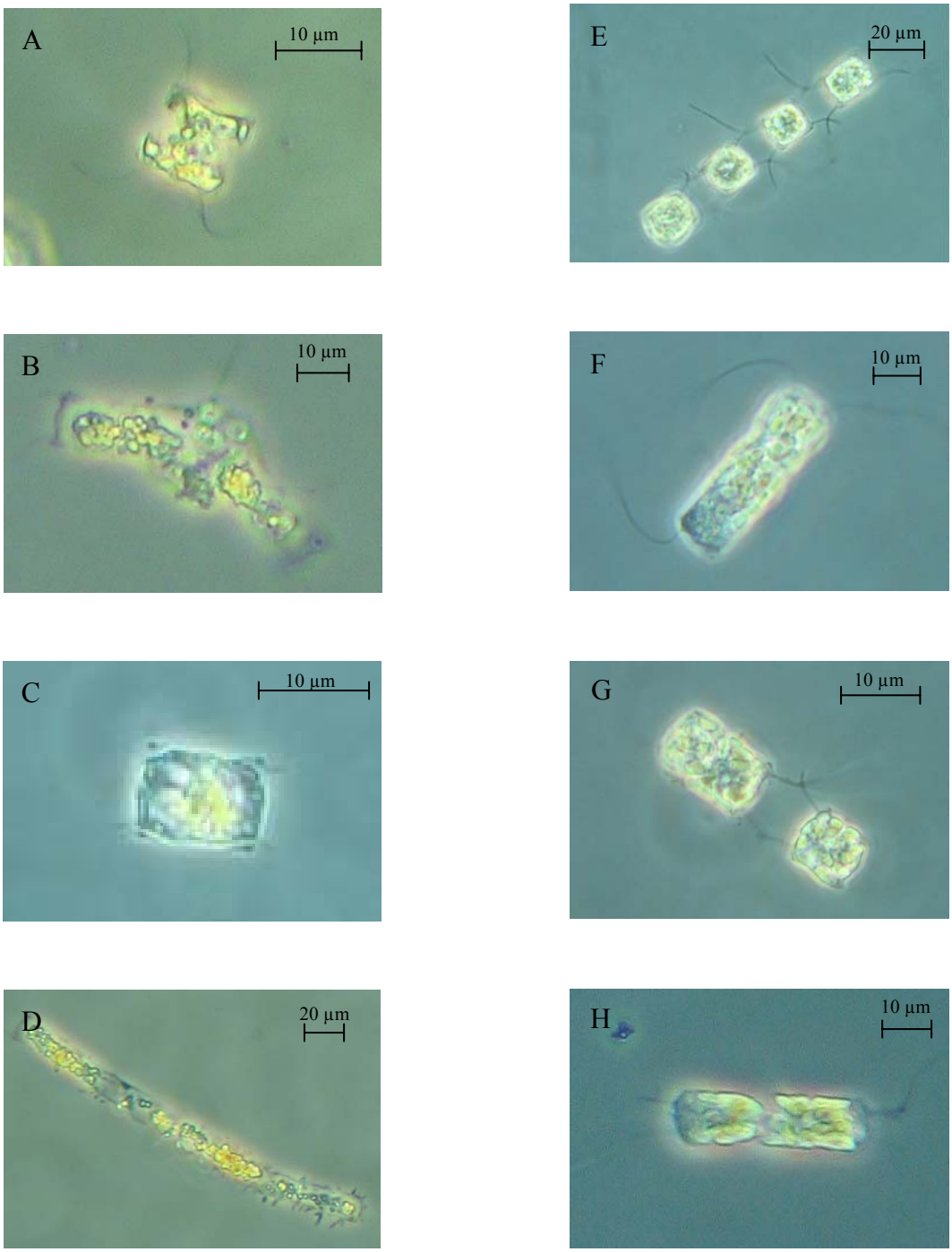

Figure 2: Light microscopy pictures of *C. dichaeta* in the treatments A-H.

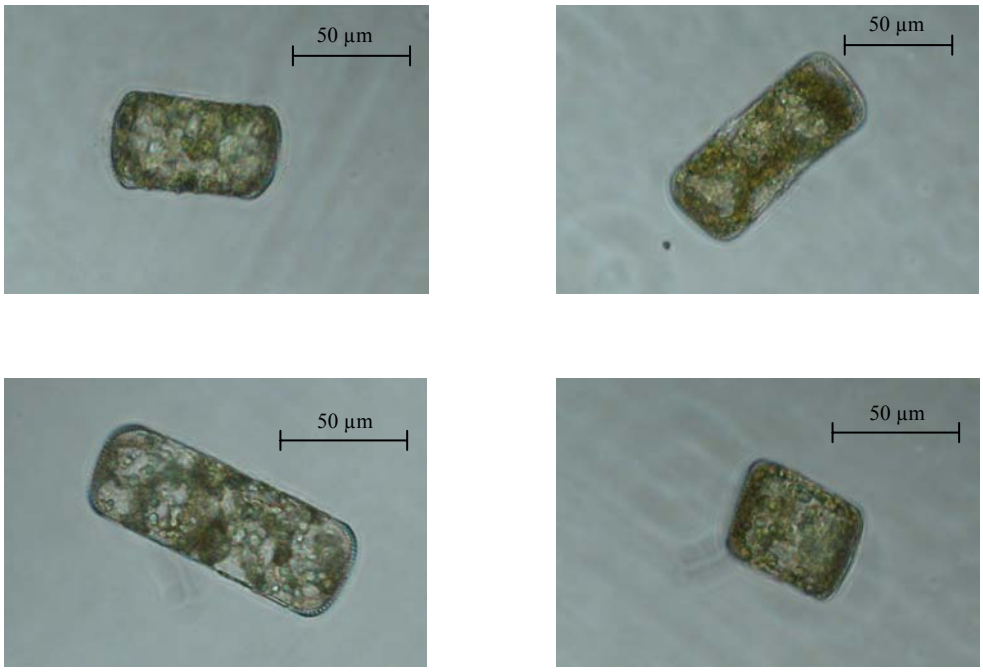

treatment F

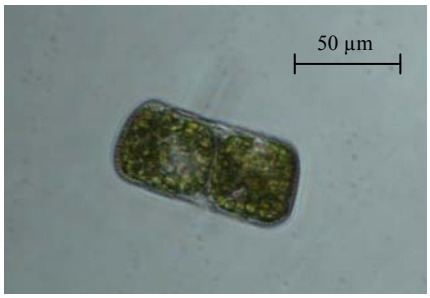

Figure 3: Light microscopy pictures of *Actinocyclus sp.* The variance in cell size and Chl content was found in all treatments. In treatment F (picture of dividing cell) all cells had visibly higher Chl concentrations per cell concentration.

Growth in iron limited and replete cultures

Under typical SO conditions with low iron concentrations and a low light environment (treatment A and B) the three diatom species *Actinocyclus sp*., *Chaetoceros dichaeta*, and *C. debilis* were able to grow moderately except for *Actinocyclus* in treatment A (Fig. 4 A and B). High silicate concentrations (treatment A) enhanced maximum cell numbers 14.9 times in *C. debilis* and 5.5 times in *C. dichaeta*, while *Actinocyclus* surprisingly showed no significant increase in cell numbers in treatment A. For all cultures Fv/Fm values were between 0.23 and 0.3 at the beginning of the experiment (Fig. 5) indicating iron limitation (Greene et al., 1992). Unlike *Actinocyclus*, both *Chaetoceros* species showed increasing Fv/Fm values within the first days of the experiment to a maximum of 0.4 (A) and 0.45 (B). In the low silicate cultures (B) the values decreased more rapidly and were slightly lower than those of the high silicate cultures (A) after day 10.

Low iron and high light conditions (treatment C and D) mimic natural SO conditions under shallow mixing. This increase in light intensity compared to the treatments A and B did not increase growth of all species tested. *Actinocyclus* cultures did not grow at all under these high light conditions. Both *Chaetoceros* species showed almost no difference between the high and low light conditions under low silicate concentrations (B compared to D). In *C. dichaeta* we observed a significantly lower increase in cell numbers under high silicate and high light conditions (C compared to A). In *C. debilis* the increase in cell numbers was initially higher in the high light treatment C compared to the low light treatment A. However, the culture grew longer under low light conditions, reaching about three times higher maximum cell numbers. Fv/Fm values for *Actinocyclus* and *C. debilis* were slightly lower compared to the low light treatments A and B.

Under high iron and low light conditions (treatment E and F) growth of all cultures was higher in the high silicate treatment E compared to all low iron treatments A – D. In the low silicate treatment (F) only the growth of *Actinocyclus* was higher compared to the equivalent low iron treatments, while both *Chaetoceros* species showed similar or even lower growth. The increase in cell numbers under high silicate concentrations in treatment E was more than 10 times higher in *C. dichaeta* and almost 40 times higher in *C. debilis* compared to treatment F. Interestingly, besides absolute growth, silicate also seems to

influence the growth behavior. Under low silicate concentrations (F) *Actinocyclus* had higher cell numbers in the beginning and was not overtaken by treatment E until day 42. *C. debilis* seems to have a longer lag phase under high silicate conditions as well. For *C. dichaeta* no cell counts in the beginning of the experiment were available. Fv/Fm values in both treatments were higher for all cultures compared to all low iron treatments. Maximum Fv/Fm values were highest in *C. debilis* cultures in both treatments reaching 0.69 (E) and 0.63 (F). However, in this species the Fv/Fm values decreased rapidly in treatment F after day 9.

Under high iron and high light conditions (G and H) no growth was detectable in the *Actinocyclus* cultures and *C. dichaeta* cultures. Only the diatom *C. debilis* was able to grow and increased its cell numbers was 20 times higher under high silicate concentrations in treatment G. Compared to the low light treatments E and F there was no significant difference in the first 27 days. However, as *C. debilis* continued growing until day 47 in treatment E, maximum cell numbers in treatment G were significantly lower. This observation is comparable to the lower maximum cell numbers in the low iron treatments C compared to A. The Fv/Fm values for all cultures were significantly lower compared to the same iron and silicate conditions under lower light (E and F). In the *Actinocyclus* cultures Fv/Fm values directly decreased below 0.2 in all treatments. While *C. debilis* showed highest maximum Fv/Fm values in treatment G (0.59) almost no change compared to the start value was observed in the low silicate treatment H. Here *C. dichaeta* cultures showed highest maximum values with 0.47.

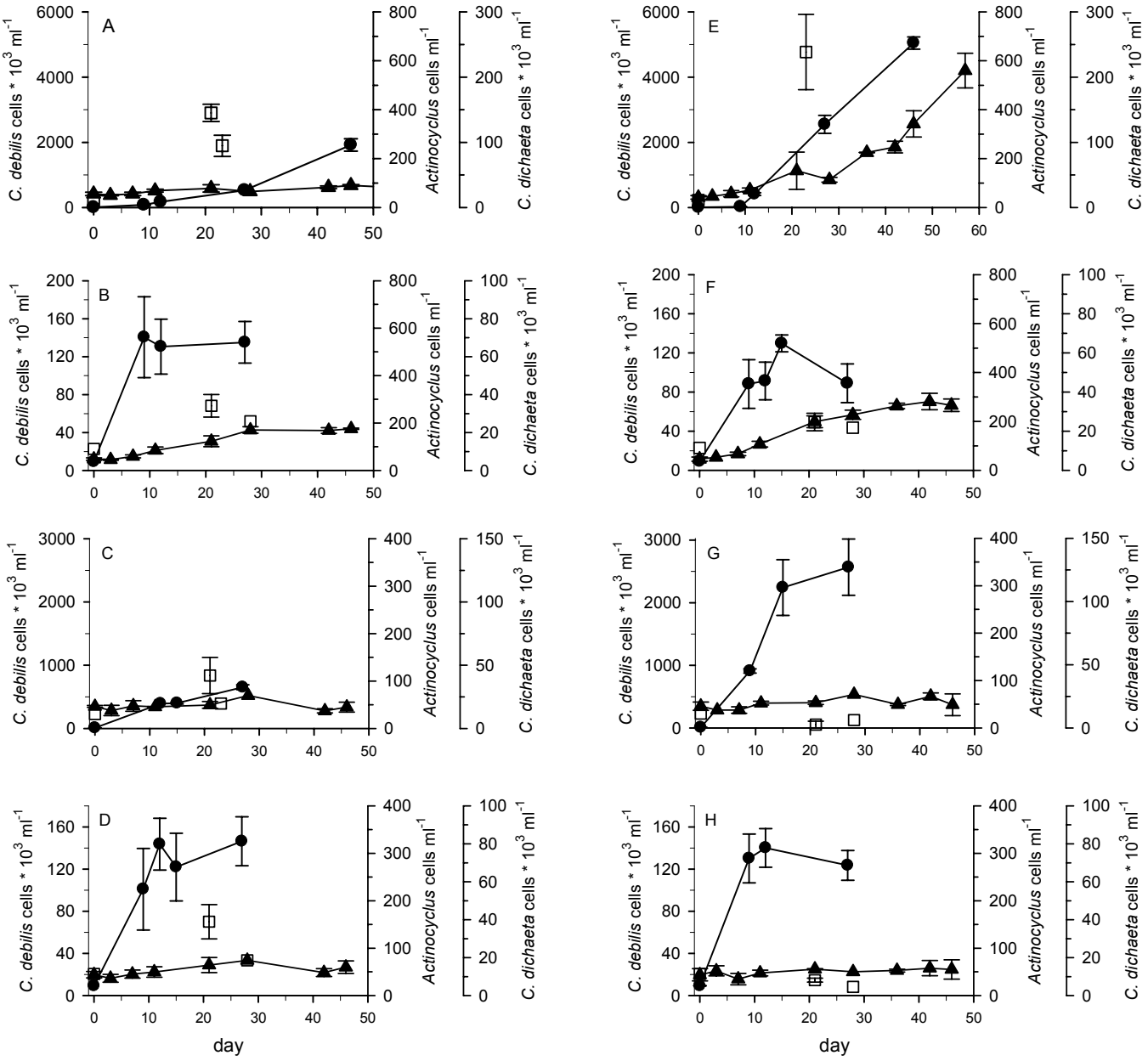

Figure 4: Cell counts of the three species *Actinocyclus sp.* (dark triangles), *Chaetoceros dichaeta (open squares)*, and *C. debilis* (dark circles) grown at the eight different treatments A-H. Note different scales for different treatments.

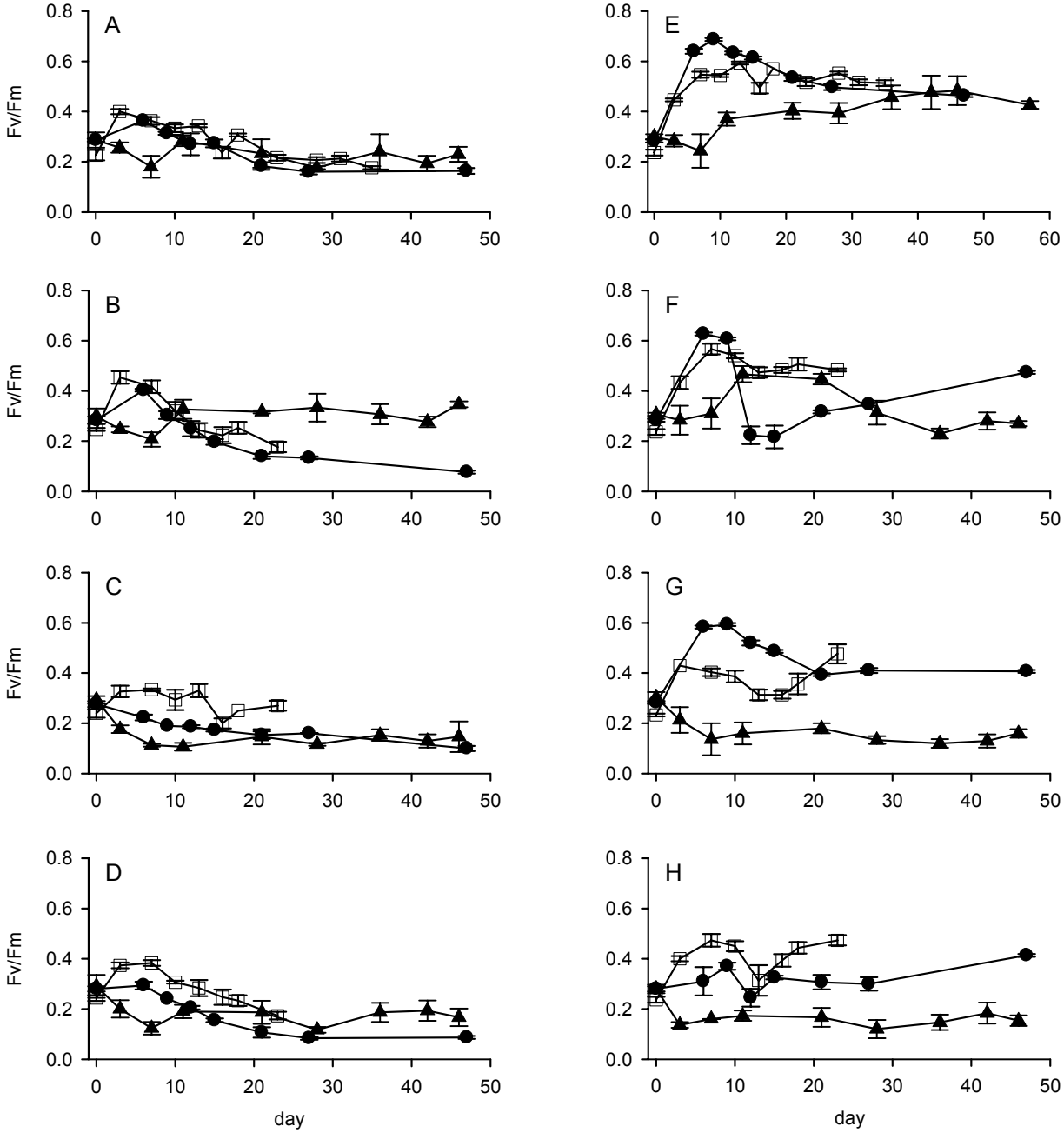

Figure 5: Fv/Fm of the three species *Actinocyclus sp.* (dark triangles), *Chaetoceros dichaeta (open squares)*, and *C. debilis* (dark circles) grown at the eight different treatments A-H.

Cellular chlorophyll and cell volume

In cultures of *Actinocyclus sp.* cellular chlorophyll concentrations were 0.08 ± 0.01 ng cell^{-1} (Fig. 6) and showed no significant difference between the treatments except for treatment F (0.16 ng cell^{-1}). In both *Chaetoceros* species cellular chlorophyll concentrations increased under low light conditions, low silicate, and under high iron concentrations. Like in *Actinocyclus*, the combination of these three factors in treatment F resulted in highest cellular chlorophyll concentrations in both *Chaetoceros* species (4.9 pg cell^{-1} in *C. dichaeta* and 0.45 pg cell^{-1} in *C. debilis*). The high cellular chlorophyll concentrations of *Actinocyclus* and *C. debilis* are clearly visible in the microscopic pictures (Fig. 1, 3).

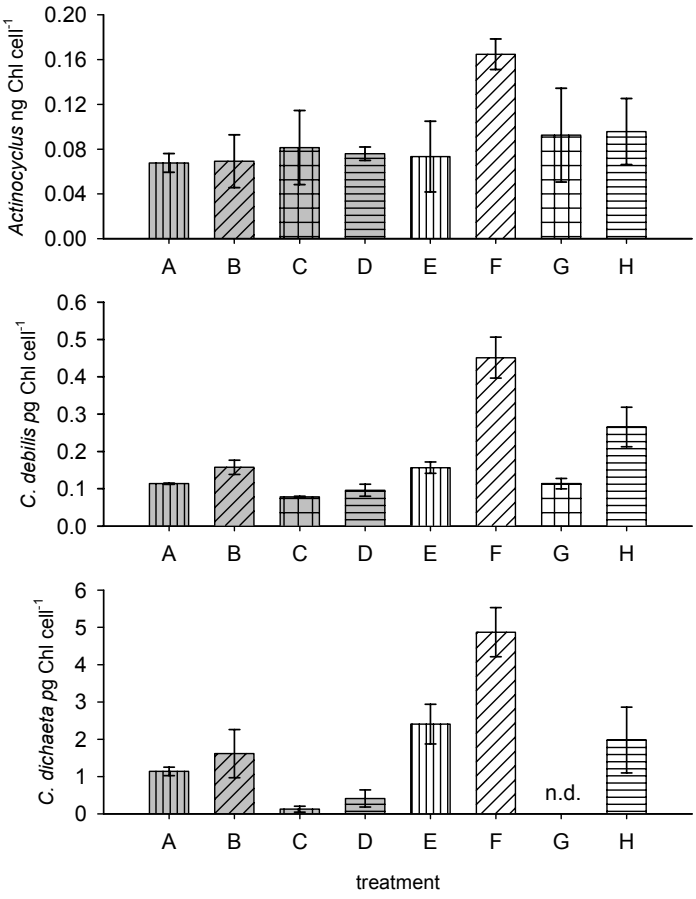

Figure 6: Cellular chlorophyll concentrations of the three species *Actinocyclus sp.* (day 46), *Chaetoceros dichaeta* (day 21), and *C. debilis* (treatment F and H day 9, all others day 27) grown at the eight different treatments. For the *C. dichaeta* cultures chlorophyll values for treatment G are missing so no chlorophyll per cell values could be estimated.

The effect of nutrient limitation on cell size was again species specific (Fig. 7). In cultures of *Actinocyclus* cell volume was between 96297 and 152440 µm³ and showed no significant changes between the eight different treatments. However, this species only grew in the three treatments B, E, and F and here cell volume was slightly lower compared to the others. In both *Chaetoceros* species cells grown under iron limitation tended to be smaller compared to the same light and silicate conditions under high iron concentrations respectively (compare treatments A and E; B and F; C and G; D and H). However, the effect of iron on cell volume was minor and often not significant compared to the effect of silicate. In *C. dichaeta*, silicate limitation led to a significant increase in cell volume of up to 4.7 times (treatment C and D). In *C. debilis* cultures, cells grown under silicate limitation again showed a significantly higher increase in cell volume of almost three times. In both species, this increase in cell volume under low silicate conditions was caused by the elongation of cells (Fig. 1 and 2).

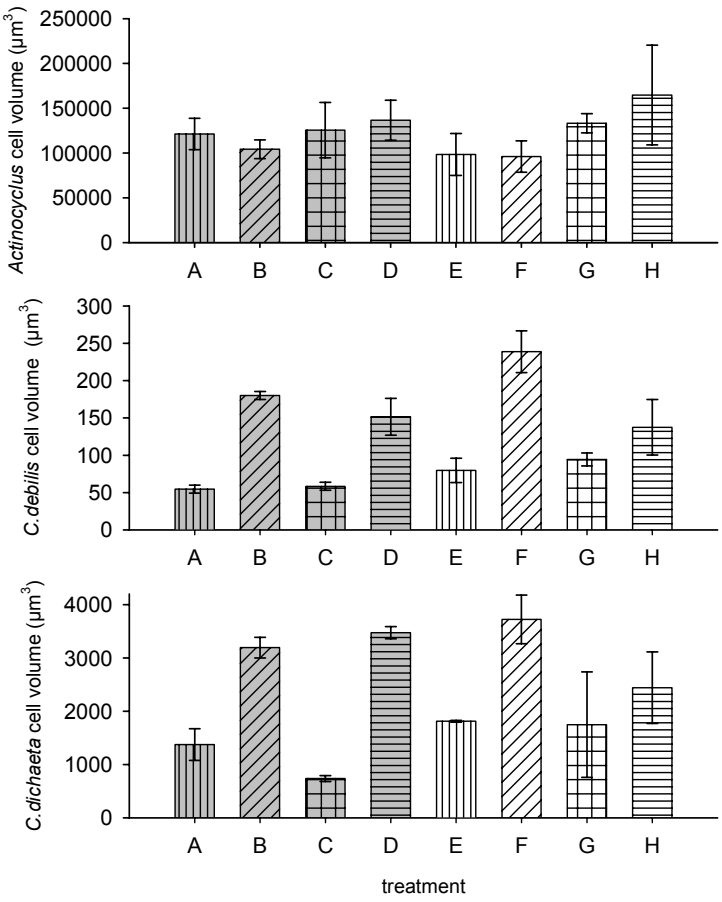

Figure 7: Cell volume of the three species *Actinocyclus sp.* (day 46), *Chaetoceros dichaeta* (day 21), and *C. debilis* (day 27) grown at the eight different treatments.

As both cellular chlorophyll concentrations and cell volume were affected by iron, silicate, and light, we determined chlorophyll concentrations per cell volume to be able to better compare the treatments. In *Actinocyclus* mean concentrations of chlorophyll per cell volume were 0.0006 pg μm^{-3} and showed no significant difference except for treatment F (Fig. 8). Here the values were three times higher (0.0018 pg μm^{-3}). In both *Chaetoceros* species mean chlorophyll per cell volume tended to be higher in the high iron treatments with mean values of 0.012 pg μm^{-3} in *C. dichaeta* and 0.018 pg μm^{-3} in *C. debilis*. As silicate limitation increased cell volume stronger than cellular chlorophyll concentrations, chlorophyll per cell volume was lower in the low Si treatments except for treatment F in *C. dichaeta*. High light intensities also lowered the concentrations of chlorophyll per cell volume. This effect was strongest in *C. dichaeta* under low iron concentrations.

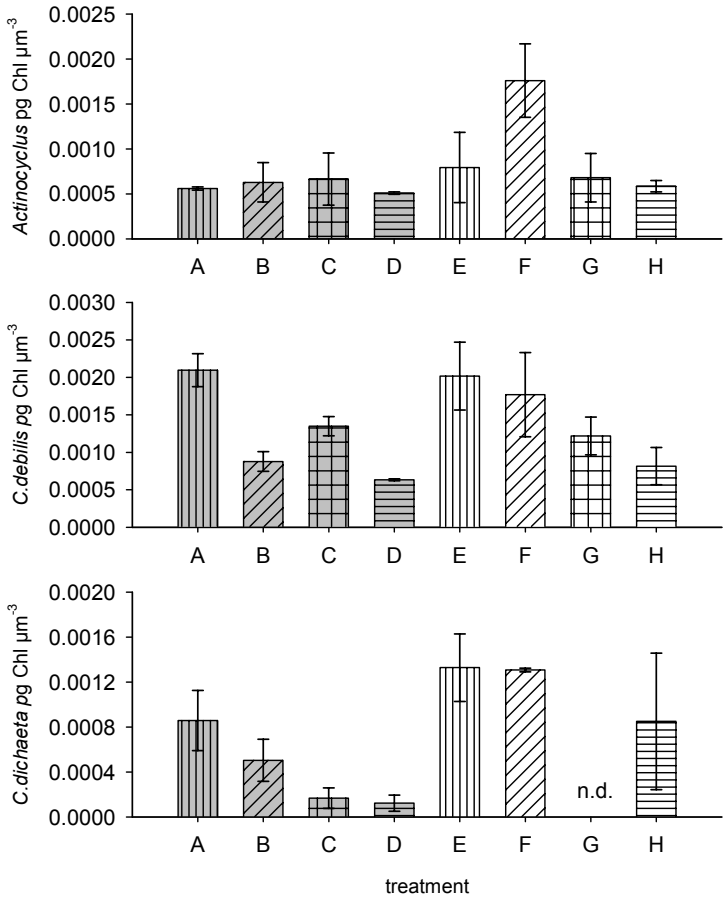

Figure 8: Chl per cell volume in *Actinocyclus* (day 46), *Chaetoceros dichaeta* (day 21), and *C. debilis* (day 27) grown at the eight different treatments. For the *C. dichaeta* cultures chlorophyll values for treatment G are missing so no chlorophyll per volume values could be estimated.

Chain length

Chaetoceros dichaeta and *C. debilis* are both chain forming diatoms. The chain length of both species was influenced by iron, light, and silicate (Fig. 9 A, B). In the low iron treatments of *C. dichaeta* cultures 90 % of all cells were single cells or in 2 - 3 cell chains (Fig. 9 A). The chain length in the iron replete treatments seemed to be influenced more by light and silicate availability than in *C. debilis* cultures. No significant changes compared to the low iron treatments were found in treatments G and H. Longest chains were found in the high iron, low light treatment E where 50 % of all cells were in chains of 3-5 (E) cells. In treatment F there also was a small tendency towards longer chains. In all *C. debilis* cultures grown under iron limitation, 90 % of all cells were single cells or in two cell chains (Fig. 9 B). High iron concentrations resulted in an increase in chain length except for the high light, low silicate treatment (H). The increase in chain length was highest in the two high iron, high silicate treatments G and E. Here 50 % of all cells were in chains of 1 - 4 (E) and 2 - 5 (G) cells. Additionally, in treatment G up to 16 cells per chain were occasionally observed (<5 %, data not shown). In the high iron, low light, low silicate treatment (F) the increase in chain length was slightly higher compared to the low iron treatments.

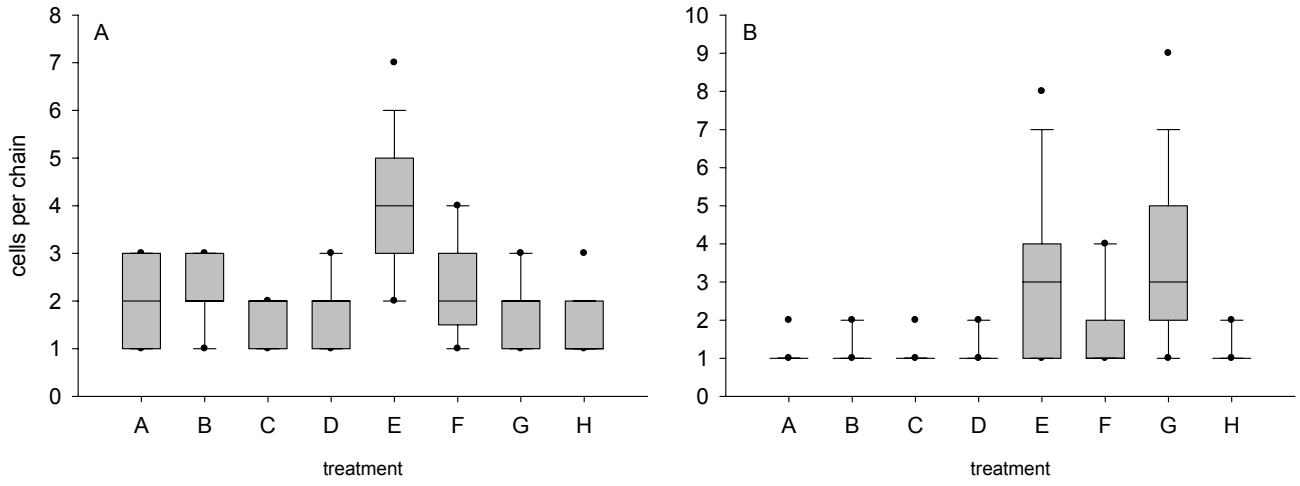

Figure 9: Chain length of *C. dichaeta* at day 21 (A) and *C. debilis* (B) at day 9 (treatments A, B), day 12 (treatments F, H and E) and day 15 (treatments C, D, G). The boundary of the box closest to zero indicates the 25th percentile, the line within the box marks the median, and the boundary of the box farthest from zero indicates the 75th percentile. Whiskers (error bars) above and below the box indicate the 90th and 10th percentiles and dark points indicate the 95th and 5th percentile.

Discussion:

The Southern Ocean is the largest HNLC region of the worlds' oceans where various factors suppress growth of primary producers despite the generally high nitrate concentrations. The low iron concentrations in the SO are known to limit algal growth in general while diatoms are additionally limited by low silicate concentrations north of the PFZ. The wind mixed layer depth in the SO is generally high and can reach up to about 100 m after storm events (de Baar et al., 2005). Because of these deep mixing events the phytoplankton cells are often exposed to very low light intensities, which are thought to additionally limit the photosynthetic activity and thus growth.

In this study we examined the effect of co-limitation of the three main parameters that may limit diatom growth in the SO: iron, silicate, and light in laboratory experiments. We are aware that laboratory experiments can only try to imitate nature and never create a truly natural environment. However, while focusing on certain key variables under controlled laboratory conditions, information about some adaptation strategies will be obtained.

The nutrient concentrations in culture media are usually much higher compared to natural conditions. This is necessary to reach sufficient biomass in a relatively small volume so that there is enough material for analysis. Nutrient concentrations that would be considered high in the field, such as the 20 μM silicate, were suitable for our low Si treatments due to the much higher biomass and showed to reduce algal growth in our experiments.

The effect of nutrient limitation on morphology

The SO is known to be a major sink of biogenic opal in the worlds' ocean and most of this opal consists of diatom frustules that grow in the euphotic zone and sink to the seafloor in aggregates or fecal pellets. Frustules found in SO sediments are commonly used to reconstruct past variations in sea surface temperature (Crosta et al., 2005; Kunz-Pirrung et al., 2002), sea ice cover (Armand et al., 2005; Gersonde and Zielinski, 2000), drifting of tropical/subtropical species to higher latitudes (Romero et al., 2005), and to trace pathways of Antarctic Bottom Water (Zielinski and Gersonde, 1997). Thereby often

the identification down to species level is essential as some species can be used as indicators for the above mentioned parameters. Nutrient limitation that may affect frustule morphology as described in this study can therefore cause difficulties in species identification and lead to misinterpretation.

The genus *Chaetoceros* is one of the most abundant diatom genera in the ocean and its distribution covers most environments from coastal temperate to polar regions. The genus is composed of about 180 species and many of them are found in the Southern Ocean. Usually *Chaetoceros* species are relatively slightly silicified compared to other diatoms, which makes them more sensitive to remineralization and leads to poorly preserved siliceous remains in sediments of the open SO. *Chaetoceros* is known to prefer nutrient rich conditions and in the SO this genera is mainly found in near shore sediments (Armand et al., 2005; Zielinski and Gersonde, 1997). In the East Antarctic Margin *Chaetoceros* species dominate the phytoplankton community and partly pure *Chaetoceros* ooze can be found in the sediments (Stickley et al., 2005). In these regions, *Chaetoceros* frustules in the sediment are used as an indicator for seasonal changes and spring sea ice melting events (Stickley et al., 2005), which are known to increase nutrient concentrations. Our data show that besides the known effects of remineralization and destruction due to grazing, frustule morphology is also affected by nutrient availability. Under Si and Fe co-limitation the frustules of *C. dichaeta* were clearly malformed and fragile while *C. debilis* and *Actinocyclus* did not show such morphological changes. This observation could be another reason for the poorly preserved *Chaetoceros* frustule in the sediments of the open SO and it is possible that *Chaetoceros* abundances in the euphotic zone are thus underestimated. To our knowledge no such malformation of SO diatom frustules in the field is described in the literature and we can not exclude that part of these morphological changes may be artifacts due to culturing. However, it is very likely that, if they are abundant in the field, malformed frustules would not be identified correctly if found in water samples or sediments. Even though it will not be possible to exactly count cell numbers if the frustules are malformed and poorly preserved, the recognition of those could be a hint for iron and silicate co-limitation in the euphotic zone. Our data could therefore provide a helpful contribution to visually identify nutrient limitation in *C. dichaeta* and possible other SO diatoms.

The observation that cells of both *Chaetoceros* species were elongated under silicate limitation are similar to those reported by Harrison et al. (1977). This suggests that low silicate concentrations not only influence the build up of new frustule material but also the mechanism of cell division itself. The cell cycle is classically divided in four phases the G1, S, G2 and M. While DNA is replicated during the S phase and mitosis and cell division take place in the M phase, G1 and G2 refer to "gaps" in between those processes. During these "gaps" most of the cell growth takes place (see review in Ragueneau et al., 2000). Silicon uptake and the formation of new frustules by diatoms are non-continuous processes that are confined to the G2 phase (Brzezinski, 1992; Brzezinski et al., 1990). It is described in the literature that nutrient limitation in general and resulting low growth rates leads to elongated G2+M phases and thus increased total silicate uptake (Claquin et al., 2002). However, cells grown under Si limitation may not be able to reach a certain intracellular silicate concentration. They may remain in the G2 phase and therefore do not enter the M phase and do not divide. We can only speculate what causes the extreme elongation of the cells under Si limitation (Fig. 1 and 2), but they may have some kind of regulatory process that stops them from dividing until they have collected a minimum amount of silicate as the new frustules may otherwise be too fragile. However, we observed that the cells continued building up plasma and that the girdle band continued growing, which resulted in the elongated shape. Similar morphological changes are described for diatoms under silicate limitation in the field and in laboratory experiments (Harrison et al., 1977; Paasche and Østergren, 1980) and are also explained by continued cell growth while cell division is blocked.

Besides the effect on growth and cell morphology, iron and silicate also influenced chain length in both *Chaetoceros* species (Fig. 9). Both species had the highest number of cells per chain under high iron and high silicate conditions. In *C. debilis* this was independent of light intensity while in *C. dichaeta* chain length was only longer in the low light treatment. The formation of chains is an important and effective way to prevent grazing (Fryxell and Miller, 1978; Pahlow et al., 1997). Besides the species specific effects of iron, light, and silicate on growth, such differences in grazing protection will have additional impacts on species composition under changing nutrient concentrations in the SO. Based on these findings we propose that under favorable nutrient conditions the cosmopolitan species *C.*

debilis can benefit from long cell chains as grazing protection independent of the season while *C. dichaeta* would be at a disadvantage at higher light intensities during periods of shallow mixing.

The effect of light intensity

Light limitation is thought to be one major reason for low phytoplankton biomass and drawdown of nutrients in the euphotic zone of the SO. Mitchell et al. (1991) modeled that under the deep mixing conditions given in the SO, only ~ 10 % of the available nutrients could be utilized due to light limitation. In accordance with this model, a negative correlation between WML depth and chlorophyll concentrations (mg m^{-3}) was observed in *in situ* iron fertilization experiments (de Baar et al., 2005). However, when integrated to mixed layer depth, chlorophyll concentrations during EIFEX were the highest compared to all other *in situ* iron fertilization experiments despite the very deep mixing (Peeken et al. unpublished data).

The importance of iron for photosynthesis stems from high concentrations in the photosystem I and II and the cytochrome b_6f complex (Raven, 1990). Under low light intensities the production of light-harvesting pigments is enhanced and thus the cellular iron requirements increase (Strzepek and Price, 2000; Sunda and Huntsman, 1997). In regions like the SO where iron is limiting, low light intensities are therefore likely to co-limit phytoplankton growth. However, it has been described recently that the oceanic diatom species *Thalassiosira oceanica* had a much lower concentration of the iron rich parts of the photosynthetic apparatus, photosystem I and cytochrome b_6f complex, compared to the coastal species *T. weissflogii* (Strzepek and Harrison, 2004). This leads to a significant decrease in cellular iron demand while growth and photosynthetic efficiency stayed at a high level, comparable to those of the coastal species. Whereas the exact physiological mechanisms remain unknown so far, this apparent paradox is explained by a higher effective absorption cross-section and turnover rate of photosystem I in the open ocean species, possible in adaptation to the low natural iron concentration (Strzepek and Harrison, 2004). Similar adaptation strategies could enable SO diatoms to sustain high growth under iron and light conditions that would limit other species.

In this study we could not find a general limiting effect of low light intensity. *Actinocyclus sp.* and *C. dichaeta* were clearly not light limited grown under 30 µmol photons m^{-2} s^{-1}. This equals about the light intensity in 16 to 42 m depth, depending on surface radiation in the open SO during EIFEX (Röttgers pers. comm.). However, in the field phytoplankton cells are never exposed to constant light intensities but undergo permanent changes in the light climate due to mixing and changes in weather conditions. Assuming surface irradiances of 100 or 500 µmol photons m^{-2} s^{-1} phytoplankton cells would be exposed to mean light intensities of 30 µmol photons m^{-2} s^{-1} when mixed between surface and 44m or to more than 200 m, respectively. Although this assumption is very theoretical it suggests that mixing depths of about 100 m, as commonly observed in the SO, may on average not result in a limiting light climate.

In our experiments, an increase by a factor of three to 90 µmol photons m^{-2} s^{-1} (mean light intensity in 1-28 m depth) at the same light : dark cycle suppressed growth and photosynthetic efficiency of *Actinocyclus* under low and high iron concentrations and of *C. dichaeta* under high iron concentrations. In contrast to our findings, laboratory experiments with single species and deck incubations with natural phytoplankton assemblages suggest an iron and light co-limitation of the SO phytoplankton. Although these experiments are difficult to compare as some laboratory experiments were not performed with SO phytoplankton species (Strzepek and Harrison, 2004; Strzepek and Price, 2000; Sunda and Huntsman, 1997) and light intensities differ from 20 to about 900 µmol photons m^{-2} s^{-1} and from light : dark cycles of 12 : 12 to 24 : 0 hours (de Baar et al., 1990; Martin et al., 1990; Sunda and Huntsman, 1997; Timmermans et al., 2001), it can be summarized that smaller species are reported to be less affected by iron and light co-limitation compared to larger ones. Timmermans et al. (2001) for example report that *C. dichaeta* was only able to grow at a light : dark cycle of 20 : 4 hours at 80 µmol photons m^{-2} s^{-1} while no growth was detected under the same light intensity at a light : dark cycle of 12 : 12 hours. They conclude that *C. dichaeta* is iron and light co-limited under short day conditions. However, in these experiments the absolute amount of photons during one light period was 3.46 mol photons m^{-2}, which is exactly twice as much as in our low light experiments (1.73 mol photons m^{-2}). This shows that the duration of irradiance is more important than the light intensity itself. The light : dark cycle in culture experiments

simulates the time of year and therefore gives no information about possible reactions to changing WML depth.

Adaptation to low light in the SO was observed during the *in situ* iron fertilization experiment EIFEX. Although it is generally assumed that no net growth is possible below the 1 % light depth, relatively high primary production of 3.4 mg C m^{-3} d^{-1} was observed at depth with 0.1 % of the surface light intensity (Peeken et al. unpublished data). The phytoplankton community of the SO is therefore able to maintain positive growth at extremely low light intensities. Similar adaptation strategies are also known for ice algae and benthic diatoms, which usually only get less than 0.1 % of the surface light intensities (Admiraal, 1977; Thomas and Dieckmann, 2002). However, to our knowledge no such adaptation strategies are reported for pelagic diatoms in the SO.

Grown under high light intensity the three species tested here showed very different responses. While *Actinocyclus* was not able to grow in any of the high light treatments, *C. debilis* seems to be able to deal with higher light intensities as the increase in cell numbers was not significantly higher in most of the low light treatments. *C. debilis* is not endemic in the SO but more or less globally distributed (Anderson et al., 2004). This means that this species has to be adapted to a variety of very different light and nutrient environments. Besides, *C. debilis* may be more susceptible to grazing than larger species. Being able to sustain high growth rates under varying environmental conditions can therefore be essential to survive. Under shallow mixing conditions such "generalists" as *C. debilis* are likely to have an advantage over low light adapted species. Surprisingly *C. dichaeta* was able to grow under high light and low iron, while no growth was detected under high light and high iron. *C. dichaeta*, as a SO species, is subjected to the deep mixing of the SO and the resulting low light conditions. When iron becomes available this species may start to increase its photosynthetic efficiency to use the low light as effective as possible. It may then not be able to deal with a surplus of light energy.

Several studies show that species specific differences in the level of iron and light co-limitation exist (Sunda and Huntsman, 1997; Timmermans et al., 2001). Timmermans et al. (2001) conclude from their findings that mainly larger diatoms are iron and light co-limited and that low iron and low light conditions in the SO will favor the growth of small

diatoms. The reason why those can not build up high biomasses is assumed due to higher grazing pressure. The importance of grazing for the size distribution of the phytoplankton community will be discussed below. In contrast to Timmermans conclusion, our findings show that the large diatoms species tested here (*Actinocyclus* sp. and *C. dichaeta*) are not light limited but that higher light intensities have a negative effect on growth. A shallower mixing and the resulting higher irradiance would therefore not favor the growth of these larger diatom species. The observation that diatom blooms in the SO are dominated by large diatoms highlights the importance of grazing to suppress the biomass of smaller diatoms.

In conclusion we assume that the importance of light limitation in the SO is overestimated. On the other hand the importance of grazing to control the biomass of smaller diatoms and to allow larger species to bloom may have been underestimated. The species specific differences in the interaction of iron and light found here and in the literature may help to complete our understanding of the development of diatoms blooms under different environmental conditions in the SO.

The effect of Fe and Si limitation on diatom growth

In situ iron fertilization in the SO showed that community growth was more enhanced by iron addition in high silicate waters compared to low silicate waters (Coale et al., 2004; Coale et al., 2003; Leblanc et al., 2005). Similar to these findings from the field, growth of all three species tested in this study was clearly co-limited by iron and silicate, as highest cell numbers were reached in the high iron, high silicate, low light treatment.

Nutrient requirements are generally assumed to be linked to cell size as uptake rates are dependent on the surface to volume ratios (Chisholm, 1992; Morel et al., 1991). Thus smaller species are less affected by nutrient limitation compared to larger species. In this context Timmermans et al. (2001) describe that growth of the small Antarctic diatom *C. brevis* was not limited by low iron concentrations while the larger *C. dichaeta* was. In contrast to that a positive effect of iron on growth of the small diatom species *Fragilariopsis cylindrus*, *Cylindrotheca closterium*, *Chaetoceros* sp., and one unidentified pennate diatom during the *in situ* iron fertilization experiment EIFEX was described by Hoffmann

et al. (2006). Sedwick et al. (2002) suggested that larger diatom species might be more silicate limited and that these species therefore bloom in high silicate waters when iron becomes available. In agreement to that enhanced growth of small pennate diatoms with iron addition in high and low silicate waters is described by Hutchins et al. (2001). They assume that these small, lightly silicified species are highly adapted to low Si growth conditions. However, our results demonstrate that there are small species that do not react in this way. The negative effect of silicate limitation on growth was highest in *C. debilis*, the smallest species, and lowest in *Actinocyclus*, the largest species tested. Larger, strongly silicified species have a higher amount of silicate per cell and in absolute numbers more silicate is needed to build up new frustules. However, relative to cell volume the amount of silicate may be even higher in small species. Especially in combination with high growth rates, such small species may be limited earlier by low silicate concentrations than slow growing larger species. Further, the extent of Fe and Si co-limitation on growth of the three diatom species was again higher in the smallest species. Under low light conditions maximum cell numbers were 36 times (*C. debilis*), 7 times (*C. dichaeta*), and 3 times (*Actinocyclus*) lower under Fe and Si co-limitation compared to Fe and Si replete conditions. Thus our data suggest that the extent of iron and silicate co-limitation is not only dependent on cell size. The differences between the species tested here and others reported in the literature suggest that the influence of nutrient co-limitation in the SO is even more complex than hitherto assumed.

Possible explanations for these observations are differences in the physiological adaptations to nutrient limitation, such as the number and activity of membrane transport proteins, that might compensate the effect of cell size. It is generally accepted that iron limitation decreases the maximum specific uptake rate (V_{max}) for silicic acid in marine diatoms, while absolute values of V_{max} differ between species (De La Rocha et al., 2000; Franck et al., 2003; Leynaert et al., 2004). This is explained by a decrease in the number of active silicate transporters in the cell membrane under iron stress (De La Rocha et al., 2000). Alternatively, it is suggested that, as Si uptake in marine diatoms is linked to aerobic respiration, iron limitation decreases the electron transport efficiency of the iron rich respiratory chain and thus causes a decrease in V_{max} (Franck et al., 2003). Thus iron limitation decreases the capacity for silicic acid uptake in marine diatoms. This may be less

relevant in the high silicate regions of the SO, but north of the PFZ iron limited diatoms will be even faster co-limited by the low silicate availability. In this study we could not find a positive effect of iron addition under silicate limitation on growth of all three species tested. However, in *C. dichaeta* frustule malformation was only observed under iron and silicate co-limitation, while under low silicate and high iron conditions cells were elongated but frustules showed no visible malformation. This suggests a better silicate uptake under increased iron availability in this species. Brzezinski et al. (2005) hypothesize that diatom growth rates are limited by iron while biogenic silica production rates and cellular silicon content may be controlled by a combined influence of both iron and silicate. Our data show that iron and silicate both have a direct influence on diatom growth. Under silicate limitation both *Chaetoceros* species tested seemed to have problems reaching their intracellular silicate concentration needed for cell division. This is supported by the observation that cell volume is significantly higher in all low silicate treatments.

Besides the general decrease in V_{max}, the half saturation constant for silicic acid uptake (K_{Si}) is extremely different between diatom species and shows no collective trend under iron limitation (De La Rocha et al., 2000; Franck et al., 2003; Leynaert et al., 2004). This suggests that while iron may have an effect on the number of active Si transporters, their affinity for silicic acid is not Fe dependent and represents species specific properties (De La Rocha et al., 2000). Brzezinski et al. (2005) reported a decrease in K_{Si} during the *in situ* iron fertilization experiment SOFEX in the low Si waters of the north patch. They suggested that either iron lowers the half saturation constants for silicic acid of individual species or causes a species shift that favors diatoms with higher Si affinity. Besides the effect of the surface to volume ratio on nutrient uptake rates, species specific adaptation mechanisms such as the amount and activity of transport proteins in the cell membrane may have an important impact on iron and silicate uptake rates and therefore determine the level of iron and silicate co-limitation in SO diatoms.

Implications for the field

Artificial iron fertilization is performed with the aim to decrease atmospheric CO_2 concentrations by increasing the carbon export to the deep sea in HNLC regions. It is therefore important to investigate the effect of iron fertilization on the community structure and carbon export in high and low Si waters of the SO.

If persistent iron fertilization in low silicate waters would shift the phytoplankton community towards diatom species with lower K_{Si} and/or those who are able to decrease K_{Si} with increasing iron availability, these species would be able to increase biomass and therefore would rapidly deplete the Si concentrations. This is consistent with findings of Coale et al. (2004) who report that even though diatoms only accounted for less than 50 % of the total biomass under low Si conditions, this phytoplankton group showed the highest increase relative to initial values after iron fertilization in the low silicate SOFEX north patch. After a diatom bloom biogenic material is known to be effectively exported to the deep sea via aggregation. Therefore it can be suggested that the system would remain Si depleted. The resulting nutrient environment would make it impossible for diatoms to bloom until the next upwelling event supplies new Si. Other phytoplankton classes as prymnesiophytes, pelagophytes, and dinoflagellates would have the advantage and it is possible that they would dominate the phytoplankton community permanently. Diatoms are known to play a major role in carbon export to the deep sea, as the heavy silicate frustules have high sinking rates (Waite and Nodder, 2001). Other phytoplankton groups have less effective protection mechanisms, such as frustules and formation of cell chains, and are therefore exposed to higher grazing pressure compared to diatoms. Thus biomass in a non-diatom dominated system would be mainly exported as fecal pellets and remineralization and recycling production would be more effective (Dubischar and Bathmann, 2002). It can be speculated that persistent iron fertilization in low silicate waters and a possibly resulting shift in species composition towards a lower diatom contribution would therefore result in a system with less efficient carbon export.

Our results suggest that iron fertilization under high silicate conditions supports growth of large and small diatoms. The general observation that large diatoms bloom in the SO when iron becomes available (see review in de Baar et al., 2005; Hoffmann et al., 2006)

shows that other factors such as grazing determine species succession in an effective way. As mentioned above small grazers are very efficient in controlling the biomass of the small phytoplankton community. Large diatom species are known to be better protected against these grazers because of their size, the silica frustules, and the formation of cell chains. In addition Dubischar and Bathmann (1997) reported that large copepod grazers, that are able to ingest large diatom species and cell chains, had a more patchy distribution and ingestion rates were to low to control the biomass of these species under favorable nutrient conditions. Only the very randomly distributed salps had ingestion rates high enough to potentially suppress such a bloom. Of the species tested in this study, *C. debilis* seems to be able to adapt best to changing environmental conditions and maintain favorable growth rates. These findings in our laboratory experiments are supported by field observations from the subarctic Pacific Ocean. It has been shown that *C. debilis* is able to exceed the growth of other species in the field and become the dominant species after *in situ* iron fertilization (Tsuda et al., 2003). The growth of *C. dichaeta* and especially *Actinocyclus* were much more affected by the availability of iron, light, and silicate. However, growth of all species showed to be co-limited by iron and silicate. If nutrient availability would be the only limiting factor of growth we would expect small "generalists" as *C. debilis* to dominate in the Southern Ocean.

In conclusion we suggest that while all diatom size classes may be able to increase growth following iron fertilization in high Si regions of the SO, the dominance of large species might be mainly caused by effective grazing control of the small phytoplankton biomass.

Acknowledgements:

We thank Jesco Peschutter and Wiekbe Schmidt for their help with cell counting. We also thank Eike Breitbarth and Peter Croot for helpful comments and discussion. This research was funded by the German Research Foundation (DFG) grant PE_565_5.

References:

Abelmann, A., and R. Gersonde, 1991. Biosiliceous particle flux in the Southern Ocean. Marine Chemistry, 35, 503-536.

Admiraal, W., 1977. Influence of light and temperature on the growth rate of estuarine benthic diatoms in culture. Marine Biology, 39, 1-9.

Anderson, M., A. Paulino, B. P. Carlsen, et al., 2004. Light climate and primary productivity in the Arctic. UNIS Publication Series, AB323 Report ISBN 82-481-0010-3, 1-95.

Armand, L. K., X. Crosta, O. E. Romero, et al., 2005. The biogeography of major diatom taxa in Southern Ocean surface sediments: 1. Sea ice related species. Palaeogeography Palaeoclimatology Palaeoecology, 223, 93-126.

Banse, K., 1991. Rates of phytoplankton cell division in the field and in iron enrichment experiments. Limnology and Oceanography, 36(8), 1886-1898.

Blain, S., P. N. Sedwick, F. B. Griffiths, et al., 2002. Quantification of algal iron requirements in the Subantarctic Southern Ocean (Indian sector). Deep-Sea Research II, 49, 3255-3273.

Brzezinski, M. A., 1992. Cell-Cycle Effects on the Kinetics of Silicic-Acid Uptake and Resource Competition among Diatoms. Journal of Plankton Research, 14(11), 1511-1539.

Brzezinski, M. A., J. L. Jones, and M. S. Demarest, 2005. Control of silica production by iron and silicic acid during the Southern Ocean Iron Experiment (SOFeX). Limnology and Oceanography, 50(3), 810-824.

Brzezinski, M. A., R. J. Olson, and S. W. Chisholm, 1990. Silicon availability and cell-cycle progression in marine diatoms. Marine Ecology Progress Series, 67, 83-96.

Chisholm, S. W., 1992, Phytoplankton size, in *Primary productivity and biogeochemical cycles in the sea*, edited by P.G. Falkowski, and A.D. Woodhead, Plenum Press, New York.

Claquin, P., V. Martin-Jézéquel, J. C. Kromkamp, et al., 2002. Uncoupling of silicon compared with carbon and nitrogen metabolisms and the role of the cell cycle in continuous cultures of *Thalassiosira pseudonana* (Bacillariophyceae) under light, nitrogen, and phosphorus control. Journal of Phycology, 38, 922-930.

Coale, K. H., K. S. Johnson, F. P. Chavez, et al., 2004. Southern Ocean iron enrichment experiment: carbon cycling in high- and low- Si waters. Science, 304, 408-414.

Coale, K. H., X. Wang, S. J. Tanner, et al., 2003. Phytoplankton growth and biological response to iron and zinc addition in the Ross Sea and Antarctic Circumpolar Current along 170°W. Deep-Sea Research II, 50(3-4), 635-653.

Crosta, X., O. E. Romero, L. K. Armand, et al., 2005. The biogeography of major diatom taxa in Southern Ocean surface sediments: 2. Open ocean related species. Palaeogeography Palaeoclimatology Palaeoecology, 223, 66-92.

Dafner, E. V., and N. V. Mordasova, 1994. Influence of biotic factors an the hydrochemical structure of surface water in the Polar Frontal Zone of the Atlantic Antarctic. Marine Chemistry, 45, 137-148.

de Baar, H. J. W., P. W. Boyd, K. H. Coale, et al., 2005. Synthesis of iron fertilisation experiments: From the iron age in the age of enlightenment. Journal of Geophysical Research, 110, C09S16, doi:10.1029/2004JC002601.

de Baar, H. J. W., A. G. J. Buma, R. F. Nolting, et al., 1990. On iron limitation of the Southern Ocean: experimental observations in the Weddell and Scotia Sea. Marine Ecology Progress Series, 65, 105-122.

De La Rocha, C. L., D. A. Hutchins, M. A. Brzezinski, et al., 2000. Effects of iron and zinc deficiency on elemental composition and silica production by diatoms. Marine Ecology Progress Series, 195, 71-79.

Dubischar, C. D., and U. V. Bathmann, 1997. Grazing impact of copepods and salps on phytoplankton in the Atlantic sector of the Southern Ocean. Deep-Sea Research II, 44(1-2), 415-433.

Dubischar, C. D., and U. V. Bathmann, 2002. The occurrence of fecal material in relation to different pelagic systems in the Southern Ocean and its importance for vertical flux. Deep-Sea Research II, 49, 3229-3242.

Franck, V. M., K. W. Bruland, D. A. Hutchins, et al., 2003. Iron and zinc effects on silicic acid and nitrate uptake kinetics in three high-nutrient, low-chlorophyll (HNLC) regions. Marine Ecology-Progress Series, 252, 15-33.

Franck, V. M., M. A. Brzezinski, K. H. Coale, et al., 2000. Iron and silicic acid concentrations regulate Si uptake north and south of the Polar Frontal Zone in the Pacific Sector of the Southern Ocean. Deep-Sea Research II, 47, 3315-3338.

Fryxell, G. A., and W. I. Miller, 1978. Chain-forming diatoms: Three araphid species. Bacillaria, 1, 113- 136.

Gersonde, R., and U. Zielinski, 2000. The reconstruction of late Quaternary Antarctic sea-ice distribution-the use of diatoms as a proxy for sea-ice. Palaeogeography Palaeoclimatology Palaeoecology, 162, 263-286.

Greene, R. M., R. J. Geider, Z. Kolber, et al., 1992. Iron-induced changes in light harvesting and photochemical energy-conversion processes in eukaryotic marine-algae. Plant Physiology, 100(2), 565-575.

Greene, R. M., Z. S. Kolber, D. G. Swift, et al., 1994. Physiological limitation of phytoplankton photosynthesis in the eastern equatorial Pacific determined from variability in the quantum yield of fluorescence. Limnology and Oceanography, 39(5), 1061-1074.

Harrison, P. J., H. L. Conway, R. W. Holmes, et al., 1977. Marine diatoms grown in chemostats under silicate or ammonium limitation. III. Cellular chemical composition and morphology of *Chaetoceros debilis*, *Skeletonema costatum*, and *Thalassosira gravida*. Marine Biology, 43, 19-31.

Hoffmann, L. J., I. Peeken, K. Lochte, et al., 2006. Different reactions of Southern Ocean phytoplankton size classes to iron fertilization. Limnology and Oceanography, 51(3), 1217-1229.

Hutchins, D. A., P. N. Sedwick, G. R. DiTullio, et al., 2001. Control of phytoplankton growth by iron and silicic acid availability in the subantarctic Southern Ocean: Experimental results from the SAZ project. Journal of Geophysical Research, 106(C12), 31559-31572.

Jeffrey, S. W., and G. F. Humphrey, 1975. New spectrophotometric equations for determining chlorophylls a, b, c_1 and c_2 in higher plants, algae and natural phytoplankton. Biochem. Physiol. Pflanzen, 167, 191-194.

Kolbowski, J., and U. Schreiber, 1995, Computer-controlled phytoplankton analyzer based on 4-wavelengths PAM chlorophyll fluorometer, in *Photosynthesis: from Light to Biosphere*, edited by P. Mathis, pp. 825-828.

Kunz-Pirrung, M., R. Gersonde, and D. A. Hodell, 2002. Mid-Brunhes century diatom sea surface temperature and sea ice records from the Atlantic sector of the Southern Ocean (OCD Leg 177, sites 1093, 1094 and core PS2089-2). Palaeogeography Palaeoclimatology Palaeoecology, 182, 305-328.

Leblanc, K., C. E. Hare, P. W. Boyd, et al., 2005. Fe and Zn effects on the Si cycle and diatom community structure in two high and low-silicate HNLC areas. Deep-Sea Research I, 52, 1842-1864.

Leynaert, A., E. Bucciarelli, P. Claquin, et al., 2004. Effect of iron deficiency on diatom cell size and silicic acid uptake kinetics. Limnology and Oceanography, 49(4), 1134-1143.

Martin, J. H., S. E. Fitzwater, and R. M. Gordon, 1990. Iron deficiency limits phytoplankton growth in antarctic waters. Global biogeochemical cycles, 4, 5-12.

Mitchell, B. G., E. A. Brody, O. Holmhansen, et al., 1991. Light limitation of phytoplankton biomass and macronutrient utilization in the Southern-Ocean. Limnology and Oceanography, 36(8), 1662-1677.

Morel, F. M. M., R. J. M. Hudson, and N. M. Price, 1991. Limitation of productivity by trace metals in the sea. Limnology and Oceanography, 36(8), 1742-1755.

Nelson, D. M., P. Tréguer, M. A. Brzezinski, et al., 1995. Production and dissolution of biogenic silica in the ocean: Revised global estimates, comparison with regional data and relationship to biogenic sedimentation. Global Biogeochemical Cycles, 9(3), 359-372.

Paasche, E., and I. Østergren, 1980. The annual cycle of plankton diatom growth and silica production in the inner Oslofjord. Limnology and Oceanography, 25(3), 481-494.

Pahlow, M., U. Riebesell, and D. A. Wolf-Gladrow, 1997. Impact of cell shape and chain formation on nutrient acquisition by marine diatoms. Limnology and Oceanography, 42(8), 1660-1672.

Ragueneau, O., P. Tréguer, A. Leynaert, et al., 2000. A review of the Si cycle in the modern ocean: recent progress and missing gaps in the application of biogenic opal as a paleoproductivity proxy. Global and Planetary Change, 26, 317-365.

Raven, J. A., 1990. Predictions of Mn and Fe use efficiencies of phototrophic growth as a function of light availability for growth and of C assimilation pathway. New Phytologist, 116, 1-18.

Romero, O. E., L. K. Armand, X. Crosta, et al., 2005. The biogeography of major diatom taxa in Southern Ocean surface sediments: 3. Tropical/Subtropical species. Palaeogeography Palaeoclimatology Palaeoecology, 223, 49-65.

Sarthou, G., K. R. Timmermans, S. Blain, et al., 2005. Growth physiology and fate of diatoms in the ocean: a review. Journal of Sea Research, 53(1-2), 25-42.

Sedwick, P. N., S. Blain, B. Quéguiner, et al., 2002. Resource limitation of phytoplankton growth in the Crozet Basin, Subantarctic Southern Ocean. Deep-Sea Research II, 49, 3327-3349.

Sigmon, D. E., D. M. Nelson, and M. A. Brzezinski, 2002. The Si cycle in the Pacific sector of the Southern Ocean: seasonal diatom production in the surface layer and export to the deep sea. Deep-Sea Research II, 49, 1747-1763.

Stickley, C. E., J. Pike, A. Leventer, et al., 2005. Deglacial ocean and climate seasonality in laminated diatom sediments, Mac.Robertson Shelf, Antartica. Palaeogeography Palaeoclimatology Palaeoecology, 227, 290-310.

Strzepek, R. F., and P. J. Harrison, 2004. Photosynthetic architecture differs in coastal and oceanic diatoms. Nature, 431, 689-692.

Strzepek, R. F., and N. M. Price, 2000. Influence of irradiance and temperature on the iron content of the marine diatom Thalassiosira weissflogii (Bacillariophyceae). Marine Ecology-Progress Series, 206, 107-117.

Sunda, W. G., and S. A. Huntsman, 1997. Interrelated influence of iron, light and cell size on marine phytoplankton growth. Nature, 390, 389-392.

Thomas, D. N., and G. S. Dieckmann, 2002. Antarctic Sea Ice - a habitat for extremophiles. Science, 295, 641-644.

Timmermans, K. R., M. S. Davey, B. van der Wagt, et al., 2001. Co-limitation by iron and light of *Chaetoceros brevis*, *C. dichaeta* and *C. calcitrans* (Bacillariophyceae). Marine Ecology Progress Series, 217, 287-297.

Tréguer, P., and G. Jacques, 1992. Dynamics of nutrients and phytoplankton, and fluxes of carbon, nitrogen, and silicon in the Antarctic Ocean. Polar Biology, 12, 149-162.

Tréguer, P., A. Kamatani, S. Gueneley, et al., 1989. Kinetics of dissolution of Antarctic diatom frustules and the biogeochemical cycle of silicon in the Southern Ocean. Polar Biology, 9(6), 397-403.

Tréguer, P., D. M. Nelson, A. J. Van Bennekom, et al., 1995. The silica balance in the World Ocean: A reestimate. Science, 268, 375-379.

Tsuda, A., S. Takeda, H. Saito, et al., 2003. A mesoscale iron enrichment in the western subarctic Pacific induces a large centric diatom bloom. Science, 300, 958-961.

van Oijen, T., M. A. van Leeuwe, E. Granum, et al., 2004. Light rather than iron controls photosynthate production and allocation in Southern Ocean phytoplankton populations during austral autumn. Journal of Plankton Research, 26(8), 885-900.

Waite, A. M., and S. D. Nodder, 2001. The effect of in situ iron addition on the sinking rates and export flux of Southern Ocean diatoms. Deep-Sea Research II, 48(11-12), 2635-2654.

Zielinski, U., and R. Gersonde, 1997. Diatom distribution in Southern Ocean surface sediments (Atlantic sector): Implications for paleoenvironmental reconstructions. Palaeogeography Palaeoclimatology Palaeoecology, 129(3-4), 213-250.

CHAPTER III

Effects of iron on the elemental stoichiometry during EIFEX and in the diatoms *Fragilariopsis kerguelensis* and *Chaetoceros dichaeta*

Linn Hoffmann, Ilka Peeken, Karin Lochte

Accepted in Biogeosciences Discussions

Abstract:

The interaction between iron availability and the phytoplankton elemental composition was investigated during the *in situ* iron fertilization experiment EIFEX and in laboratory experiments with the Southern Ocean diatom species *Fragilariopsis kerguelensis* and *Chaetoceros dichaeta*. Contrary to other *in situ* iron fertilization experiments we observed an increase in the bPSi : POC, bPSi : PON, and bPSi : POP ratios within the iron fertilized patch during EIFEX. This is possibly caused by a relatively stronger increase in diatom abundance compared to other phytoplankton groups and does not necessarily represent the amount of silicification of single diatom cells. In laboratory experiments with *F. kerguelensis* and *C. dichaeta* no changes in the POC : PON, PON : POP, and POC : POP ratios were found with changing iron availability in both species. BPSi : POC, bPSi : PON, and bPSi : POP ratios were significantly lower in the high iron treatments compared to the controls. In *F. kerguelensis* this is caused by a decrease in cellular bPSi concentrations and therefore possibly less silicification. In *C. dichaeta* no change in cellular bPSi concentration was found. Here lower bPSi : POC, bPSi : PON, and bPSi : POP ratios were caused by an increase in cellular C, N, and P under high iron conditions. We therefore assume that iron limitation does not generally increase silicification of diatoms and that changes in the bPSi : POC, bPSi : PON, and bPSi : POP ratios under iron fertilization in the field are caused by a variety of different mechanisms. These results imply that the effect of iron on nutrient uptake is more complex than hitherto assumed.

Introduction:

Recent studies showed that the canonical Redfield ratio of 106 : 16 : 1 for C : N : P is not a general stoichiometric optimum for all marine phytoplankton species but rather represents an average of species specific ratios, which can differ extremely from the Redfield ratio (Ho, et al., 2004; Klausmeier, et al., 2004; Quigg, et al., 2003; Twining, et al., 2004). It is reported that while the POC : PON ratio is often close to the Redfield ratio, diatoms in general have lower than the Redfield PON : POP and POC : POP ratios (Ho, et al., 2004; Quigg, et al., 2003). This is supported by observations from the Southern Ocean (SO) where waters dominated by diatoms have lower PON : POP and POC : POP

ratios compared to waters dominated by the haptophyte *Phaeocystis antarctica* (Arrigo, et al., 2002; Arrigo, et al., 1999).

Beside these differences in the elemental composition of different phytoplankton classes, nutrient availability can influence stoichiometry of individual species. As a possible explanation for deviations from the Redfield ratio the trace metal iron is discussed. Iron is needed in the nitrogen metabolism of phytoplankton cells as it is essential in the enzymes for nitrate reduction, nitrate and nitrite reductase. Therefore in High Nutrient Low Chlorophyll (HNLC) regions like the SO, where iron limits phytoplankton growth, higher POC : PON and lower PON : POP ratios compared to the Redfield ratio may be expected. However, as the POC : PON ratio is rather constant independent of phytoplankton species (Ho, et al., 2004; Quigg, et al., 2003) and iron concentration (Greene, et al., 1991; Price, 2005), while the POC : POP and PON : POP ratios are much more variable, intracellular phosphate seems to be more influenced by iron availability. The exact mechanisms how the elemental composition of phytoplankton is influenced by iron and why there are large species specific differences remain unknown.

Besides the impact on POC, PON, and POP composition, one important effect of iron limitation on the elemental stoichiometry is an increase in the bPSi : POC, bPSi : PON, and bPSi : POP ratio of diatoms (Hutchins and Bruland, 1998; Price, 2005; Takeda, 1998; Timmermans, et al., 2004; Twining, et al., 2004). It has been generally assumed that this is caused by an increase in cellular silicate concentrations rather than a decrease in cellular C, N, and P. However, data on the cellular elemental composition of SO diatoms under different iron availabilities are rare and not always a decrease of cellular bPSi with increasing iron availability is observed (Takeda, 1998). It is therefore not certain that iron fertilization generally decreases frustule silicification and the resulting effects on grazing protection, sinking rates, and remineralization have to be considered in relation to the species specific response to iron availability.

In this study we examined the effect of iron deplete and replete growth conditions on the elemental composition of two Antarctic diatom species *Fragilariopsis kerguelensis* and *Chaetoceros dichaeta*. These species were selected because of their important contribution to the diatom biomass in the SO community. Further, they represent two different degrees

of silicification with *F. kerguelensis* being stronger silicified compared to *C. dichaeta*. These results were compared to size fractionated bPSi : POC, bPSi : PON, and bPSi : POP ratios during the *in situ* iron fertilization experiment EIFEX.

Aim of this study is to investigate the effect of iron on silicification of two important SO diatom species and thus to help interpreting changes in the bPSi : POC, bPSi : PON, and bPSi : POP ratio observed in field experiments.

Material and Methods:

A detailed description of the phytoplankton community structure and of the total POC, PON, POP, and bPSi concentrations during EIFEX is given by Hoffmann et al. (2006) (Chapter I). Additionally the POC : PON, POC : POP, and PON : POP ratios of the total plankton community, the >20 μm, 2-20 μm, and the <2 μm size fraction and the total bPSi : POC ratios are presented. In the manuscript at hand we supplement this data set with POC, PON, POP, and bPSi concentrations as well as the bPSi : POC, bPSi : PON, and the bPSi : POP ratios of the >20 μm and the <20 μm size fraction during EIFEX since bPSi was only measured in these size classes. These data are completed with results from laboratory experiments, performed with the SO diatom species *F. kerguelensis* and *C. dichaeta*.

F. kerguelensis and *C. dichaeta* were isolated on board RV "Polarstern" during the SO iron fertilization experiment EIFEX. Isolation procedure, cultivation conditions, and trace metal clean handling were the same as described in Chapter II.

Two experiments with three iron treatments and three replicates each were carried out. In one treatment no iron was added to the culture media, in the other two high iron treatments 100 and 1000 nM Fe were added. In these treatments free iron concentrations were 1.55 nM Fe' (all inorganic Fe species) and 15.5 nM Fe', respectively, estimated after Timmermans et al. (2001). We additionally grew *F. kerguelensis* without iron and EDTA addition, to investigate if this chelator has an effect on growth and stoichiometry. Culture conditions and treatment labels are listed in table 1.

Chlorophyll measurements, cell counts, and determination of the photosynthetic efficiency Fv/Fm were performed as described in Chapter II.

Table 1: Iron and EDTA concentrations in the different treatments of the two laboratory experiments.

Species	Treatment			
	A	B	C	D
F. kerguelensis	no Fe addition no EDTA	no Fe addition 10 μM EDTA	1.55 nM Fe' 10 μM EDTA	15.5 nM Fe' 10 μM EDTA
C. dichaeta	-	no Fe addition 10 μM EDTA	1.55 nM Fe' 10 μM EDTA	15.5 nM Fe' 10 μM EDTA

Size fractionated samples for POC, PON, POP, and bPSi measurements during EIFEX were taken as described by Hoffmann et al. (2006). POC, PON, POP, and bPSi samples from the laboratory experiments were not size fractionated. However, the filters used and sample storage was the same as for the EIFEX samples.

POC and PON measurements of the EIFEX and *F. kerguelensis* samples as well as all POP, bPSi, and HPLC pigments measurements were carried out as described by Hoffmann et al. (2006). The POC and PON content of the *C. dichaeta* cultures was analyzed using an Euro EA-CN IRMS elemental analyzer linked to Finnegan Delta Plus radio isotope mass spectrometer as described by Carman and Fry (2002). Acetanelid and peptone were used as standards.

Growth rates were calculated as $\mu = (t_2 - t_1)^{-1} \cdot \ln(N_2 / N_1)$ where μ is the net growth rate d^{-1} and N_1 and N_2 are the cell concentrations at t_1 and t_2 respectively. Growth rates were calculated form the beginning until the day of highest cell numbers. For statistical analysis Students t-test was used. Differences found are reported as significant in the text if $p < 0.05$.

Results:

Size fractionated particulate organic matter during EIFEX

During the *in situ* iron fertilization experiment EIFEX, the particulate organic matter (POM) showed a different behavior in the >20 µm and the <20 µm size fractions inside the iron fertilized patch (Fig. 1). Almost no changes were found in the >20 µm size fraction during the first 16 days of the experiment followed by a 4.1, 1.9, 4.1, and 1.4 times increase in bPSi, POC, PON, and POP concentrations, respectively (Fig. 1 A). In the <20 µm size fraction no changes in POC, PON, and POP concentrations were found while bPSi concentrations increased continuously during the whole 37 days of the experiment by a factor of 2.5 (Fig. 1 B).

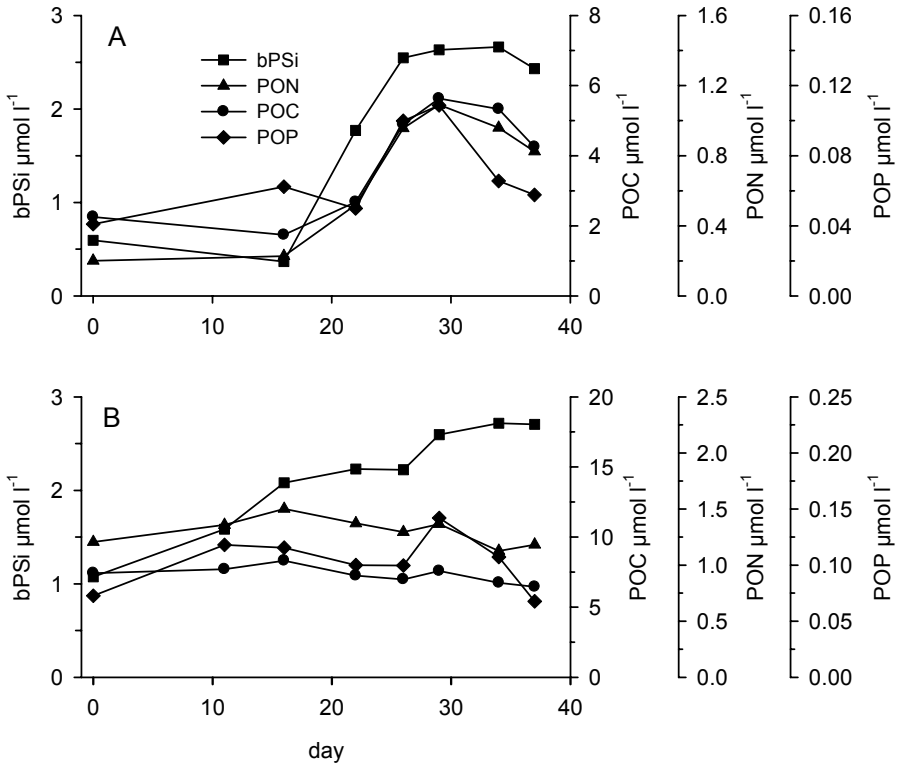

Figure 1: Concentrations of bPSi, POC, PON, and POP in the >20 µm size fraction (A) and in the <20 µm size fraction (B).

The bPSi : POC, bPSi : PON, and bPSi : POP ratios of the total biomass increased 2.1, 1.3, and 2.6 times respectively during the experiment inside the fertilized patch, while no trend was observed outside the patch (Table 2). Separation of the total biomass in >20 μm and <20 μm size fractions shows that the same trends were found in the molar ratios of both size classes (Fig. 2). The bPSi : POC, bPSi : PON, and bPSi : POP ratios increased continuously in the <20 μm size fraction from 0.1, 0.9, and 14.8 at the start of the experiment to 0.4, 2.3, and 40.0 at day 37 inside the fertilized patch. Outside the patch the values were lower in the second half of the experiment. In the >20 μm fraction the elemental ratios did not increase steadily. The values were 0.3 (bPSi : POC), 3.0 (bPSi : PON), and 14.5 (bPSi : POP) in the beginning and decreased within the first 16 days of the experiment, followed by a large increase at day 21 to 0.7, 3.4, and 35.5. During the rest of the experiment the values stayed at an elevated level.

Table 2: Molar ratios of bPSi : POC, bPSi : PON, and bPSi : POP of the total biomass during the iron fertilization experiment EIFEX in- and outside the iron fertilized patch. *Hoffmann et al. 2006.

Day	bPSi : POC*	bPSi : PON	bPSi : POP
inpatch	μmol : μmol	μmol : μmol	μmol : μmol
0	0.24	1.52	17.19
11	0.23	1.39	15.46
16	0.29	1.89	16.99
22	0.44	2.46	28.84
26	0.40	2.18	27.16
29	0.38	1.99	21.88
34	0.40	2.12	25.15
37	0.50	2.80	45.51
outpatch			
0	0.24	1.52	17.19
12	0.36	2.03	19.18
18	0.27	1.45	15.65
27	0.21	1.08	12.24
35	0.37	2.01	22.64

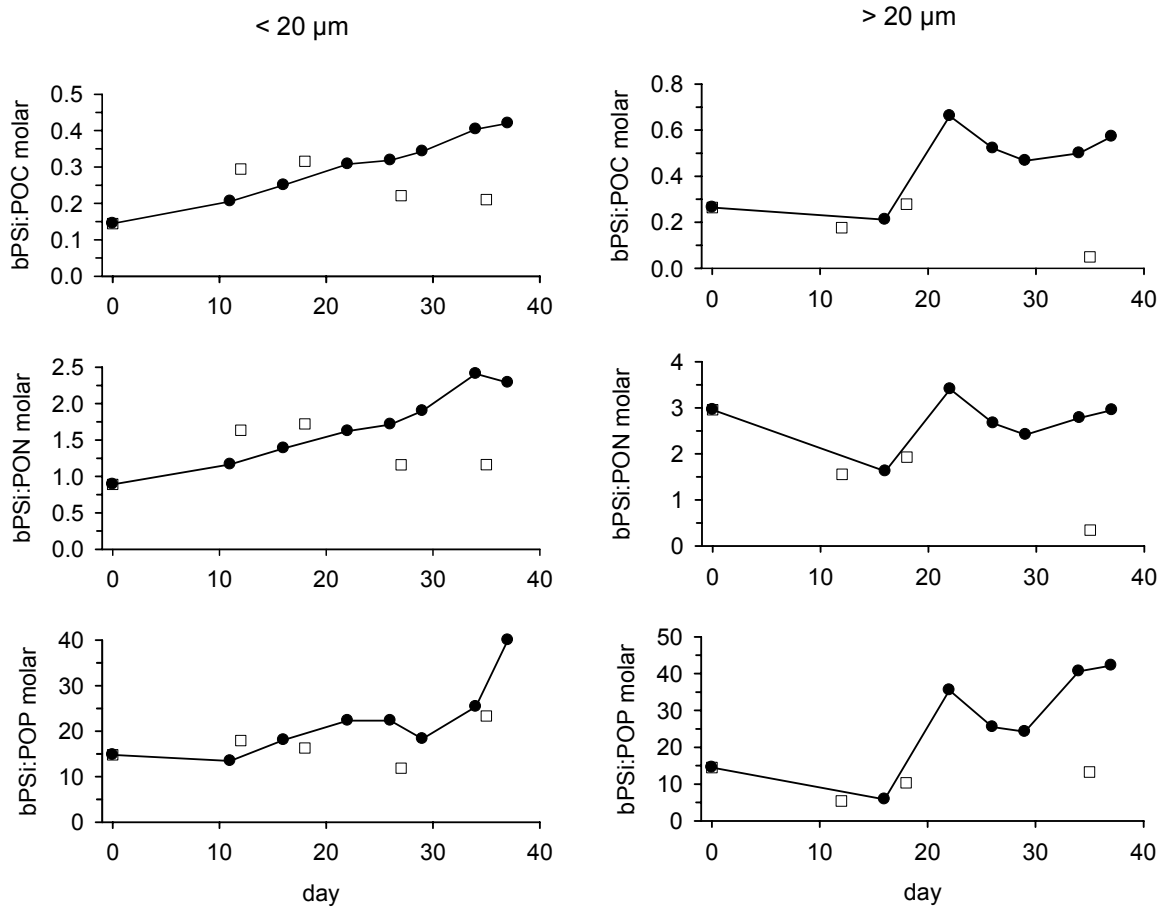

Figure 2: Molar ratios of the < 20 µm and the > 20 µm size fraction inside the iron fertilized patch (dark circles) and outside the iron fertilized patch (open squares).

Growth parameters in the laboratory experiments

In *F. kerguelensis* and *C. dichaeta* cultures, iron fertilization resulted in a significant increase in maximum growth rate, chlorophyll concentrations, and photosynthetic efficiency (Fv/Fm) compared to the non fertilized treatments (Fig. 3 and Tab. 3). In *F. kerguelensis* growth rates, Chl concentrations, and Fv/Fm were not statistically different (t-test; p = 0.3 - 0.6) in both low iron treatments A and B. Iron addition resulted in a distinct increase in each of these parameters with higher values at 15.5 nM Fe' compared to 1.55 nM Fe'. Mean chlorophyll concentrations were 0.8 µg l^{-1} at the beginning of the experiment for all treatments. The chlorophyll concentrations increased to 15.4 µg l^{-1} in 34 days without iron and EDTA addition (Fig. 3 A). Under EDTA addition Chl concentrations were slightly lower (8.1 µg l^{-1}). The addition of 1.55 nM Fe' resulted in a significant increase in the chlorophyll concentrations compared to both treatments without iron addition (t-test; p =

0.003 and 0.0007). After 34 days Chl concentrations reached a value of 76 μg l^{-1}, which is a 95 times increase. Higher iron concentrations of 15.5 nM Fe' additionally increased Chl concentrations to a value of 96.4 μg l^{-1}. Fv/Fm values of *F. kerguelensis* were between 0.15-0.29 at the beginning of the experiment. These low values indicated that the start culture was iron limited before the experiment. However, the variance here and in the low iron treatments throughout the experiment was relatively high, possibly caused by the very low biomass. Without iron addition maximum Fv/Fm values of 0.29 were reached. Under iron addition Fv/Fm values increased to 0.44 (treatment C) and 0.6 (treatment D) (Tab. 3). Maximum growth rates roughly doubled from 0.10 and 0.12 in the low iron treatments to 0.18 and 0.2 in the high iron treatments (Tab. 3).

In *C. dichaeta* Chl concentrations in both high iron treatments increased rapidly by about 30 times to 96.1 and 97.0 μg l^{-1} in 25 days (Fig. 3 B). Thereafter concentrations levelled off and highest values were reached at day 36 with 113.9 μg l^{-1} (treatment C) and 112.8 μg l^{-1} (treatment D). In the low iron treatment Chl concentrations increased only 11.6 times until day 25. However, growth continued throughout the experiment reaching concentrations almost as high as the high iron treatments of 87.3 μg l^{-1} at day 42. Fv/Fm values were between 0.19 and 0.21 at the beginning of the experiment and increased more than two times reaching maximum values of 0.54 (treatment C) and 0.56 (treatment D) after iron addition (Tab. 3). Under iron limitation maximum Fv/Fm value was 0.32. Maximum growth rate in the low iron treatment was 0.22 (Tab. 3). Unlike *F. kerguelensis*, we found no difference between the addition of 1.55 and 15.5 nM Fe'. In both high iron treatments the maximum growth rate was 0.31.

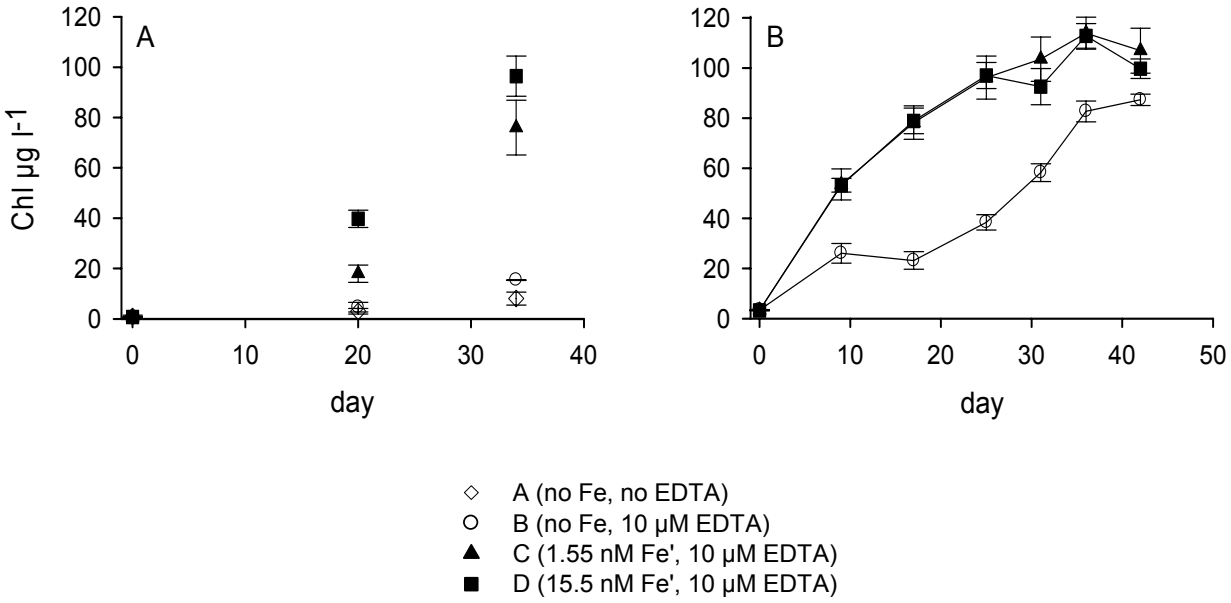

Figure 3: Chlorophyll concentrations in *F. kerguelensis* (A) and *C. dichaeta* (B) in the different treatments.

Elemental ratios in the laboratory experiments

In both species no significant changes in the POC : PON, POC : POP, and PON : POP ratio were found between the high and low iron treatments and the different growth periods (Fig. 4 and 5). However, all elemental ratios were below the Redfield ratio of C : N : P 106 : 16 : 1. *C. dichaeta* and *F. kerguelensis* had mean POC : PON ratios of 5.8 and 5.5, which is lower than the Redfield ratio of 6.6. More severe are the differences in the POC : POP and PON : POP ratios which are 44.6 and 7.7 in *C. dichaeta* and 17.8 and 3.3 in *F. kerguelensis* respectively. Here the difference from the Redfield POC : POP ratio of 106 is 58 % (*C. dichaeta*) and 83 % (*F. kerguelensis*). The deviation from the Redfield PON : POP ratio of 16 is 52 % (*C. dichaeta*) and 80 % (*F. kerguelensis*). In both species high iron concentrations resulted in lower bPSi : POC, bPSi : PON, and bPSi : POP ratios compared to the low iron treatments. At day 34 (*F. kerguelensis*) and day 31 (*C. dichaeta*) the ratios were roughly twice as high in the low iron treatment compared to the high iron treatments.

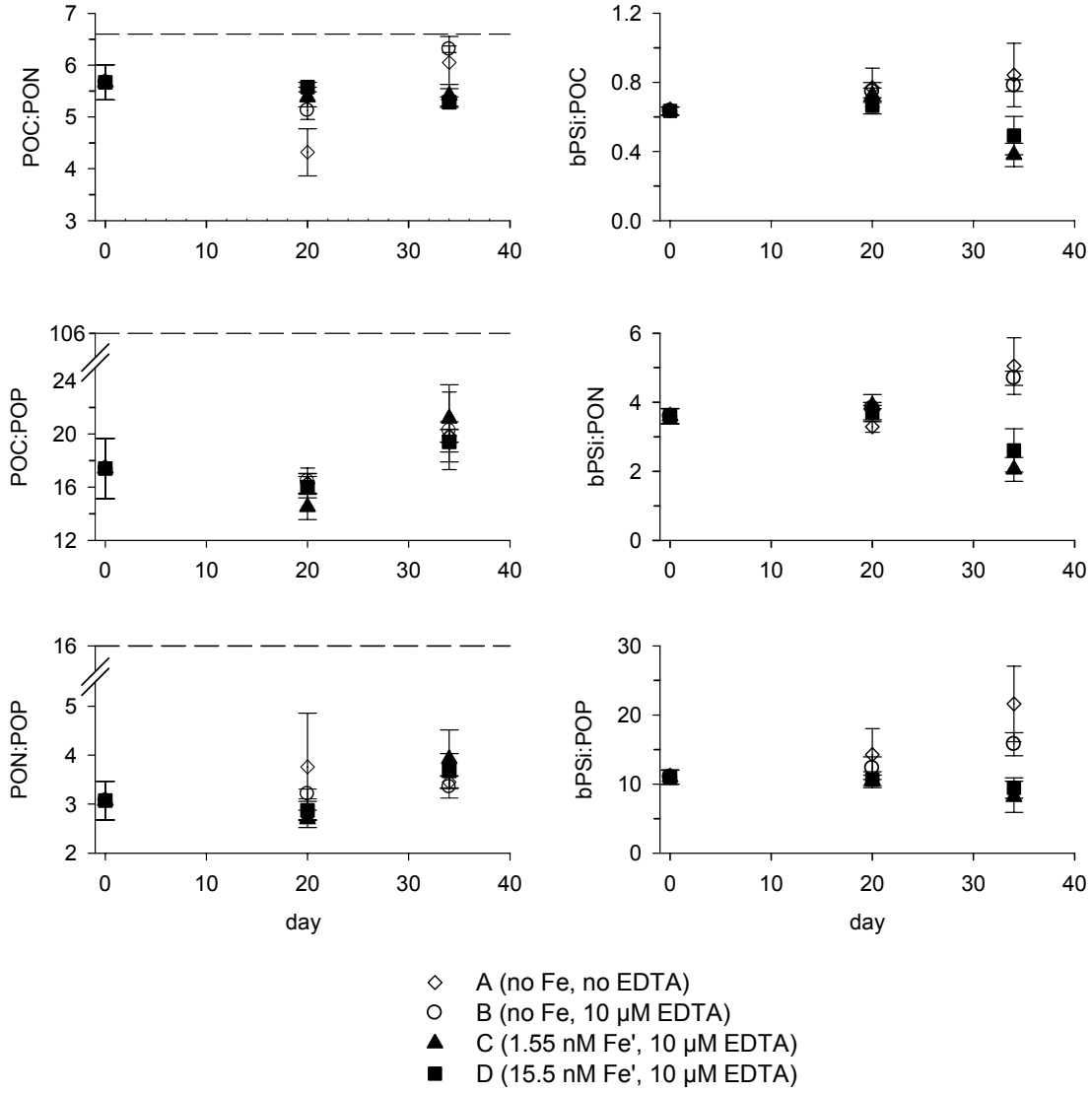

Figure 4: Molar elemental ratios in *F. kerguelensis* grown under different iron and EDTA concentrations. The dashed line represents the Redfield ratio.

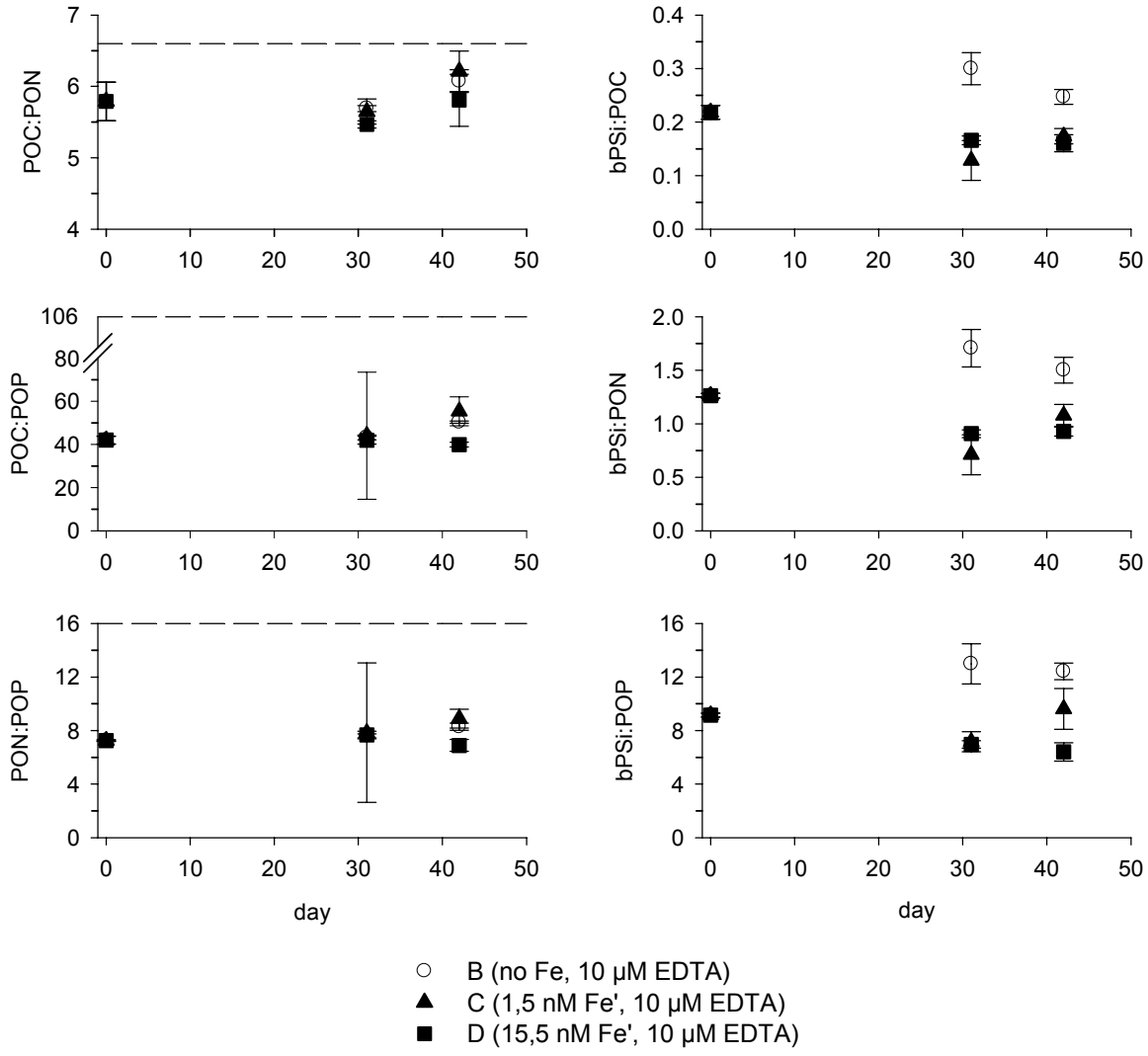

Figure 5: Molar elemental ratios in *C. dichaeta* grown under different iron and EDTA concentrations. The dashed line represents the Redfield ratio.

Cellular composition

Chl per cell increased in all high iron treatments in both species. Cellular chlorophyll concentrations of *F. kerguelensis* and *C. dichaeta* were about two times higher in the high iron treatments (Tab. 3). Interestingly the cellular elemental composition shows different strategies of the two species both resulting in lower bPSi : POC, bPSi : PON, and bPSi : POP ratios under high iron concentrations. Mean cellular C, N, and P concentrations of all treatments were 18.9, 3.6, and 1.0 pmol cell^{-1} in *F. kerguelensis* showing no significant changes due to iron concentrations (t-test; p = 0.1 – 0.9). However, bPSi concentrations per cell were significantly higher in both low iron treatments compared to the high iron treatments (t-test; P = 0.035 and 0.039). In contrast to that no significant change in the cellular bPSi concentration in *C. dichaeta* was found (mean of 0.7 pmol cell^{-1}; t-test; p = 0.2 – 0.9), while cellular C, N, and P concentrations were about twice as high under high iron concentrations.

Table 3: Cellular elemental composition and chlorophyll concentration, growth rate and maximum Fv/Fm of *F. kerguelensis* at day 34 in the two low iron treatments A and B and the high iron treatments C and D and of *C. dichaeta* at day 31 in the low iron treatment B and the high iron treatments C and D. Values marked with * were significantly different (t-test; p < 0.05) between high and low iron treatments. Values marked with ° were only significantly different between treatment B and C.

				Elemental composition			
Treatment	μmax d^{-1}	Fv/Fm max	Chl pg cell^{-1}	C pmol cell^{-1}	N pmol cell^{-1}	P pmol cell^{-1}	Si pmol cell^{-1}
F. kerguelensis	*	*	*				*
A	0.12 ± 0.01	0.29 ± 0.08	1.9 ± 0.8	17.4 ± 4.1	2.9 ± 0.5	0.7 ± 0.2	14.2 ± 0.5
B	0.10 ± 0.01	0.29 ± 0.05	2.3 ± 0.9	15.7 ± 1.3	2.5 ± 0.2	0.7 ± 0.1	12.0 ± 1.0
C	0.18 ± 0.0	0.44 ± 0.06	3.6 ± 0.8	21.5 ± 2.6	4.0 ± 0.3	1.0 ± 0.2	9.0 ± 1.2
D	0.20 ± 0.01	0.60 ± 0.05	4.5 ± 0.9	19.3 ± 6.3	3.7 ± 1.3	1.0 ± 0.2	9.1 ± 1.3
C. dichaeta	*	*	*	°	°	°	
B	0.22 ± 0.01	0.32 ± 0.00	0.4 ± 0.2	2.0 ± 0.03	0.4 ± 0.0	0.05 ± 0.0	0.6 ± 0.1
C	0.31 ± 0.03	0.54 ± 0.02	1.1 ± 0.2	6.1 ± 0.7	1.1 ± 0.1	0.1 ± 0.03	0.7 ± 0.1
D	0.31 ± 0.02	0.56 ± 0.02	0.8 ± 0.1	3.5 ± 0.7	0.6 ± 0.1	0.08 ± 0.02	0.6 ± 0.2

Discussion:

Deviation from the Redfield ratio

The elemental composition of diatoms is known to be extremely variable between different species (Sarthou, et al., 2005). A general observation from laboratory experiments (Ho, et al., 2004; Price, 2005; Quigg, et al., 2003) and field studies (Arrigo, et al., 1999; Coale, et al., 2004; Hoffmann, et al., 2006) is that the mean POC : PON ratio of diatoms is close to the Redfield ratio of 6.6 and shows only minor changes due to environmental conditions. In agreement to that we found mean POC : PON ratios of 5.5 for *F. kerguelensis* and 5.8 for *C. dichaeta* that showed no significant changes with iron concentration. The PON : POP and POC : POP ratios of diatoms are generally lower than the Redfield ratio (Fu, et al., 2005; Ho, et al., 2004; Quigg, et al., 2003; Sarthou, et al., 2005) and are much more susceptible to changes in nutrient supply. For *Thalassiosira weissflogii* a higher accumulation of P and resulting lower PON : POP and POC : POP ratios are reported under iron limiting conditions in laboratory experiments (Price, 2005). It remains unknown if this is due to a luxury uptake and storage of P or if specific physiological processes under iron limitation force the cell to a higher P usage. However, the elemental PON : POP and POC : POP ratios of both species tested in this study were not affected by the iron concentration of the growth medium (Fig. 4 and 5). Similar findings are reported for the PON : POP ratio *C. dichaeta* and *Nitzschia* sp. (Takeda, 1998) and *Phaeodactylum tricornutum* (Greene, et al., 1991). Takeda (1998) showed that in vitro iron fertilization can lead to opposed changes in the ratio of NO_3^- : PO_4^{3-} consumption depending on the oceanic region. While he found an increase in the ratio of NO_3^- : PO_4^{3-} consumption in the SO, no changes were found in the Subarctic North Pacific and a decrease is reported from waters of the Equatorial Pacific. Hoffmann et al. (2006) report a wide variability between the PON : POP and POC : POP ratios of the different phytoplankton size classes after iron fertilization in the SO. While both ratios increased from far below Redfield values to close to Redfield values in the microplankton, the opposite trend was observed in the nanoplankton. Here start values close to the Redfield ratio decreased to far lower values after iron fertilization.

Although we found no changes in the relative elemental composition of both species and in the absolute cellular C, N, and P concentrations in *F. kerguelensis*, total cellular C, N, and P concentrations roughly doubled with higher iron concentration in *C. dichaeta* (Tab. 3). This effect may partly be caused by a change in cell volume. We found an increase in the cell volume of *C. dichaeta* by a factor of 1.3 with higher iron concentrations (data not shown) that was similar to those reported in Chapter II. However, this increase in cell volume would only result in cellular C, N, and P concentrations of 2.7, 0.5, and 0.06 pmol $cell^{-1}$ respectively and can therefore not explain all of the observed increase (compare Table 3). Additionally a higher C, N, and P accumulation must have taken place in this species under high iron concentrations. It can be speculated that increased C uptake due to higher photosynthetic activity and higher nitrate uptake under high iron concentrations are responsible for this observation. To our knowledge no physiological effect is known that could explain increased P uptake under high iron concentrations. No change in cell size of *F. kerguelensis* was found during this experiment, which is consistent with findings reported by Timmermans et al. (2004) for the same species. These authors showed that the cellular nutrient consumption ratios of four SO diatom species grown under different iron concentrations differ extremely and showed no collective trend. Cellular N consumption increased in *Actinocyclus* sp., *Thalassiosira* sp., and *C. pennatum* with increasing iron concentration, while no changes were found in *F. kerguelensis*. In agreement with our observations, none of the species tested by Timmermans et al. (2004) showed higher cellular P uptake under iron limitation.

These results show that luxury P consumption, as reported by Price (2005) for *T. weissflogii*, is not a general mechanism controlled by iron availability, but rather a species specific reaction. It has been recently shown that phytoplankton cells absorb P on their cell surfaces in an amount of 14 % to 57 % of total cellular P (Fu, et al., 2005; Sanudo-Wilhelmy, et al., 2004). The measured PON : total POP and POC : total POP ratios might therefore generally be lower than the truly intracellular stoichiometry and thus may falsify our interpretation of the nutritional status of the cells. When corrected for the surface bound P Fu et al. (2005) describe an increase in the C : intracellular P and N : intracellular P ratios of a factor of 1.2 to 2 in all species tested, including one Southern Ocean *Chaetoceros* species. It can only be speculated what the effect of these observations on the

proposed POP export may be. It is possible that sinking cells would lose a lot of the surface bound P during sinking due to microbial uptake. This could possibly decrease the amount of total P exported to the deep sea greatly. These uncertainties lead us to the suggestion to use PON : POP and POC : POP ratios with great caution in terms of nutrient drawdown ratios and for biogeochemical modeling. The general observation that the POC : PON ratio is less affected by environmental conditions and generally closer to the Redfield ratio makes it a far better proxy for these purposes.

Impact of iron on silicification

A collective observation from *in situ* iron fertilization experiments is that the growth of diatoms, especially large species, is stimulated to a greater degree than other phytoplankton groups. In these experiments, besides the increase in cell counts and chlorophyll concentrations, the drawdown of nitrate in iron fertilized waters is often used to follow the biomass development. As iron is an essential component in the enzymes responsible for nitrogen uptake, nitrate and nitrite reductase, it was not surprising to see that nitrate uptake was greatly enhanced by iron fertilization. More remarkable was the observation that higher iron availability decreased the bPSi : PON ratio in bottle incubation experiments in all HNLC regions (Brzezinski, et al., 2003; De La Rocha, et al., 2000; Franck, et al., 2003; Franck, et al., 2000; Hutchins and Bruland, 1998; Martin and Fitzwater, 1988; Takeda, 1998; Watson, et al., 2000). This phenomenon is not only caused by increasing N uptake but also by lower cellular bPSi concentrations (Hutchins and Bruland, 1998; Takeda, 1998) and thus also affected the bPSi : POC and bPSi : POP ratios. Because of the relative increase in bPSi under iron limitation, Boyle (1998) suggested that iron-limited diatoms grow thicker and thus heavier silica shell, which sink faster to the sea floor and are less remineralized. This is thought to be a reason for the high accumulation rates of diatom frustules in SO sediments despite relatively low bPSi production in the euphotic zone, known as the "opal paradox" (Nelson, et al., 1995; Tréguer, et al., 1995).

Contrary to other *in situ* iron fertilization experiments, which showed decreasing bPSi : PON and bPSi : POC ratios, respectively (Boyd, et al., 2005; Coale, et al., 2004; Gall, et

al., 2001), the bPSi : POC, bPSi : PON, and bPSi : POP ratios of the total biomass increased 1.8 to 2.6 times during EIFEX (Tab. 2). This is caused by a stronger increase of bPSi concentrations compared to POC, PON, and POP concentrations, which can be explained by a relative increase in the diatom abundance and a shift towards diatom species that are stronger silicified compared to others (Hoffmann, et al., 2006).

In the >20 µm size fraction concentrations of bPSi, POC, PON, and POP increased inside the fertilized patch (Fig. 1 A). Here again increasing bPSi : POC, bPSi : PON, and bPSi : POP ratios result from a stronger enhancement in bPSi concentrations compared to the other parameters. As this size fraction was dominated by diatoms from the beginning (Hoffmann, et al., 2006), this observation can only be caused by a shift in the diatom community structure towards heavily silicified species. In the <20 µm size faction no increase in POC, PON, and POP concentrations was found, while bPSi concentrations increased steadily throughout the experiment (Fig. 1 B). In this size fraction cell counts and HPLC pigment data show a shift from a haptophyte dominated towards a diatom dominated phytoplankton community (Hoffmann, et al., 2006). This resulted in increasing bPSi concentrations, while POC related biomass showed no changes. Changes in species composition during EIFEX may have been more pronounced compared to other *in situ* iron fertilization experiments. Thus the increasing bPSi : POC, bPSi : PON, and bPSi : POP ratios during EIFEX may not necessarily contradict the theory of weaker silicification with iron fertilization, however, species specific differences and reactions of the heterotrophic biomass may falsify the picture.

To further understand these mechanisms and explain the differences between EIFEX and other experiments, we performed laboratory experiments with two SO diatoms *F. kerguelensis* and *C. dichaeta*, which were both important species during EIFEX, and determined cellular POC, POP, PON, and bPSi concentrations. The bPSi : POC and bPSi : PON ratios of both species were relatively close to those found in the field, while the bPSi : POP ratios were lower in both cultures (Fig. 4, 5 and Table 2). As described above the cellular P pool is more complex than the C and N pools due to the existence of surface bound P. The surface bound P concentration is dependent on the amount of surface bound Mn (Sanudo-Wilhelmy, et al., 2004), which is explained by the adsorption

of P to cell-surface-bound Mn hydroxides and oxides. In the SO Mn concentrations are known to be very low (Martin, et al., 1990). It is therefore possible that in this region surface bound P concentrations and thus total cellular P concentrations are lower compared to our laboratory experiments, where all trace metals, including Mn, were added in excess. This could possibly explain the higher Si : P ratios observed during in the field during EIFEX. This assumption is further supported by the observation that C : P and N : P ratios of all size classes during EIFEX reported by Hoffmann et al. (2006) were higher compared to those found in *F. kerguelensis* and *C. dichaeta* in this study (Fig. 4 and 5).

Our laboratory experiments show that increased cellular bPSi concentrations under iron limitation are not a general phenomenon of all diatom species. In both species tested we observed higher bPSi : POC, bPSi : PON, and bPSi : POP ratios under low iron availability. However, while bPSi concentrations per cell were significantly increased under iron limitation in *F. kerguelensis*, no changes were found in *C. dichaeta* (Tab. 3). In the latter species the increase in the bPSi : POC, bPSi : PON, and bPSi : POP ratios is caused by lower cellular C, N, and P concentrations as described above. Analysis of Si consumption per cell led to similar results showing higher cellular Si accumulation under low iron concentrations in *Actinocyclus* sp., *Thalassiosira* sp., and *F. kerguelensis*, but no significant change in cellular Si accumulation in *Corethron pennatum* (Timmermans, et al., 2004). We assume that species specific changes in the elemental composition as well as the reactions of other phytoplankton groups and the heterotrophic biomass conceal the effect of iron on diatom silicate uptake in the field. Changes in the bPSi : POC, bPSi : PON, and bPSi : POP ratios with iron fertilization should thus be carefully interpreted in terms of diatom silicification.

The reason for changes in nutrient uptake and storage under changing iron availability is, with the exception of nitrate, not well understood. Fe limitation directly decreases the uptake rates of SO diatoms for silicic acid (Brzezinski, et al., 2005; De La Rocha, et al., 2000; Franck, et al., 2003; Franck, et al., 2000). However, it is generally accepted that increased Si uptake is caused by an increased duration of the cell wall synthesis phase. Si uptake is closely related to the G_2+M phase of the cell cycle. Nutrient (N, Fe), light, or

temperature limitation that prolong this phase lead to higher silicification in diatoms (see review in Martin-Jézéquel, et al., 2000). Despite lower uptake rates under Fe limitation the increased period available for Si uptake resulted in higher silicification of diatom frustules. However, our results and those of previous studies show that this phenomenon is not valid for all diatom species. As we observed that bPSi : POC, bPSi : PON, and bPSi : POP ratios were not affected by the changes in the cellular concentrations, these mechanisms will be of less importance for analysis of nutrient budgets. However, they can possibly affect the sinking behavior as well as the remineralization of frustules in the sediments. As *in situ* iron fertilization experiments are performed with the aim to increase the uptake of atmospheric CO_2 and carbon export to the deep sea, impact of iron on sedimentation and remineralization is of great interest. Higher sinking rates were observed for iron limited cells of *Actinocyclus* sp. (Muggli, et al., 1996) and of *F. kerguelensis*, *Nitzschia* sp., and *Navicula* sp. during the *in situ* iron fertilization experiment SOIREE (Waite and Nodder, 2001). This phenomenon is thought to be a mechanism for the preservation of a seed population or could possibly give the cells access to higher nutrient concentrations in deeper waters (De La Rocha, et al., 2000). Additionally it can be speculated that a stronger silicification of the frustules could increase the cell wall stability and therefore provide a better grazing protection under unfavorable growth conditions. It is also possible that iron limitation decreases the ability of diatoms to maintain buoyancy. Usually diatom cells control buoyancy by the selective exchange of heavier and lighter ions in the vacuole, the so-called ionic pump, which requires a lot of energy (Anderson and Sweeney, 1978). Iron limitation might reduce the efficiency of energy-producing pathways needed by the cells to maintain buoyancy (Sarthou, et al., 2005). However, diatoms are known to dominate the phytoplankton community in turbulent waters (Harris, 1986). It is therefore not likely that a successful phytoplankton group such as diatoms suffer from permanent stress to maintain cell buoyancy in regions like the SO, which are characterized by low iron concentrations and extremely deep mixing throughout the year. We therefore assume that increased sinking rates are mainly caused by a stronger silicification. However, the largest diatom cells during SOIREE, *Trichotoxon* sp. and *Thalassiothrix* sp., showed only little changes in sinking rates (Waite and Nodder, 2001). These species specific differences may

result from different impacts of iron on silicification as shown here and in previous studies.

The sediments of the SO mainly consist of diatom frustules of *Fragilariopsis kerguelensis*. This species is heavily silicified and has shown to increase silicification under low iron conditions in laboratory experiments including this study. Therefore, high accumulation rates of silica frustules in the sediment are probably mainly caused by strong silicification in this species under iron limitation. We therefore assume that a decrease in silicification and lower sinking rates of *F. kerguelensis*, as observed by Waite and Nodder (2001), could decrease the dominant contribution of this species to the Si export under long-term iron fertilization in the SO. Less silicified frustules could additionally be more affected by grazing and remineralization and thus decrease carbon export as well. However, the observation that the cellular Si content of *C. dichaeta* was not dependent on the iron availability, as well as the observation that *Trichotoxon* sp. and *Thalassiothrix* sp. did not change their sinking rates (Waite and Nodder, 2001), imply that other, also important SO diatom species, would not be affected. If all of those species would increase their cellular C concentrations similar to our observations of *C. dichaeta*, this could even increase the carbon export with iron fertilization.

In conclusion we suggest that changes in the bPSi : C, bPSi : N, and bPSi : P ratios with changing iron availability should be carefully interpreted in terms of nutrient export. Changes in the phytoplankton community structure as well as sinking rates and grazing protection of dominant species might be of greater importance for biomass export and remineralization.

References:

Anderson, L. W. J., and B. M. Sweeney (1978), Role of inorganic ions in controlling sedimentation rate of a marine centric diatom *Ditylum brightwelli*, Journal of Phycology, 14, 204-214.

Arrigo, K. R., R. B. Dunbar, M. P. Lizotte, and D. H. Robinson (2002), Taxon-specific differences in C/P and N/P drawdown for phytoplankton in the Ross Sea, Antarctica, Geophysical Research Letters, 29, [doi:10.1029/2002GL015277].

Arrigo, K. R., D. H. Robinson, D. L. Worthen, R. B. Dunbar, G. R. DiTullio, M. VanWort, and M. P. Lizotte (1999), Phytoplankton community structure and the drawdown of nutrients and CO_2 in the Southern Ocean, Science, 283, 365-367.

Boyd, P. W., R. Strzepek, S. Takeda, G. Jackson, C. S. Wong, R. M. McKay, C. Law, H. Kiyosawa, H. Saito, N. Sherry, K. Johnson, J. Gower, and N. Ramaiah (2005), The evolution and termination of an iron-induced mesoscale bloom in the northeast subarctic Pacific, Limnology and Oceanography, 50, 1872-1886.

Boyle, E. (1998), Pumping iron makes thinner diatoms, Nature, 393, 733-734.

Brzezinski, M. A., M.-L. Dickson, D. M. Nelson, and R. Sambrotto (2003), Ratios of Si, C and N uptake by microplankton in the Southern Ocean, Deep-Sea Research II, 50, 619-633.

Brzezinski, M. A., J. L. Jones, and M. S. Demarest (2005), Control of silica production by iron and silicic acid during the Southern Ocean Iron Experiment (SOFeX), Limnology and Oceanography, 50, 810-824.

Carman, K. R., and B. Fry (2002), Small-sample methods for $\delta^{13}C$ and $\delta^{15}N$ analysis of the diets of marsh meiofaunal species using natural-abundance and tracer-addition isotope techniques, Marine Ecology Progress Series, 240, 85-92.

Coale, K. H., et al. (2004), Southern Ocean iron enrichment experiment: carbon cycling in high- and low- Si waters, Science, 304, 408-414.

De La Rocha, C. L., D. A. Hutchins, M. A. Brzezinski, and Y. Zhang (2000), Effects of iron and zinc deficiency on elemental composition and silica production by diatoms, Marine Ecology Progress Series, 195, 71-79.

Franck, V. M., K. W. Bruland, D. A. Hutchins, and M. A. Brzezinski (2003), Iron and zinc effects on silicic acid and nitrate uptake kinetics in three high-nutrient, low-chlorophyll (HNLC) regions, Mar Ecol-Prog Ser, 252, 15-33.

Franck, V. M., M. A. Brzezinski, K. H. Coale, and D. M. Nelson (2000), Iron and silicic acid concentrations regulate Si uptake north and south of the Polar Frontal Zone in the Pacific Sector of the Southern Ocean, Deep-Sea Research II, 47, 3315-3338.

Fu, F.-X., Y. Zhang, K. Leblanc, S. A. Sanudo-Wilhelmy, and D. A. Hutchins (2005), The biological and biogeochemical consequences of phosphate scavenging onto phytoplankton cell surfaces, Limnology and Oceanography, 50, 1459-1472.

Gall, M. P., R. Strzepek, M. Maldonado, and P. W. Boyd (2001), Phytoplankton processes. Part 2. Rates of primary production and factors controlling algal growth during the Southern Ocean Iron RElease Experiment (SOIREE), Deep-Sea Res Pt Ii, 48, 2571-2590.

Greene, R. M., R. J. Geider, and P. G. Falkowski (1991), Effect of iron limitation on photosynthesis in a marine diatom, Limnology and Oceanography, 36, 1772-1782.

Harris, G. P. (1986), Phytoplankton ecology: Structure, function, and fluctuation, edited, Chapman and Hall, London.

Ho, T. Y., A. Quigg, Z. V. Finkel, A. J. Milligan, K. Wyman, P. G. Falkowski, and F. M. M. Morel (2004), The elemental composition of some marine phytoplankton, Journal of Phycology, 39, 1145-1159.

Hoffmann, L. J., I. Peeken, K. Lochte, P. Assmy, and M. Veldhuis (2006), Different reactions of Southern Ocean phytoplankton size classes to iron fertilization, Limnology and Oceanography, 51, 1217-1229.

Hutchins, D. A., and K. W. Bruland (1998), Iron-limited diatom growth and Si:N uptake ratios in a coastal upwelling regime, Nature, 393, 561-564.

Klausmeier, C. A., E. Litchman, T. Daufresne, and S. A. Levin (2004), Optimal nitrogen-to-phosphorus stoichiometry of phytoplankton, Nature, 429, 171-174.

Martin-Jézéquel, V., M. Hildebrand, and M. A. Brzezinski (2000), Silicon metabolism in diatoms: implications for growth, Journal of Phycology, 36, 821-840.

Martin, J. H., and S. E. Fitzwater (1988), Iron deficiency limits phytoplankton growth in the north-east Pacific subarctic, Nature, 331, 341-343.

Martin, J. H., R. M. Gordon, and S. E. Fitzwater (1990), Iron in Antarctic waters, Nature, 345, 156-158.

Muggli, D. L., M. Lecourt, and P. J. Harrison (1996), Effects of iron and nitrogen source on the sinking rate, physiology and metal composition of an oceanic diatom from the subarctic Pacific, Marine Ecology Progress Series, 132, 215-227.

Nelson, D. M., P. Tréguer, M. A. Brzezinski, A. Leynaert, and B. Queguiner (1995), Production and dissolution of biogenic silica in the ocean: Revised global estimates, comparison with regional data and relationship to biogenic sedimentation, Global Biogeochemical Cycles, 9, 359-372.

Price, N. M. (2005), The elemental stoichiometry and composition of an iron-limited diatom, Limnology and Oceanography, 50, 1159-1171.

Quigg, A., Z. V. Finkel, A. J. Irwin, Y. Rosenthal, T.-Y. Ho, J. R. Reinfelder, O. Schofield, F. M. M. Morel, and P. Falkowski (2003), The evolutionary inheritance of elemental stoichiometry in marine phytoplankton, Nature, 425, 291-294.

Sanudo-Wilhelmy, S. A., A. Tovar-Sanchez, F. X. Fu, D. G. Capone, E. J. Carpenter, and D. A. Hutchins (2004), The impact of surface-adsorbed phosphorus on phytoplankton Redfield stoichiometry, Nature, 432, 897-901.

Sarthou, G., K. R. Timmermans, S. Blain, and P. Treguer (2005), Growth physiology and fate of diatoms in the ocean: a review, Journal of Sea Research, 53, 25-42.

Takeda, S. (1998), Influence of iron availability on nutrient consumption ratio of diatoms in oceanic waters, Nature, 393, 774-777.

Timmermans, K. R., M. S. Davey, B. van der Wagt, J. Snoek, R. J. Geider, M. J. W. Veldhuis, L. J. A. Gerringa, and H. J. W. de Baar (2001), Co-limitation by iron and light of *Chaetoceros brevis*, *C. dichaeta* and *C. calcitrans* (Bacillariophyceae), Marine Ecology Progress Series, 217, 287-297.

Timmermans, K. R., B. van der Wagt, and H. J. W. de Baar (2004), Growth rates, half saturation constants, and silicate, nitrate, and phosphate depletion in relation to iron availability of four large open-ocean diatoms from the Southern Ocean, Limnology and Oceanography, 49, 2141-2151.

Tréguer, P., D. M. Nelson, A. J. Van Bennekom, D. J. DeMaster, A. Leynaert, and B. Queguiner (1995), The silica balance in he World Ocean: A reestimate, Science, 268, 375-379.

Twining, B. S., S. B. Baines, and N. S. Fisher (2004), Element stoichiometries of individual plankton cells collected during the Southern Ocean Iron Experiment (SOFeX), Limnology and Oceanography, 49, 2115-2128.

Waite, A. M., and S. D. Nodder (2001), The effect of in situ iron addition on the sinking rates and export flux of Southern Ocean diatoms, Deep-Sea Research II, 48, 2635-2654.

Watson, A. J., D. C. E. Bakker, A. J. Ridgwell, P. W. Boyd, and C. S. Law (2000), Effect of iron supply on Southern Ocean CO_2 uptake and implications for glacial atmospheric CO_2, Nature, 407, 730-733.

CHAPTER IV

Subduction zone volcanic ash can fertilize the surface ocean and stimulate phytoplankton growth: Evidence from biogeochemical experiments and satellite data

Svend Duggen, Peter Croot, Ulrike Schacht, and Linn Hoffmann

Geophysical Research Letters,
VOL. 34, L01612, doi:10.1029/2006GL027522, 2007

GEOPHYSICAL RESEARCH LETTERS, VOL. 34, L01612, doi:10.1029/2006GL027522, 2007

Subduction zone volcanic ash can fertilize the surface ocean and stimulate phytoplankton growth: Evidence from biogeochemical experiments and satellite data

Svend Duggen,[1,2] Peter Croot,[3] Ulrike Schacht,[4] and Linn Hoffmann[3]

Received 10 July 2006; revised 10 November 2006; accepted 6 December 2006; published 13 January 2007.

[1] Volcanoes confront Earth scientists with new fundamental questions: Can airborne volcanic ash release nutrients on contact with seawater, thereby excite the marine primary productivity (MPP); and, most notably, can volcanoes through oceanic fertilization affect the global climate in a way that is so far poorly understood? Here we present results from biogeochemical experiments showing that 1) volcanic ash from subduction zone volcanoes rapidly release an array of nutrients (co-)limiting algal growth in vast oceanic areas, 2) at a speed much faster (minute-scale) than hitherto known and that marine phytoplankton from low-iron oceanic areas can swiftly, within days, utilize iron from volcanic sources. We further present satellite data possibly indicating an increase of the MPP due to the seaward deposition of volcanic particulate matter. Our study supports the hypothesis that oceanic (iron) fertilization with volcanic ash may play a vital role for the development of the global climate. **Citation:** Duggen, S., P. Croot, U. Schacht, and L. Hoffmann (2007), Subduction zone volcanic ash can fertilize the surface ocean and stimulate phytoplankton growth: Evidence from biogeochemical experiments and satellite data, *Geophys. Res. Lett.*, *34*, L01612, doi:10.1029/2006GL027522.

1. Introduction

[2] The availability of nutrients in the surface ocean strongly affects the MPP and can therefore have a substantial influence on the development of the global climate [*Falkowski et al.*, 1998; *Morel and Price*, 2003]. Almost two decades ago it was discovered that iron limits phytoplankton growth in vast oceanic areas [*Martin and Fitzwater*, 1988]. Since then it was hypothesized that particulate matter from major volcanic eruptions (e.g. Pinatubo 1991, Philippines subduction zone) may release sufficient iron and other nutrients to the surface ocean to stimulate the MPP and trigger global atmospheric CO_2-drawdown [*Sarmiento*, 1993; *Watson*, 1997]. Moreover, oceanic fertilization with Fe from volcanic ash is thought to be partly responsible for a termination of global warmth at the Paleocene/Eocene boundary and for millennial climate change through MPP feedback [*Bains et al.*, 2000; *Bay et al.*, 2004].

[3] The rapid fertilizing potential of volcanic ash particles arises from a coating containing nutrient-bearing soluble salts formed from the gas phase during the eruption (e.g. condensed volcanic gases and adsorbed aerosols) [*Frogner et al.*, 2001]. A pioneer study with seawater and a single ash sample from the Icelandic Hekla volcano shows that ash from volcanoes in hot spot tectonic settings can release substantial amounts of macro- and micro-nutrients such as PO_4^{3-}, Si, Fe, Zn, Mn, Ni, Co and Cu within 1–2 hours [*Frogner et al.*, 2001]. However, volcanic gases from hot spot and subduction zone (SZ) volcanoes strongly differ in composition [*Oppenheimer*, 2004] and therefore volcanic ash coatings from these fundamentally different tectonic settings can be expected to have different nutrient contents and ratios underlining the necessity to examine the nutrient mobilization behaviour of subduction zone volcanic ash.

[4] This is particularly important for future quantitative assessments of the significance of volcanoes for oceanic fertilization, since most of the >5,300 historical subaerial volcanic eruptions occurred in subduction zones and due to their explosive nature SZ volcanoes are capable of transporting huge amounts of ash far into the ocean basins [*Sigurdsson et al.*, 2000], where trace metal levels usually are low. The majority of SZ volcanoes in turn are found in the Pacific Ring of Fire encircling the Pacific Ocean covering almost 50% of the Earth's oceanic surface and, notably, hosting the largest surface ocean area with very low-iron concentrations (Figure 1).

[5] Rapid stimulation of the MPP upon seaward volcanic ash deposition can only be expected at water depths where phytoplankton thrives, i.e. in the sunlit euphotic zone of the surface ocean (~100 m). Yet it remains unclear whether nutrients from SZVA particles, while sinking through the water column, are mobilized sufficiently swiftly, i.e. within the euphotic zone, or in the darkness of the sea. For the ocean-atmosphere interchange of CO_2 diatoms appear to take centre stage (e.g. due to the high C/Fe ratio of their tissue) [*Smetacek*, 2000; *Watson*, 1997] but, although generally expected, it is until now uncertain if marine diatoms can utilize volcanic iron for building up biomass, which may depend on the speciation of iron and the contemporaneous release of toxic metal ions. Together, short time-scale studies of the nutrient and toxic metal mobilization behaviour of SZVA and biogeochemical experiments are presently important for improving our understanding of the causal connection between volcanism, oceanic (iron) fertilization, enhancement of the MPP, the ocean-atmosphere interchange

[1] Geological Institute, University of Copenhagen, Copenhagen, Denmark.
[2] Now at Dynamics of the Ocean Floor Division, Leibniz-Institute for Marine Sciences, IFM-GEOMAR, Kiel, Germany.
[3] Marine Biogeochemistry and Chemical Oceanography Division, Leibniz-Institute for Marine Sciences, IFM-GEOMAR, Kiel, Germany.
[4] SFB 574, Leibniz-Institute for Marine Sciences, IFM-GEOMAR, Kiel, Germany.

0094-8276/07/2006GL027522$05.00

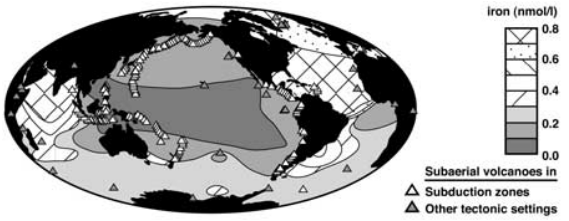

Figure 1. Map illustrating the surface ocean iron concentrations (modified from *Parekh et al.* [2005]) and distribution of subaerially active volcanoes [*Sigurdsson et al.*, 2000] on Earth. Subduction zone volcanoes are concentrated along the Pacific Ring of Fire encircling the largest ocean basin and the global minimum of surface ocean iron concentration.

of CO_2 and sulfur compounds, and ultimately global climate development.

2. Samples and Results

[6] The volcanic ash samples used for geochemical experiments in this study stem from subduction zone volcanoes located thousands of kilometers apart in the Pacific Ring of Fire: Arenal in Costa Rica, Sakura-jima in Japan and Mt. Spurr in Alaska (Figure 1). As airborne volcanic ash particles have soluble coatings containing nutrients [*Frogner et al.*, 2001] it is crucial to conduct oceanic fertilization studies with ash that has neither been in contact with rain- nor seawater following deposition (unhydrated ash). The release of 1) trace metals was determined *in situ* in low-metal Antarctic seawater by means of Anodic Stripping Voltammetry and 2) fixed N species, PO_4^{3-} and SiO_4^{4-} in the course of agitation experiments using low-nutrient Atlantic seawater. Details about analytical methods and data tables are found in the online auxiliary material[1].

[7] As illustrated in Figure 2a, on contact with ocean water, unhydrated SZVA swiftly release significant amounts of an array of important nutrients. Despite the wide distribution of their volcanic sources, the ash samples exhibit remarkably similar mobilization patterns with the highest mobilization rates within the initial 5–15 minutes and a fairly restricted variation of their nutrient release. Within 20 minutes each gram of ash liberated between 10–60 nmol of Fe, 2–27 nmol of Zn and 0–50 nmol of Cu (Figure 2a). Fe concentrations rose further within the first hour and thereafter even redoubled at 15 hours contact time as measured for the Arenal ash sample. The subsequent slight but steady decrease of the Zn and Cu concentrations following an initial pulse may be attributed to partial re-adsorption of Zn and Cu to ash particle surfaces. Only trace amounts of Cd and Pb, however, came off. Agitation experiments illustrate that SZVA instantly mobilize fixed N in significant amounts but, remarkably, primarily as NH_4^+ (~81–98% of the total N) rather than NO_3^- and NO_2^-, along with some PO_4^{3-} and Si (Figure 2a). Each gram of ash released between 200–1,100 nmol NH_4^+, 10–450 nmol NO_3^-, <50 nmol NO_2^-, 10–100 nmol PO_4^{3-} and 50–200 nmol Si. Trace metals are apparently released on a similar time scale as from Saharan aeolian dust [*Nimmo et al.*, 1998].

[8] In order to examine the possible biological effect of SZVA in iron-limited oceanic areas we performed bio-incubation experiments with the diatom *Chaetoceros dichaeta*, a common phytoplankton species in the Southern Ocean. We used Antarctic seawater doped with vitamins and nutrients (f/2 concentrations) except iron thereby creating an iron-limited system. For three of the six culture experiments the seawater was additionally in very brief contact (only 15–20 minutes!) with selected SZVA material having high initial mobilization rates for Fe as based on geochemical experiments (Figure 2a). As illustrated in Figures 3a and 3b, the phytoplankton in the bottles with SZVA-fertilized seawater show both a significant enhancement of the photosynthetic efficiency Fv/Fm and biomass (chlorophyll *a*) compared to the cultures that were grown without SZVA-fertilization. Within the first three days the SZVA-fertilized cultures exhibited a rapid increase of the photosynthetic efficiency that in the subsequent fourteen days stayed at a relatively high level ranging from 0.52 to 0.42 ± 0.03 (Figure 3a). This is significantly above the values observed for iron limited systems (<0.3, e.g. 0.20–0.25 in the Southern Ocean) [*Coale et al.*, 2004], whereas the cultures in the experiments without SZVA-fertilization swiftly fell back towards this level. After day six and until the termination of the experiment (after day 18) the increase of chlorophyll *a* in the SZVA-fertilized treatments was almost three times as high as for the populations grown under Fe-limited conditions (Figure 3b).

3. Discussion

[9] Our geochemical data for the first time provide a basis to explore the chemical impact of SZVA on surface ocean water. Based on Stokes' law and assuming deposition of individual grains, volcanic ash particles have euphotic zone residence times ranging from only a few minutes through 1–2 hours to 1–2 days for, resp., coarse (2,000–500 μm), intermediate (250–150 μm) and fine (<50 μm) ash particles. Aggregates of ash particles are frequently formed in the ash clouds of volcanic eruptions and are inferred to have high settling velocities in seawater (>1,670 meters/day) [*Wiesner et al.*, 1995], showing that even fine ash particles, as clusters, pass the euphotic zone swiftly within 1–2 hours.

[10] Since the mobilization rates are highest during the initial minutes (Figure 2a), the upper section (50 m) of the euphotic zone will be more prone to oceanic fertilization with SZVA: An ash layer of about 1 mm thickness distributed on a surface of 1 dm^2 (corresponding to ~20 g of ash at 30% porosity) could raise the Fe concentration by about 0.4–2.4 nmol/l, Zn by 0.1–1.1 nmol/l, Cu by 0–2.0 nmol/l, total fixed N expressed as NO_3^- by 1–3.2 μmol/l (Figure 2a), PO_4^{3-} by 0.4–4.0 nmol/l and Si by 2.0–8.0 nmol/l (Figure 2b) (calculated for 50 m mixed layer depth). For an ~1 cm ash layer these values would roughly be 10-fold and it is therefore important to emphasize that ash layers on the centi-, decimetre- and metre-scale were frequently found at numerous drill sites in the ocean basins [*Cao et al.*, 1995]. Notably, it was estimated that volcanic material makes up ca. 23% of the marine sediments in the Pacific about half of

[1]Auxiliary material data sets are available at ftp://ftp.agu.org/apend/gl/2006GL027522. Other auxiliary material files are in the HTML.

which comes from subduction zones [*Straub and Schmincke*, 1998].

[11] SZVA would most likely have their largest impact on the ocean water chemistry where the concentrations of one or more nutrients are low. This is usually the case in the euphotic zone but becomes extreme in regions where the MPP is under-productive due to restricted nutrient availability (e.g. Fe) [*Martin and Fitzwater*, 1988]. In general these areas are the low- and high-nutrient- but low-productivity (LNLP and HNLP) areas in the Central Pacific, Central Atlantic, Central Indian and Southern Ocean (Figure 1) [*Chester*, 2000] that in terms of biologically important trace metal levels may be considered some of the most devilish habitats on Earth [*Morel and Price*, 2003]. In the surface ocean water of LNLP areas the nutrient concentrations are extraordinarily low (e.g. Fe and Zn <0.5 nmol/l, Cu <1 nmol/l and NO_3^- <~50 nmol/l) [*Bruland and Lohan*, 2004; *Dugdale and Wilkerson*, 1992] (Figures 1 and 2b). HNLP areas such as the Southern Ocean have excess NO_3^- (~20–30 μmol/l), variable Si ($\leq$5 μmol/l in low-Si- and $\geq$60 μmol/l in high-Si areas) but very low Fe contents (<0.5 nmol/l) [*Boyd et al.*, 2004; *Coale et al.*, 2004] (Figures 1 and 2b). Therefore, seaward deposition of even very thin layers of volcanic ash can significantly increase fixed N, Fe, Zn and Cu concentrations in LNLP areas and Fe, Zn and Cu in HNLP regions (Figure 2b). Consequently, SZVA can have an impact on the euphotic zone nutrient budget in as much as ~70% of the oceanic areas on Earth. However, drill core data for Pacific marine sediments suggest that most of the SZVA is deposited in the vicinity, i.e. <1,000 kilometers, of subduction zones, which in the Pacific Ocean is well within the low-productivity oceanic areas [*Straub and Schmincke*, 1998].

[12] Recent open ocean bioassay experiments show that oceanic fertilization is more effective when a combination of nutrients is added to surface ocean water rather than an individual growth-limiting element [*Mills et al.*, 2004]. This is associated with co-limitation of algal growth by additional nutrients that may play a crucial role for the acquisition and uptake of carbon, nitrogen, phosphorous and silica by marine phytoplankton (e.g. Fe, Zn and Cu in metalloenzymes and Si for silica shells in diatoms) and hence the build-up of biomass in the oceans. SZVA not only release the key trace metal Fe but also Zn, Cu, P, Si, and NH_4^+ (Figure 2) that is more readily incorporated into algae tissue than NO_3^-. Therefore, SZVA can be considered as a natural and rapidly working multi-fertilizer having the potential to excite the MPP in various oceanic areas.

[13] To our knowledge this study provides the first direct evidence that marine diatoms can utilize iron from volcanic sources. The swift coupled enhancements of Fv/Fm and Chl *a* in the bio-incubation experiments with SZVA as displayed in Figure 3 are similar to those observed for the MPP during meso-scale iron-fertilization experiments in the Southern Ocean [*Coale et al.*, 2004]. Our results illustrate that SZVA can indeed act as high-speed fertilizer and has the potential

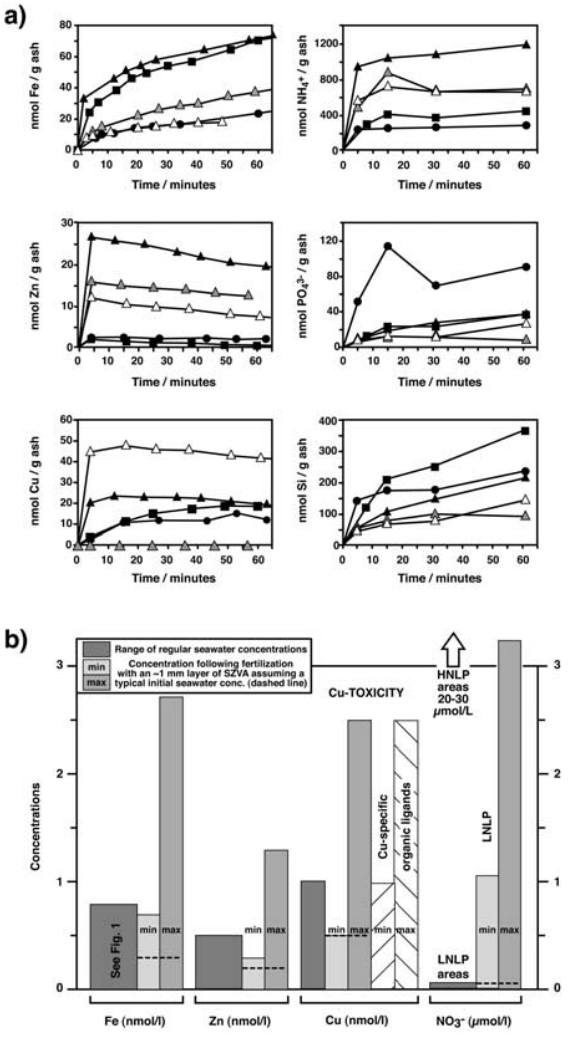

Figure 2. Effect of unhydrated subduction zone volcanic ash on seawater. (a) Results for nutrient release of unhydrated SZVA on contact with natural seawater from time-dependent geochemical experiments measured by means of Anodic Stripping Voltammetry and standard photometry. The SZVA stem from different eruptions of volcanoes in the Pacific Ring of Fire: Sakura-jima volcano in Japan sampled 11 June 1986 (on the campus of the Kagoshima university), 18 November 1987 (at the eastern foot of the volcano) and 12 June 1999 (again on campus) (white, grey and black triangles, respectively), Mt. Spurr sampled 18 August 1991 in Anchorage, Alaska (black circles) and permanently active Arenal volcano 1993 sampled at the foot of the volcano in Costa Rica (black squares). Natural seawater was sampled cleanly during cruises with large research vessels in the Antarctic and Atlantic Oceans. (b) Bar chart schematically displaying the effect on the nutrient budget of the upper section (mixed layer depth = 50 m) of the marine euphotic zone upon seaward deposition of a relatively thin, ~1 mm volcanic ash layer. The calculations are based on a short seawater-SZVA contact time of ~20 minutes as inferred from Figure 2a. Fixed nitrogen species were recalculated to nitrate. The bars denote the absolute range of surface ocean concentrations for individual trace metals and NO_3^- (see Figure 1). Concentrations of Fe, Zn, Cu and NO_3^- in LNLP and HNLP oceanic areas prior to fertilization and of Cu-specific organic ligands in oligotrophic regions governing the level of Cu-toxicity as discussed in the main text and Figure 1.

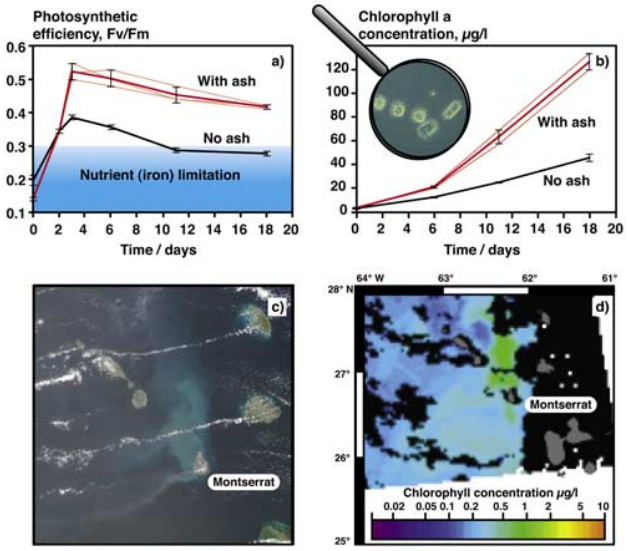

Figure 3. (a, b) Results from bio-incubation experiments with subduction zone volcanic ash and the diatom *Chaetoceros dichaeta* in natural seawater and (c, d) satellite data possibly indicating a phytoplankton bloom around ash-erupting Soufrière Hills volcano on Montserrat Island in the Lesser Antilles subduction zone. Figures 3a and 3b exhibit the increase of the photosynthetic efficiency Fv/Fm (Figure 3a) and chlorophyll *a* (biomass) concentrations (Figure 3b) during biogeochemical experiments with diatom phytoplankton (*Chaetoceros dichaeta,* shown in the reading-glass inset) in low-iron Antarctic seawater and SZVA as an iron-fertilizer in three of six experiments. Thin red lines display the results of single experiments, whereas thick red and black lines represent the geometric mean including error bars (s.d.). For nutrient limited conditions Fv/Fm is below ~0.3. Figure 3c shows an AQUA MODIS true colour space image showing Montserrat Island on 14th of July 2003 and a ~160 km by ~40 km sized greenish-blue seawater discolouration and Figure 3d processed SEASTAR SeaWiFs satellite data for the 17th of July illustrating that the seawater discolouration may result from an increase of chlorophyll concentration caused by a phytoplankton bloom.

to increase the MPP in at least iron-limited if not even all low-iron oceanic areas, making up the majority of the Earth's oceans (Figure 1). Natural manifestation for enhanced diatom growth following volcanic ash deposition is found in a drill core from the Southern Ocean showing a significant increase of the relative abundance of *Thalassiosira oestrupii* immediately after the deposition of a ~10 cm ash layer ~450 ka ago [*Kunz-Pirrung et al.*, 2002]. The association of a large number of ash layers and diatomites in the Danish mo clay formation [*Bøggild*, 1918] also suggests stimulation of diatom growth linked to volcanic ash deposition.

[14] However, whether volcanic particulate matter stimulates phytoplankton growth or not may depend on the presence or absence of toxic effects associated with the liberation of trace metals. Some metal ions are essential but can at elevated concentrations also have a negative (toxic) effect on the MPP. Such a 'Goldilocks' metal (not too little, not too much) [*Bruland and Lohan*, 2004] is Cu that can be released rapidly in significant amounts from SZVA (Figures 2a and 2b) and in general is more toxic to algae than Cd and Zn [*Bruland and Lohan*, 2004; *McKnight et al.*, 1981]. Cu is toxic as free cations but not when complexed with organic ligands, i.e. toxicity very much depends on the euphotic zone free-ion/complexed-ion ratio. In oligotrophic regions dominated by Cu-sensitive picoplankton [*Mann et al.*, 2002; *Morel et al.*, 2004] seawater concentrations of strong Cu-specific organic ligands are low (e.g. 1–2.5 nmol/l) [*Coale and Bruland*, 1988; *Moffet*, 1995], and free copper levels may be substantially and swiftly enhanced by SZVA eventually reaching toxicity (Figure 2b). On the other hand, phytoplankton species have different tolerances for and responses to Cu-toxicity [*Croot et al.*, 2000; *Mann et al.*, 2002; *Morel et al.*, 2004] and ash deposited in HNLP regions dominated by Cu-tolerant diatoms may have limited toxic effects. The toxic elements Pb and Cd, however, were only released in traces from SZVA and are unlikely to cause toxicity. In summary, our results illustrate that Cu-toxicity may be a relevant issue for the MPP upon seaward deposition of volcanic ash. A detailed understanding of this process, however, has to await results from open ocean bioassay experiments.

[15] Natural evidence for biological response to the seaward deposition of subduction zone volcanic particulate matter comes from satellite images and data of the bio-optical properties of seawater. A region of about 160 km by 40 km of greenish-blue seawater discoloration in the ash fall area around the active Soufrière Hills Volcano (Montserrat Island in the Lesser Antilles) was detected mid-July 2003 by the Moderate Resolution Imaging Spectroradiometer (MODIS) on board the AQUA and TERRA satellites (Figure 3c). Such a seawater discoloration in true color satellite images may be interpreted as a phytoplankton bloom. In order to verify this, we processed data provided by the Sea-viewing Wide Field-of-view Sensor (SeaWiFS) on board the SEASTAR satellite (Figure 3d). The data indicate that the seawater discoloration may have been caused by a considerable increase in chlorophyll levels (~1 μg/l). However, the satellite data furthermore point to a significant raise of the surface reflectance at 555 nm, which could indicate suspended volcanic ash particles that in turn may bias the appraised chlorophyll value. Stokes' law estimates and data from the Pinatubo eruption [*Wiesner et al.*, 1995] suggest that this ash signal should have been removed by the time the image was acquired. Unfortunately, there is not sufficient ash reflectance data available for a quantification of the pseudo-chlorophyll signal and we encourage researchers focusing on the bio-optical properties of seawater to examine this phenomenon in more detail.

[16] The metabolism of marine biomass production is directly linked to the atmospheric (greenhouse) gas budget. Therefore, a massive stimulation of the MPP has the capability to cause a short- and long-term drawdown of atmospheric CO_2 and to release significant amounts of biogenic dimethyl sulfide (DMS) to the atmosphere forming a main precursor of cloud condensation nuclei [*Charlson et al.*, 1987; *Sarmiento*, 1993; *Watson*, 1997]. The combination of lower atmospheric CO_2 contents and a higher cloud frequency could ultimately provide a cooling component to the development of the global climate. It was argued recently that the 1991 eruption of the Pinatubo subduction

zone volcano enhanced the MPP in the Southern Ocean causing an atmospheric CO_2-drawdown associated with an excess O_2-pulse [*Frogner et al.*, 2001; *Keeling et al.*, 1996; *Sarmiento*, 1993; *Watson*, 1997]. Using our iron mobilization data (average for 20 minutes contact time) (Figure 2a, Table 1) and assuming a typical carbon/iron ratio of 10^5 for phytoplankton in Fe-limited areas [*Watson*, 1997], we calculated that rapid Fe-fertilization with, on average, $\sim 6.3 \times 10^{15}$ g of SZVA could have caused the estimated loss of CO_2 ($\sim 1.6 \times 10^{15}$ g of C applied to the Northern Hemisphere) following the Pinatubo eruption [*Sarmiento*, 1993]. This amount of ash, however, corresponds to ~35–48% of the material erupted during the 1991 Pinatubo eruption ($1.3–1.8 \times 10^{16}$ g) [*Oppenheimer*, 2004], much of which was deposited seaward. Integrating our new data from biogeochemical experiments with data from the literature therefore suggest that oceanic and atmospheric biogeochemical cycles may be affected swiftly and for years following major volcanic eruptions.

4. Conclusions

[17] Subduction zone volcanic ash has a substantial potential to alter the nutrient budget of the surface ocean and to stimulate the growth of diatoms and other phytoplankton in iron-limited and other low-productivity oceanic areas. Hence, oceanic fertilization with SZVA may play a vital role for the ocean-atmosphere gas interchange and ultimately the development of the global climate.

[18] **Acknowledgments.** We are hugely grateful to C. Neal, G. Alvarado Induni and T. Kobayashi for kindly providing the ash samples and H. Johannsen for analytical assistance. We thank C. Neal, T. Ruedas and D. Wallace for comments and are grateful to S. Reynir Gislason and an anonymous reviewer for constructive criticism. The study was supported by the German Research Foundation (Deutsche Forschungsgemeinschaft) and is SFB 574 "Volatiles and fluids in subduction zones" contribution 83.

References

Bains, S., et al. (2000), Termination of global warmth at the Palaeocene/Eocene boundary through productivity feedback, *Nature*, *407*, 171–174.

Bay, R. C., et al. (2004), Bipolar correlation of volcanism with millennial climate change, *Proc. Natl. Acad. Sci. U. S. A.*, *101*, 6341–6345.

Bøggild, O. B. (1918), Den vulkanske Aske i Moleret samt en Oversigt over Danmarks ældre Tertiærbjergarter, *Dans. Geol. Unders., Raekke 2*, *33*, 159.

Boyd, P. W., et al. (2004), The decline and fate of an iron-induced subarctic phytoplankton bloom, *Nature*, *428*, 549–553.

Bruland, K. W., and M. C. Lohan (2004), Controls of trace metals in seawater, in *The Oceans and Marine Geochemistry (Treatise on Geochemistry 6)*, edited by H. Elderfield, pp. 23–47, Elsevier, New York.

Cao, L.-Q., et al. (1995), Geochemistry and petrology of volcanic ashes recovered from Sites 881 through 884: A temporal record of Kamchatka and Kurile volcanism, *Proc. Ocean Drill. Program Sci. Results*, *145*, 345–381.

Charlson, R. J., et al. (1987), Oceanic phytoplankton, atmospheric sulphur, cloud albedo and climate, *Nature*, *326*, 655–661.

Chester, R. (2000), *Marine Geochemistry*, 2nd ed., 506 pp., Blackwell Sci., Malden, Mass.

Coale, K. H., and K. W. Bruland (1988), Copper complexation in the northeast Pacific, *Limnol. Oceanogr.*, *33*, 1084–1101.

Coale, K. H., et al. (2004), Southern Ocean iron enrichment experiment: Carbon cycling in high- and low-Si waters, *Science*, *304*, 408–414.

Croot, P., et al. (2000), Production of extracellular Cu complexing ligands by eucaryotic phytoplankton in response to Cu stress, *Limnol. Oceanogr.*, *45*, 619–627.

Dugdale, R. C., and F. P. Wilkerson (1992), Nutrient limitation of new production, in *Primary Productivity and Biogeochemical Cycles in the Sea*, edited by P. G. Falkowski and A. D. Woodhead, pp. 107–122, Springer, New York.

Falkowski, P. G., et al. (1998), Biogeochemical controls and feedbacks on ocean primary production, *Science*, *281*, 200–206.

Frogner, P., et al. (2001), Fertilizing potential of volcanic ash in ocean surface water, *Geology*, *29*, 487–490.

Keeling, R. F., et al. (1996), Global and hemispheric CO_2 sinks deduced from changes in atmospheric O_2 concentration, *Nature*, *381*, 218–221.

Kunz-Pirrung, M., et al. (2002), Mid-Brunhes century-scale diatom sea surface temperature and sea ice records from the Atlantic sector of the Southern Ocean (ODP Leg 177, sites 1093, 1094 and core PS2089-2), *Palaegeogr. Palaeoclimatol. Palaeoecol.*, *182*, 305–328.

Mann, E. L., et al. (2002), Copper toxicity and cyanobacteria ecology in the Sargasso Sea, *Limnol. Oceanogr.*, *47*, 976–988.

Martin, J. H., and S. E. Fitzwater (1988), Iron deficiency limits phytoplankton growth in the north-east Pacific subarctic, *Nature*, *331*, 341–343.

McKnight, D. M., et al. (1981), Toxicity of volcanic-ash leachate to a blue-green alga: Results of a preliminary bioassay experiment, *Environ. Sci. Technol.*, *15*, 362–364.

Mills, M. M., et al. (2004), Iron and phosphorus co-limit nitrogen fixation in the eastern tropical North Atlantic, *Nature*, *429*, 292–294.

Moffet, J. W. (1995), The spatial and temporal variability of copper complexation by strong organic ligands in the Sargasso Sea, *Deep Sea Res.*, *42*, 1273–1295.

Morel, F. M. M., and N. M. Price (2003), The biogeochemical cycles of trace metals in the oceans, *Science*, *300*, 944–947.

Morel, F. M. M., et al. (2004), Marine bioinorganic chemistry: The role of trace metals in the oceanic cycles of major nutrients, in *The Oceans and Marine Geochemistry (Treatise on Geochemistry 6)*, edited by H. Elderfield, pp. 113–143, Elsevier, New York.

Nimmo, M., et al. (1998), Atmospheric deposition: A potential source of trace metal organic complexing ligands to the marine environment, *Croat. Chem. Acta*, *71*, 323–341.

Oppenheimer, C. (2004), Volcanic degassing, in *The Crust (Treatise on Geochemistry 3)*, edited by R. L. Rudnick, pp. 123–166, Elsevier, New York.

Parekh, P., et al. (2005), Decoupling of iron and phosphate in the global ocean, *Global Biogeochem. Cycles*, *19*, GB2020, doi:10.1029/2004GB002280.

Sarmiento, J. L. (1993), Atmospheric CO_2 stalled, *Nature*, *365*, 697–698.

Sigurdsson, H., , et al. (Eds.) (2000), *Encyclopedia of Volcanoes*, Elsevier, New York.

Smetacek, V. (2000), The giant diatom dump, *Nature*, *406*, 574–575.

Straub, S. M., and H.-U. Schmincke (1998), Evaluating the tephra input into Pacific Ocean sediments: Distribution in space and time, *Geol. Rundsch.*, *87*, 461–476.

Watson, A. J. (1997), Volcanic Fe, CO_2, ocean productivity and climate, *Nature*, *385*, 587–588.

Wiesner, M. G., et al. (1995), Fallout of volcanic ash to the deep South China Sea induced by the 1991 eruption of Mount Pinatubo (Philippines), *Geology*, *23*, 885–888.

P. Croot and L. Hoffmann, Marine Biogeochemistry and Chemical Oceanography Division, Leibniz-Institute for Marine Sciences, IFM-GEOMAR, Dienstgebäude Westufer, Düsternbrooker Weg 20, D-24105 Kiel, Germany.

S. Duggen, Dynamics of the Ocean Floor Division, Leibniz-Institute for Marine Sciences, IFM-GEOMAR, Dienstgebäude Ostufer, Wischhofstrasse 1-3, D-24148 Kiel, Germany. (sduggen@ifm-geomar.de)

U. Schacht, SFB 574, Leibniz-Institute for Marine Sciences, IFM-GEOMAR, Dienstgebäude Ostufer, Wischhofstrasse 1-3, D-24148 Kiel, Germany.

Methods

Time-dependent geochemical experiments were performed under clean laboratory conditions by mixing defined quantities of unhydrated ash and seawater (~1:20 and ~1:50 mass ratios for the trace metals and the other nutrients, respectively). Seawater used for the geochemical experiments was filtered through 0.2 μm PTFE cartridges (Sartorius) and UV irradiated for 90 minutes to remove biology and natural organic ligands. The ash samples were not sieved and therefore particle size distribution resembles that of a natural sample. Concentrations of Zn, Cu, Cd and Pb were determined *in situ* in low-metal Antarctic surface ocean water using Anodic Stripping Voltammetry with a hanging mercury drop electrode using a Metrohm VA757 under standard operating conditions. Labile Fe measurements were performed using an established technique for seawater (Croot and Johansson, 2000). The release of NH_4^+, PO_4^{3-}, Si, NO_3^- and NO_2^- was examined by means of leaching experiments with short agitation times in low-nutrient Atlantic seawater followed by rapid filtration through a 1 μm mesh PTFE filter (Sartorius) and standard routine photometry. All containers used were made of cleaned quartz glass, PE or PTFE. The geochemical data are found in Table 1 in the Online Supplemental Data.

Bio-incubation experiments were performed under trace metal clean laboratory conditions. 3.75 g of unhydrated ash (corresponding to ~0.2 mm ash layer on a surface of 1 dm^2 at 30 % porosity) from Arenal volcano was added to a batch of 1.5 L Antarctic surface ocean water that was sampled and sterilized on board the research vessel POLARSTERN in a mobile clean lab container by means of a 0.2 μm PTFE filter. After brief agitation the seawater was separated from the volcanic particulate matter with a 0.2

μm sieve resulting in a short reaction time of 15-20 minutes and then split into three portions that were doped with EDTA, nutrients (except iron) and vitamins (f/2 concentrations) and finally the diatom *Chaetoceros dichaeta* that were pre-cultured and adapted to low-iron conditions for several generations. Based on the time-dependent geochemical experiments results the Fe concentrations rose to ~115 nmol/l. The cultures were grown in 0.5 L polycarbonate bottles at 3°C exposed to artificial sunlight in marine biological laboratories. The biogeochemical data are found in Table 2 in the Online Supplemental Data.

Croot, P., and M. Johansson (2000), Determination of iron speciation by cathodic stripping voltammetry in seawater using the competing ligand 2-(2-Thiazolylazo)-*p*-creasol (TAC), *Electroanalysis*, *12*, 565-576.

Table 1: Results from time-dependent geochemical experiments with natural seawater and subduction zone volcanic ash, recalculated to nmole and µmole per gram ash. Trace metals were determined by Anodic Stripping Voltammetrie, remaining nutrients by photometry.

Mt- Spurr volcano	nmole Fe		nmole Zn	nmole Cu		µmole	µmole NO_3^-	µmole NO_2^-	µmole	µmole Si
time / min	per g ash	time / min	per g ash	per g ash	time / min	per g ash	per g ash	per g ash	per g ash	per g ash
0	0.0	0								
6	11.9	4	2.61	2.52	5	0.25	0.05	0.03	0.05	0.14
8	14.3	15	2.58	10.62	15	0.26	0.05	0.03	0.11	0.18
12	15.1	27	2.35	11.68	31	0.27	0.06	0.03	0.07	0.18
19	18.3	43	2.30	11.66	61	0.29	0.06	0.04	0.09	0.24
25	19.7	53	2.24	15.20						
34	20.6	63	2.21	12.02						
60	27.5									
75	30.6									

Arenal volcano	nmole Fe		nmole Zn	nmole Cu		µmole	µmole NO_3^-	µmole NO_2^-	µmole	µmole Si
time / min	per g ash	time / min	per g ash	per g ash	time / min	per g ash	per g ash	per g ash	per g ash	per g ash
0	0.0	0								
4	24.0	4	2.08	3.48	8	0.31	0.01	0.01	0.01	0.12
7	30.4	16	1.59	11.19	15	0.41	0.01	0.03	0.02	0.21
13	38.4	25	1.39	14.94	31	0.37	0.02	0.03	0.02	0.25
18	46.0	38	1.19	17.04	61	0.45	0.02	0.04	0.04	0.37
23	49.2	49	0.65	18.43						
30	54.0	60	0.60	18.51						
38	56.6	70	0.31	19.79						
51	64.2									
60	70.1									
71	73.8									

Sakura-jima 1986	nmole Fe		nmole Zn	nmole Cu		µmole	µmole NO_3^-	µmole NO_2^-	µmole	µmole Si
time / min	per g ash	time / min	per g ash	per g ash	time / min	per g ash	per g ash	per g ash	per g ash	per g ash
0	0.0	0								
3	8.4	4	12.41	45.13	5	0.58	0.44	0.01	0.01	0.05
5	9.9	16	10.86	48.26	15	0.73	0.46	0.02	0.01	0.07
11	12.2	26	10.07	46.43	31	0.68	0.45	0.02	0.01	0.08
20	14.7	37	9.66	46.22	61	0.68	0.47	0.03	0.03	0.15
26	15.6	51	8.39	43.53						
32	17.4	61	7.91	42.19						
40	18.2	78	7.42	38.88						
48	18.8	86	6.50	38.24						

Sakura-jima 1987	nmole Fe		nmole Zn	nmole Cu		µmole	µmole NO_3^-	µmole NO_2^-	µmole	µmole Si
time / min	per g ash	time / min	per g ash	per g ash	time / min	per g ash	per g ash	per g ash	per g ash	per g ash
0	0.0	0								
5	12.5	4	16.24	0.00	5	0.50	0.07	0.01	0.01	0.06
8	15.8	14	15.48	0.00	15	0.89	0.07	0.02	0.01	0.09
20	22.9	25	14.77	0.00	31	0.69	0.09	0.02	0.02	0.10
27	26.9	36	14.37	0.00	61	0.71	0.08	0.01	0.01	0.10
34	29.3	46	13.53	0.00						
40	30.7	57	12.91	0.00						
50	35.3									
59	37.9									
93	47.5									

Sakura-jima 1999	nmole Fe		nmole Zn	nmole Cu		µmole	µmole NO_3^-	µmole NO_2^-	µmole	µmole Si
time / min	per g ash	time / min	per g ash	per g ash	time / min	per g ash	per g ash	per g ash	per g ash	per g ash
0	0.0	0								
2	33.5	4	26.99	20.59	5	0.95	0.16	0.01	0.01	0.06
12	46.4	12	26.09	23.80	15	1.05	0.17	0.02	0.02	0.11
16	51.5	22	25.18	23.43	31	1.09	0.18	0.03	0.03	0.15
21	54.9	33	23.28	23.36	61	1.20	0.19	0.04	0.04	0.22
26	58.3	41	22.23	22.87						
42	64.8	51	20.92	21.24						
57	71.0	63	19.87	19.97						
65	74.2	74	18.66	18.76						

Table 2: Results from time-dependent bio-incubation experiments with the diatom *Chaetoceros dichaeta*, natural seawater and volcanic ash.

Day	Bottle	Ash	Fv /Fm	mean	s.d.	Chl a conc. (µg/l)	mean	s.d.
Zero	1	No ash	0.19	0.19	0.02	2.3	2.2	0.13
	2		0.21			2.0		
	3		0.18			2.3		
	4	With	0.14	0.14	0.01	3.1	2.6	0.42
	5		0.14			2.3		
	6		0.13			2.5		
Day	Bottle	Ash	Fv /Fm	mean	s.d.	Chl a conc. (µg/l)	mean	s.d.
Two	1	No ash	0.34	0.34	0.01	n.a.		
	2		0.35					
	3		0.34					
	4	With	0.35	0.35	0.00	n.a.		
	5		0.35					
	6		0.35					
Day	Bottle	Ash	Fv /Fm	mean	s.d.	Chl a conc. (µg/l)	mean	s.d.
Three	1	No ash	0.42	0.40	0.02	n.a.		
	2		0.38					
	3		0.39					
	4	With	0.50	0.52	0.03	n.a.		
	5		0.52					
	6		0.55					
Day	Bottle	Ash	Fv /Fm	mean	s.d.	Chl a conc. (µg/l)	mean	s.d.
Six	1	No ash	0.37	0.36	0.01	11.4	11.7	0.49
	2		0.35			12.3		
	3		0.36			11.5		
	4	With	0.48	0.50	0.03	20.2	20.2	0.90
	5		0.53			21.1		
	6		0.50			19.3		
Day	Bottle	Ash	Fv /Fm	mean	s.d.	Chl a conc. (µg/l)	mean	s.d.
Eleven	1	No ash	0.29	0.29	0.01	24.2	24.2	0.48
	2		0.29			24.7		
	3		0.28			23.7		
	4	With	0.44	0.45	0.02	63.7	62.8	5.79
	5		0.48			68.1		
	6		0.44			56.7		
Day	Bottle	Ash	Fv /Fm	mean	s.d.	Chl a conc. (µg/l)	mean	s.d.
Eighteen	1	No ash	0.30	0.28	0.02	43.3	45.1	2.99
	2		0.27			48.5		
	3		0.28			43.4		
	4	With	0.42	0.42	0.01	125.7	126.3	6.86
	5		0.42			133.4		
	6		0.41			119.7		

5 DANKSAGUNG

Ich danke Ilka Peeken für die Möglichkeit, an diesem Projekt zu arbeiten, und für die gute Betreuung während meiner Doktorarbeit. Danke für all die Arbeit und Mühe, die Du in den letzten Jahren investiert hast. Außerdem möchte ich Karin Lochte für ihre Hilfe, Betreuung und die vielen Kommentare zu meinen Manuskripten danken.

Ich danke meinen Co-Autoren Philipp Assmy und Marcel Veldhuis für die erfolgreiche Zusammenarbeit an meiner ersten Veröffentlichung.

Svend Duggen bin ich dankbar für die Möglichkeit mit Vulkanasche arbeiten zu können. Schön zu sehen, was aus einer zufälligen Begegnung im Flur, ein paar Krümeln Asche und viel Enthusiasmus alles werden kann!

Peter Fritsche, Kerstin Nachtigall und Tania Klüver danke ich ganz herzlich für die Hilfe bei allen kleinen und großen Laborproblemen, bei denen sie mir mit Rat und Tat und vor allem guter Laune zur Seite gestanden haben.

Vielen Dank an Peter Croot für all die Fragen, die er mir über Eisen und alles was dazugehört beantwortet hat.

Meinen HiWis Sebastian Krug, Christin Krieger, Jesco Peschutter, Wiebke Schmidt und Susanne Wilken möchte ich ganz herzlich für ihre gewissenhafte Arbeit danken. Ohne Jesco, Wiebke und Susanne hätte ich es nie geschafft, während meiner Schwangerschaft die letzten Experimente zu beenden. Vielen Dank, dass Ihr so zuverlässig ward.

Ich danke allen EIFEX Teilnehmern für zehn anstrengende aber tolle Wochen am stürmischen und kalten "Ende der Welt".

Für immer gute Stimmung auf dem Schiff, im Kaffeeraum, auf dem Flur, im Labor, im Büro, beim Mittagsessen etc. danke ich Jan Schröder, Katrin Bluhm, Marius Müller, Julia Wohlers, Kirsten Schäfer, Susanne Wilken, Sebastian Krug, Sven Neulinger, Rebecca Langlois, Diana Hümmer, Kerstin Suffrian, Martina Blümel, Vera Thiel und Marcus Tank.

Ein großes Dankeschön an alle Notfallbabysitter in den letzten Monaten, ganz besonders an Anna, Karin und Jens!

Maria Linkogle und ihren Söhnen Sander und Daniel danke ich von ganzem Herzen für die liebevolle Betreuung meiner Tochter während der letzten Monate. Ich wusste Nuka bei Euch immer in guten Händen und es ist schön zu sehen, wie sehr die Lütten sich inzwischen mögen.

Ich danke allen meinen Freunden, die mich gerade im letzten Jahr sehr unterstützt haben und immer für mich da waren. Ganz besonders möchte ich hier Birte Siem, Dirk Steinbach und Mona Borchert erwähnen auf die ich mich immer verlassen kann.

Mein besonderer Dank geht an meine Eltern, die immer hinter mir stehen und an meine Schwestern, die mich oft am besten verstehen können. Zu wissen, dass Ihr immer da seid ist sehr wichtig für mich.

Ich danke meiner Tochter Nuka dafür, dass sie so ein wunderbares und unkompliziertes Baby ist und uns so viel Freude bereitet. Ein Lächeln von Dir lässt die Welt gleich wieder sonnig aussehen, egal wie viel Stress und wie wenig Schlaf wir haben!

Eike, danke dafür, dass Du immer an meiner Seite bist und immer an mich glaubst. Es tut so gut zu wissen, dass wir zu zweit sind. Ohne Dich, Deine Unterstützung und Hilfe hätte ich es nie geschafft. Danke, dass Du mir in den letzten Monaten so sehr den Rücken freigehalten hast. Ich weiß, zusammen können wir alles schaffen!

Abschließend möchte ich allen danken, die nie daran gezweifelt haben, dass ich es auch mit Kind schaffen werde, diese Arbeit zu beenden!!